Nuclear Science
NEA/NSC/WPFC/DOC(2012)15
June 2012
www.oecd-nea.org

Spent Nuclear Fuel Reprocessing Flowsheet

NUCLEAR ENERGY AGENCY

Nuclear Science NEA/NSC/WPFC/DOC(2012)15

A Report by the WPFC Expert Group on Chemical Partitioning
of the NEA Nuclear Science Committee

Spent Nuclear Fuel Reprocessing Flowsheet

NUCLEAR ENERGY AGENCY
ORGANISATION FOR ECONOMIC CO-OPERATION AND DEVELOPMENT

ORGANISATION FOR ECONOMIC CO-OPERATION AND DEVELOPMENT

The OECD is a unique forum where the governments of 34 democracies work together to address the economic, social and environmental challenges of globalisation. The OECD is also at the forefront of efforts to understand and to help governments respond to new developments and concerns, such as corporate governance, the information economy and the challenges of an ageing population. The Organisation provides a setting where governments can compare policy experiences, seek answers to common problems, identify good practice and work to co-ordinate domestic and international policies.

The OECD member countries are: Australia, Austria, Belgium, Canada, Chile, the Czech Republic, Denmark, Estonia, Finland, France, Germany, Greece, Hungary, Iceland, Ireland, Israel, Italy, Japan, Luxembourg, Mexico, the Netherlands, New Zealand, Norway, Poland, Portugal, the Republic of Korea, the Slovak Republic, Slovenia, Spain, Sweden, Switzerland, Turkey, the United Kingdom and the United States. The European Commission takes part in the work of the OECD.

OECD Publishing disseminates widely the results of the Organisation's statistics gathering and research on economic, social and environmental issues, as well as the conventions, guidelines and standards agreed by its members.

NUCLEAR ENERGY AGENCY

The OECD Nuclear Energy Agency (NEA) was established on 1 February 1958. Current NEA membership consists of 30 OECD member countries: Australia, Austria, Belgium, Canada, the Czech Republic, Denmark, Finland, France, Germany, Greece, Hungary, Iceland, Ireland, Italy, Japan, Luxembourg, Mexico, the Netherlands, Norway, Poland, Portugal, the Republic of Korea, the Slovak Republic, Slovenia, Spain, Sweden, Switzerland, Turkey, the United Kingdom and the United States. The European Commission also takes part in the work of the Agency.

The mission of the NEA is:

- to assist its member countries in maintaining and further developing, through international co-operation, the scientific, technological and legal bases required for a safe, environmentally friendly and economical use of nuclear energy for peaceful purposes, as well as
- to provide authoritative assessments and to forge common understandings on key issues, as input to government decisions on nuclear energy policy and to broader OECD policy analyses in areas such as energy and sustainable development.

Specific areas of competence of the NEA include the safety and regulation of nuclear activities, radioactive waste management, radiological protection, nuclear science, economic and technical analyses of the nuclear fuel cycle, nuclear law and liability, and public information.

The NEA Data Bank provides nuclear data and computer program services for participating countries. In these and related tasks, the NEA works in close collaboration with the International Atomic Energy Agency in Vienna, with which it has a Co-operation Agreement, as well as with other international organisations in the nuclear field.

Corrigenda to OECD publications may be found online at: *www.oecd.org/publishing/corrigenda*.

Foreword

Under the auspices of the NEA Nuclear Science Committee (NSC), the Working Party on Scientific Issues of the Fuel Cycle (WPFC) has been established to co-ordinate scientific activities regarding various existing and advanced nuclear fuel cycles, including advanced reactor systems, associated chemistry and flowsheets, development and performance of fuel and materials, and accelerators and spallation targets. The WPFC has different expert groups to cover a wide range of scientific fields in the nuclear fuel cycle.

The Expert Group on Chemical Partitioning was created in 2001 to (1) perform a thorough technical assessment of separations processes in application to a broad set of partitioning and transmutation (P&T) operating scenarios and (2) identify important research, development and demonstration necessary to bring preferred technologies to a deployable stage and (3) recommend collaborative international efforts to further technological development.

This report aims to collect spent nuclear fuel reprocessing flowsheet of various processes developed by member states: aqueous, pyro and fluoride volatility.

Acknowledgements

The NEA Secretariat expresses its sincere gratitude to Mr. Byung-Chan Na and Mr. Isao Yamagishi for giving their best effort to initiate and continue the report.

Table of contents

List of figures

List of tables

Chapter 1: Hydrometallurgy process

1.1. Standard PUREX

1.1.1. Process description

The model adopted for the processing of LWR (light-water reactor) fuel by the standard PUREX route consists of the following unit steps and is shown schematically in Figure 1:

- fuel dissolution;
- off-gas treatment;
- chemical separation;
- conversion of fission product and minor actinide wastes to vitrified product.

Figure 1: Schematic description of standard PUREX flowsheet

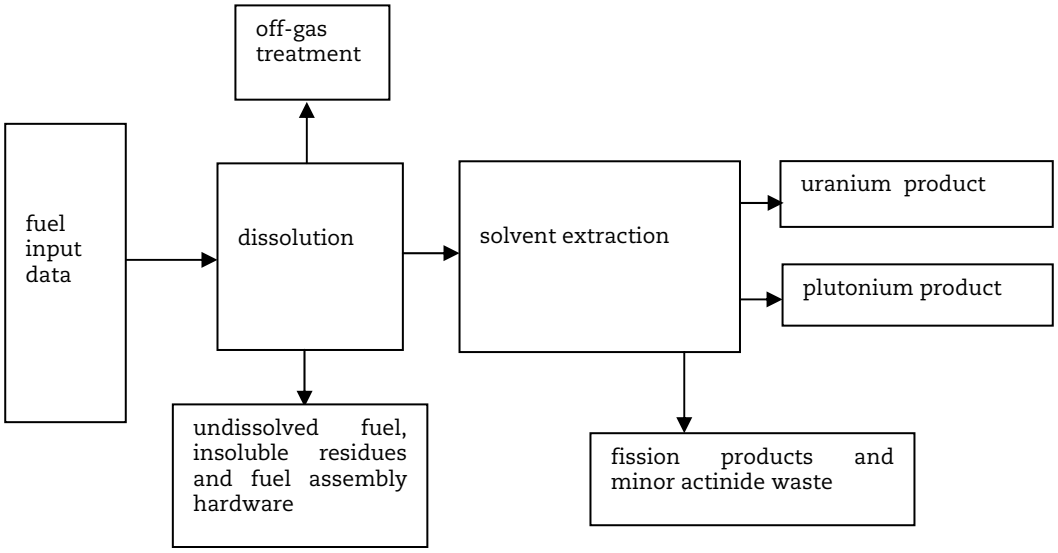

The standard PUREX process is well known, described in detail in many publications and hence only a summary of the process is given here.

Irradiated fuel following cooling for a period typically not less than 5 years is processed using the technique of solvent extraction to give uranium and plutonium oxide products. The initial processing step is exposing the fuel material from within its cladding to a nitric acid solution in order to allow dissolution. This is generally achieved

by the shearing of fuel assemblies into lengths typically of the order of 5 cm. The exposed fuel then dissolves to give a nitrate solution of uranium, plutonium, minor actinides and fission products. Volatile elements including iodine, krypton and xenon are volatilised during the dissolution process. The off-gas is treated to remove those isotopes of radiological significance. A proportion of the more noble fission elements remain undissolved following this process. In addition, a small amount of the fuel may remain with the undissolved fuel assembly hardware being trapped either within an oxide layer on the internal surface of the cladding or within fuel sections to which there has been limited acid access during the dissolution process for whatever reason.

Dissolved species are conditioned to the required uranium concentration, acidity and, in the case of plutonium, valency. This solution is then fed forward to the solvent extraction process where separation occurs as a result of different affinities with the aqueous (nitric acid) and organic (tri-butyl phosphate/diluent) phases. In the first instance this results in the co-separation of fission products and minor actinides from the uranium and plutonium. Subsequently, after manipulation of the plutonium valence state to make it less extractable into the organic phase, uranium and plutonium are separated from each other. Lastly uranium is recovered from the organic phase by reducing the acidity of the aqueous phase.

The purified, aqueous uranium and plutonium solutions are converted to storage as solid products through direct thermal denitration in the case of uranium and, for plutonium, oxalate precipitation and calcination. The waste solution containing fission products and minor actinides is evaporated to reduce its storage volume before being converted to its final waste form by calcination and vitrification. Insoluble fission products arising from the fuel dissolution process are incorporated with the calcined fission products prior to vitrification.

1.1.2. Process assumptions for flowsheeting exercise

Source data

The ORIGEN data used US experimental data which considers irradiation levels and storage periods without any manipulation. This was augmented by ^{14}C data calculated using the British FISPIN code on the assumption of an initial nitrogen impurity level of 25 ppm with respect to uranium.

Dissolution

The fission products of 0.2% other than Ru & Rh (each 0.6%) assumed to remain undissolved following the dissolution process together with 0.03% of U, Np, Am and Cm and 0.15% Pu. These should be considered as maximum values accounting for materials in pin ends and any crimped sections resulting from shearing which exhibit slower dissolution kinetics than usual and elements trapped within the oxide layer at the fuel/cladding interface.[1]

Additionally, 50% of the remaining Ru and Rh, 20% Pd and Mo, 10% Tc and 5% Zr were assumed to be insoluble when processing UO_2 fuels, the Tc value increasing to 30% for MOx fuels, values for other elements being unchanged.[2]

[1] Initially a 0.05% loss of all species was proposed, the more detailed and increased levels assumed here have been adopted to be consistent with those proposed for the Advanced Purex Option. These values are believed to be based on the information presented in Report EUR 10923, J.P. Gue *et al*. Determination of the composition and radioactivity of hulls from industrial processing of fuel from light-water reactors, European Commission, 1986.

[2] Initially a loss of 50% Ru & Rh, 25% Pd, 15% Tc & Mo and 10% Zr was proposed based on Thorp development work. These values have been adjusted to the current values to ensure consistency with the values proposed. The small difference between the two sets is less than

98% of iodine and all ^{14}C and nobles gases volatilised. Tritium was not considered.[3]

Fuel assembly hardware compacted to 130 L/tonne fuel processed.[4]

Off-gas treatment

All noble gases escape into atmosphere.

99% of ^{14}C and 0.4% of iodine precipitated as $BaCO_3$, remainder to aerial (C) or marine (I) discharge.[5]

13.63 L $BaCO_3$ slurry produced per tonne of fuel processed, encapsulated at 40 vol.% i.e. 13.63/0.4 = 34.08 L/tonne encapsulated ^{14}C waste.[6]

Solvent extraction

Decontamination factors for elements generally so high that all elements fed through from the dissolution process other than U and Pu can be assumed to be routed to the high level waste. All elements assumed to exhibit decontamination factors of at least 10^7 apart from Np (1.5×10^4) and Tc (5×10^3) relative to the uranium product and U (5×10^4), Np (100) and Tc(100) relative to the plutonium product.[7]

200 g U and 50 g of Pu per tonne lost to highly active raffinate and solvent washes, routed to vitrification.[8]

High-level waste processing

A 25% weight incorporation of waste oxides was assumed and a glass density of 2.8 g/cm^3.[9]

Waste oxide formulae were assumed to be as follows:

- M_2O Ag, Cs
- MO Sr, Pd, Cd and Ba
- M_2O_3 Y, Rh, In, Sb, La, Nd, Pm, Sm, Eu, Gd, Tb, Dy, Ho and Am
- M_6O_{11} Pr
- MO_2 Zr, Tc, Ru, Te, Ce, U, Np, Pu and Cm
- M_2O_5 Nb
- MO_3 Mo

that which might be expected when using slightly different fuel dissolution conditions and processing fuels of different irradiation history.

3 Based on Thorp development work. No ^3H or ^{14}C figures in ORIGEN data supplied by Jim Laidler, ANL. ^{14}C figure assumed by reference to similar calculations (FISPIN) using a nitrogen impurity level of 25 ppm. No ^3H figure calculated as its relatively short half-life makes it insignificant with respect to long-term waste behaviour.

4 Figure taken from: Extension of Dutch Reprocessing, X. Coeytaux and Y. Marignac, WISE-Paris, June 2004, see http://www.wise-paris.org/english/ reports 040622EPZReproc-Report.pdf, reported to be based on information from COGEMA.

5 Based on Thorp development work.

6 Based on Thorp effluent encapsulation flowsheet. The $BaCO_3$ slurry volume is not sensitive to ^{14}C content and thus is fixed irrespective of fuel burn-up and cooling time. The volume is not necessarily the minimum required.

7 Based on Thorp development work.

8 Assumed maximum losses to aqueous raffinates and solvent washes, based on Thorp development work.

9 Assumed waste loading for future vitrification process, current operation achieves ~ 20% waste loading.

1.1.3. Flowsheet predictions

The above assumptions lead to the following predictions:

- 99.87% recovery of uranium;
- 99.36 – 99.51% recovery of Pu[10];
- A small proportion (<1% for all elements) of fuel remains adhered to the fuel cladding following dissolution;
- 130 L per tonne of compacted fuel assembly hardware;
- 34 L per tonne of encapsulated barium carbonate waste incorporating 99% of ^{14}C and 0.3% of iodine present in irradiated fuel;
- vitrified waste volumes of 61.9 to 88.4 L per tonne emitting 0.87 to 3.94 kW/tonne for the range of fuels considered as shown in Table 1, below.

Table 1: Summary of vitrified waste predictions

Fuel*	U 45	U 45	U 60	U 60	M 45	M 45	M 60	M 60
Cooling/year	5	30	5	30	5	30	5	30
L/tonne	61.9	62.7	82.0	82.9	65.4	68.9	85.2	88.4
kW/tonne	2.12	0.87	2.99	1.16	2.80	1.30	3.94	1.67

* U 45 and U 60 represent UO_2 fuels irradiated to 45 and 60 GWd/tonne respectively. M 45 and M 60 represent MOx fuels irradiated to 45 and 60 GWd/tonne respectively.

1.2. Extended PUREX

1.2.1. Process description

The model adopted for the processing of LWR fuel by the Extended Purex route consists of the same unit steps as the standard PUREX route except concerning chemical separation where (Figure 2):

- the separation of neptunium (and Tc) is included in the PUREX process through an adaptation of the first TBP purification cycle;
- the recovery of the other minor actinides (Am and Cm) is realised by the DIAMEX-SANEX process;
- and, if needed, the americium-curium separation can be realised by solvent extraction using diamide.

[10] The variation in the plutonium recovery predictions arises from the assumption of a 50 g Pu/tonne loss to the aqueous raffinates and solvent washes irrespective of a particular fuel's plutonium content. This assumption arises from a difficulty in substantiating a lower figure on the basis of operational information due to issues of analytical sensitivity and process variation. A 50 g Pu/tonne loss represents a slightly higher proportion of the total plutonium content in the case of UO_2 fuels than it does for MOx fuels.

Figure 2: Extended PUREX process

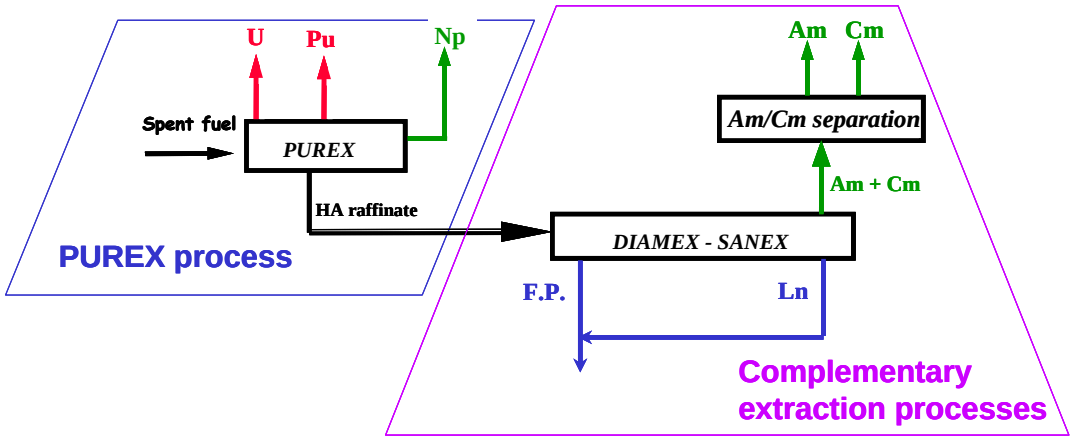

The main differences for the PUREX purification cycles process with regard to the standard PUREX concern the first cycle where (Figure 3):

- a first U-Pu co-decontamination from Tc is realised through a specific Tc scrubbing step (as in the La Hague plants);
- the co-extraction of Np with U and Pu is enhanced by an increase of the acidity of the feed up to 4 to 4.5 mol/L (less than 1% of Np is left in the raffinate).

Figure 3: PUREX 1st purification cycle - Extraction-scrubbing steps

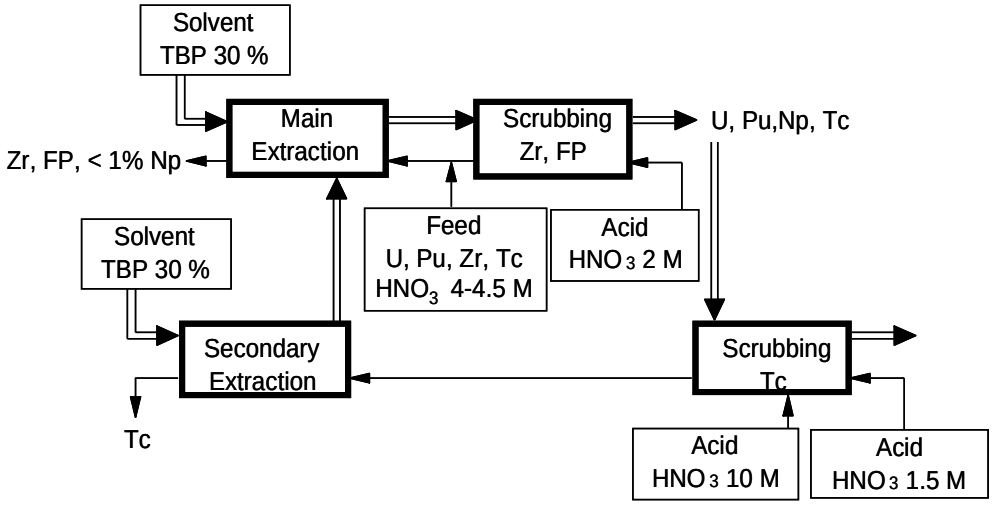

Different processes are proposed and developed for the Am-Cm recovery from the PUREX raffinate (TRUEX-TALSPEAK, NEXT, DIAMEX-SANEX…); we choose the DIAMEX-SANEX process for this flowsheeting exercise.

This process is based on:

- co-extraction of actinides and lanthanides using the DMDOHEMA (DiMethyl-DiOctyl-HexylEthoxy MalonAmide);
- followed by a selective stripping of the trivalent actinides from loaded diamide solvent using an aqueous selective complexing agent;
- and finally the stripping of the lanthanides.

This process allows the trivalent actinides and lanthanides to be co-extracted and separated in a single liquid-liquid extraction cycle.

The feasibility of this process has been demonstrated (recovery yield of An ~99.9% and less than 0.3% in mass of Ln in An) by testing a flowsheet (Figure 4) in which the DIAMEX solvent was supplemented by an acidic extractant, diethylhexylphosphoric acid (HDEHP), to ensure effective extraction at pH > 2. A mixture of HEDTA (actinide-selective polyamino-carboxylate complexing agent) and citric acid (pH 3 buffer) was selected for the selective stripping of the trivalent actinides.

Figure 4: DIAMEX-SANEX process tested on genuine solution in 2000

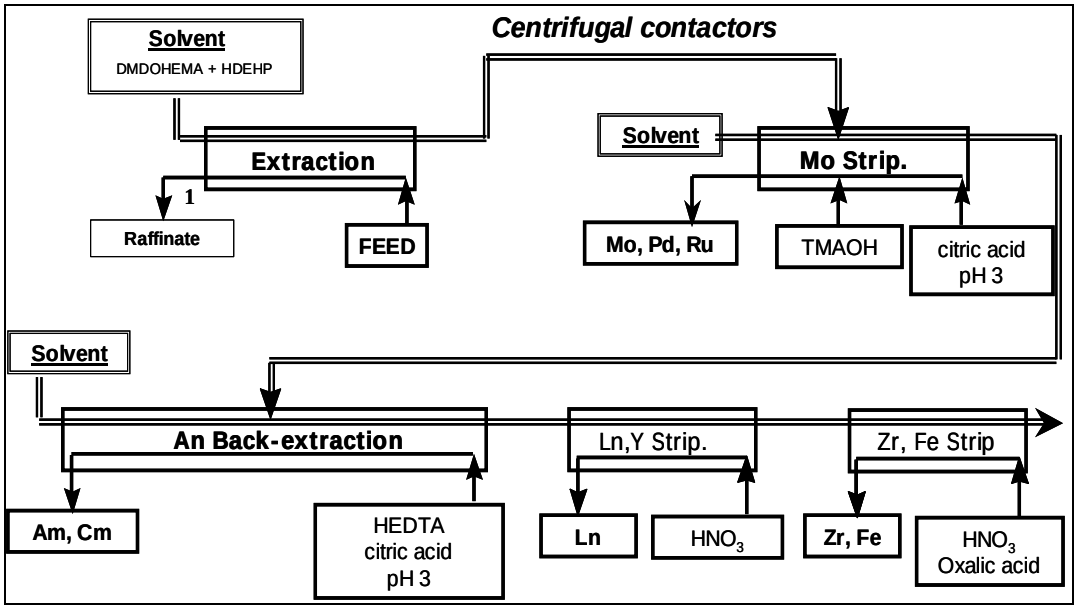

The process assumptions for the flowsheeting exercise are based on the results of this 2 000 run.

Concerning the Am/Cm splitting, the process chosen for this separation is based on the difference of the affinity of the DIAMEX solvent (DMDOHEMA) for americium and curium (Am/Cm separation factor ~ 1.6). As this difference is relatively small, this process requires a large number of stages and the performances are then sensitive to flowsheet parameters. However, such a flowsheet was successfully tested in 2002 (Figure 5) using surrogate solution without significant difficulties.

The performances obtained during this test are summarised hereafter:

- 0.6% of Am within Cm product solution;
- 0.7% of Cm within Am product solution;
- 0.02% of Am and 0.01% of Cm within the stripped solvent.

Figure 5: Am/Cm separation tested on surrogate solution in 2002

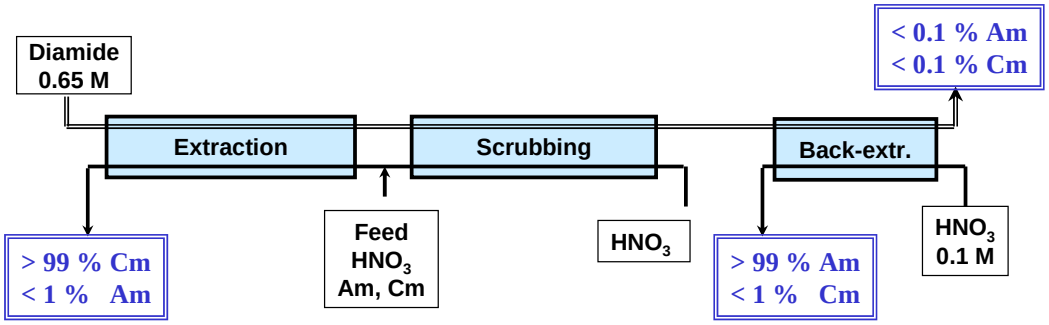

1.2.2. Process assumptions for flowsheeting exercise

The process assumption for the PUREX extraction cycles are the same as for the standard PUREX flowsheets and are recalled hereafter:

a. Dissolution step

- ~100% of volatile FPs (I, Kr, Xe) in dissolution off-gas
- Hulls residual contamination (267 kg/t)
  - FPs ~0.2%, except Ru-Rh ~0.6%
  - U, Np, Am, Cm < 0.03 % and Pu < 0.15%
- Dissolution sludge
  - Ru-Rh ~50%, Mo ~20%, Zr ~5 %, Pd ~20%,
  - Tc ~10% for UOX and ~30% for MOX
  - U-Am-Cm-Np < 0.1% and Pu < 0.3%

b. Extraction-scrubbing step

- All soluble FPs in main extraction raffinate
- [U] < 50 mg/L, [Pu] < 0.5 mg/L in main extraction raffinate
- [U] < 25 mg/L, [Pu] < 0.5 mg/L in secondary extraction raffinate

c. Vitrification step: 2 cases

- FPs oxides 18 weight% (+ sludge + Na), glass density ~2.75
- FPs oxides 25 weight% (+ sludge + Na), glass density ~2.85

The decontamination factors (Table 2) used for the DIAMEX-SANEX process and Am-Cm separation are based on experimental results of DIAMEX and DIAMEX-SANEX tests on

genuine solutions. It should be noted that some decontamination factors (DFs) are underestimated due to the sensitivity limit of the analytical methods.

Table 2: Decontamination factors for the DIAMEX-SANEX process and Am-Cm separation

Element	DF DIAMEX-SANEX	Am DF for Am/Cm separation
Rb	> 10 000**	1
Sr	> 450**	1
Fe	10***	1
Zr	> 500*	1
Mo	> 330*	1
Tc	10	1
Ru	~ 83*	1
Rh	> 120	1
Pd	> 500*	1
Ag	> 28	1
Cd	> 30	1
Sb	> 14 000	1
Cs	> 10 000	1
Ba	> 450	1
Y	> 3 000	1
La	1 000	1
Ce	> 660	1
Pr	1 250	1
Nd	900	1
Sm	> 270	1
Eu	> 3 000	100
Gd	> 3 000	100
U	10	10
Np	10	10
Pu	10	10
Am	1	1
Cm	1	100
Bk	1	1
Cf	1	1

The flowsheets obtained using these assumptions are presented in the following figures:

- Figure 6: flowsheet for UOX fuel 45 GWd/t 5-year cooled;
- Figure 7: flowsheet for UOX fuel 60 GWd/t 5-year cooled;
- Figure 8: flowsheet for MOX fuel 45 GWd/t 5-year cooled;
- Figure 9: flowsheet for MOX fuel 60 GWd/t 5-year cooled.

Figure 6: Flowsheet for UOX fuel 45 GWd/t 5-year cooled

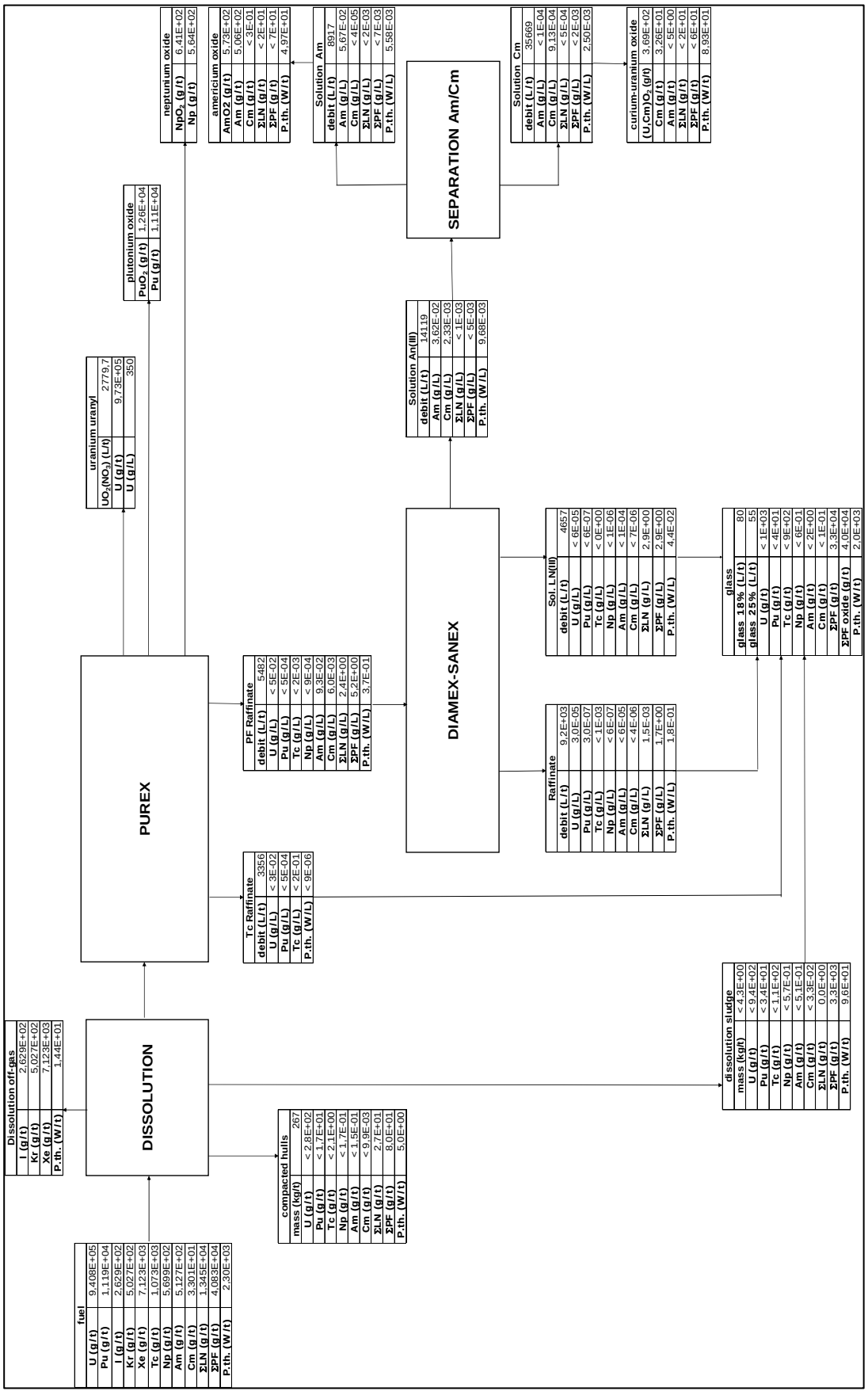

Figure 7: Flowsheet for UOX fuel 60 GWd/t 5-year cooled

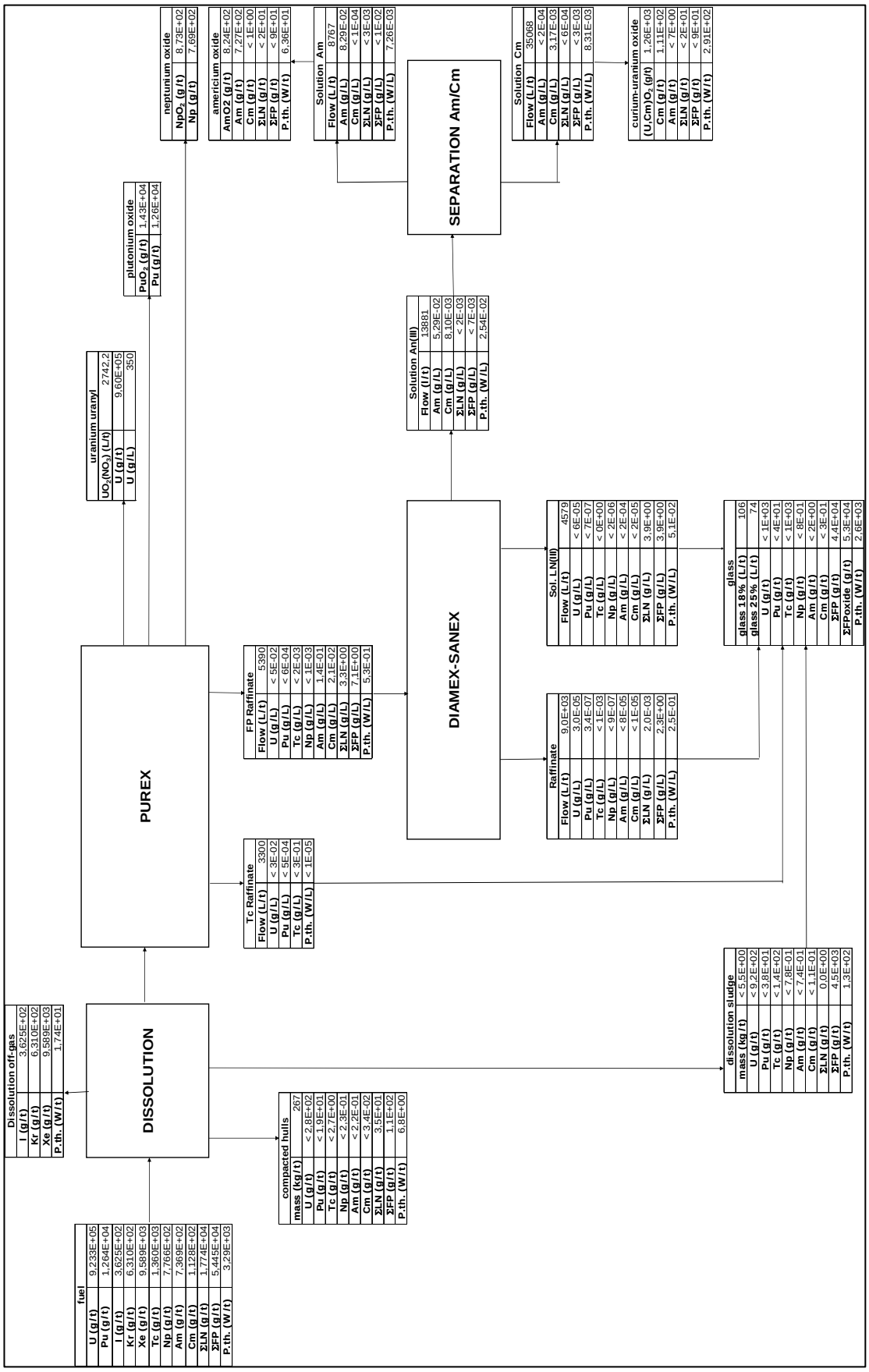

Figure 8: Flowsheet for MOX fuel 45 GWd/t 5-year cooled

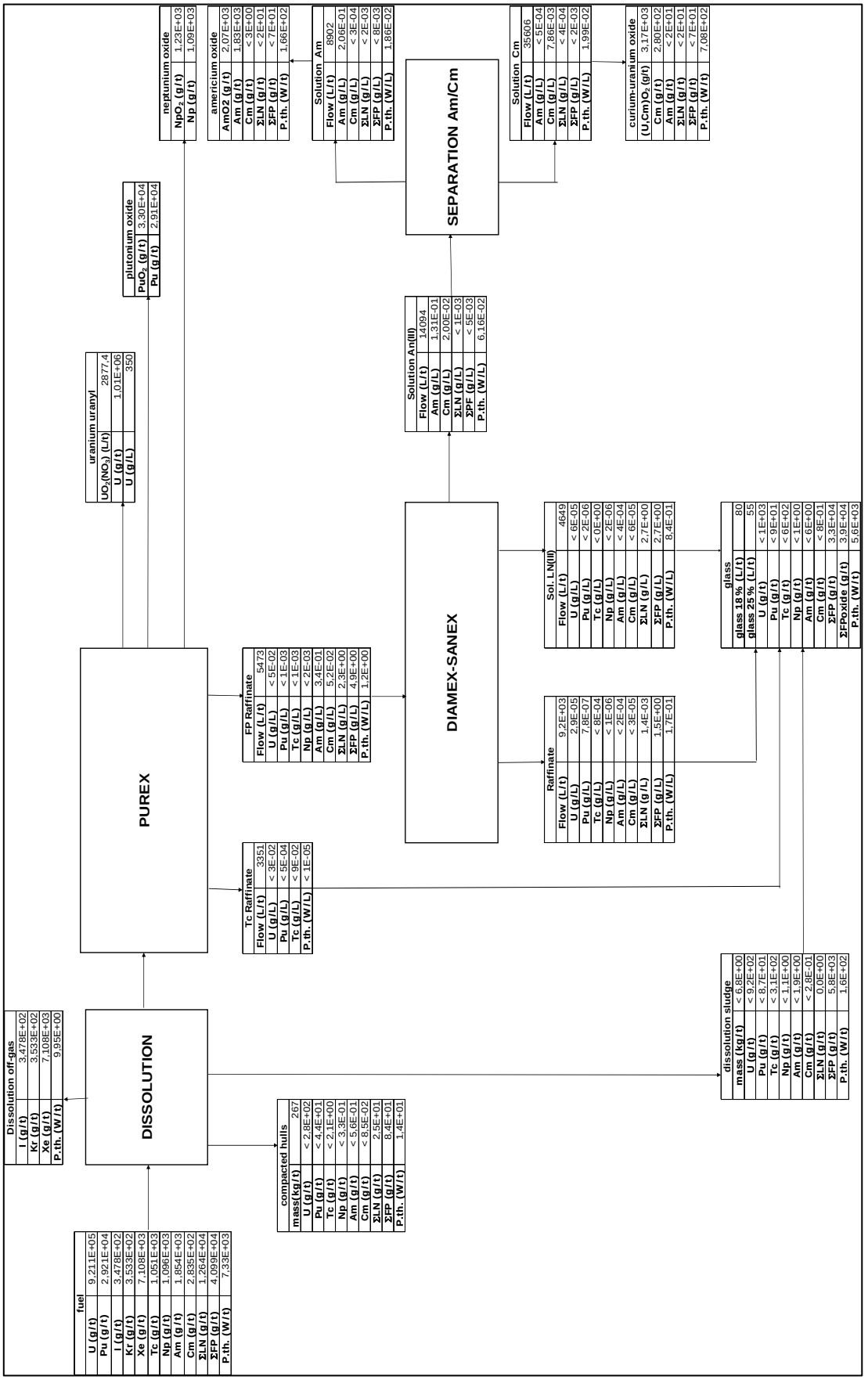

Figure 9: Flowsheet for MOX fuel 60 GWd/t 5-year cooled

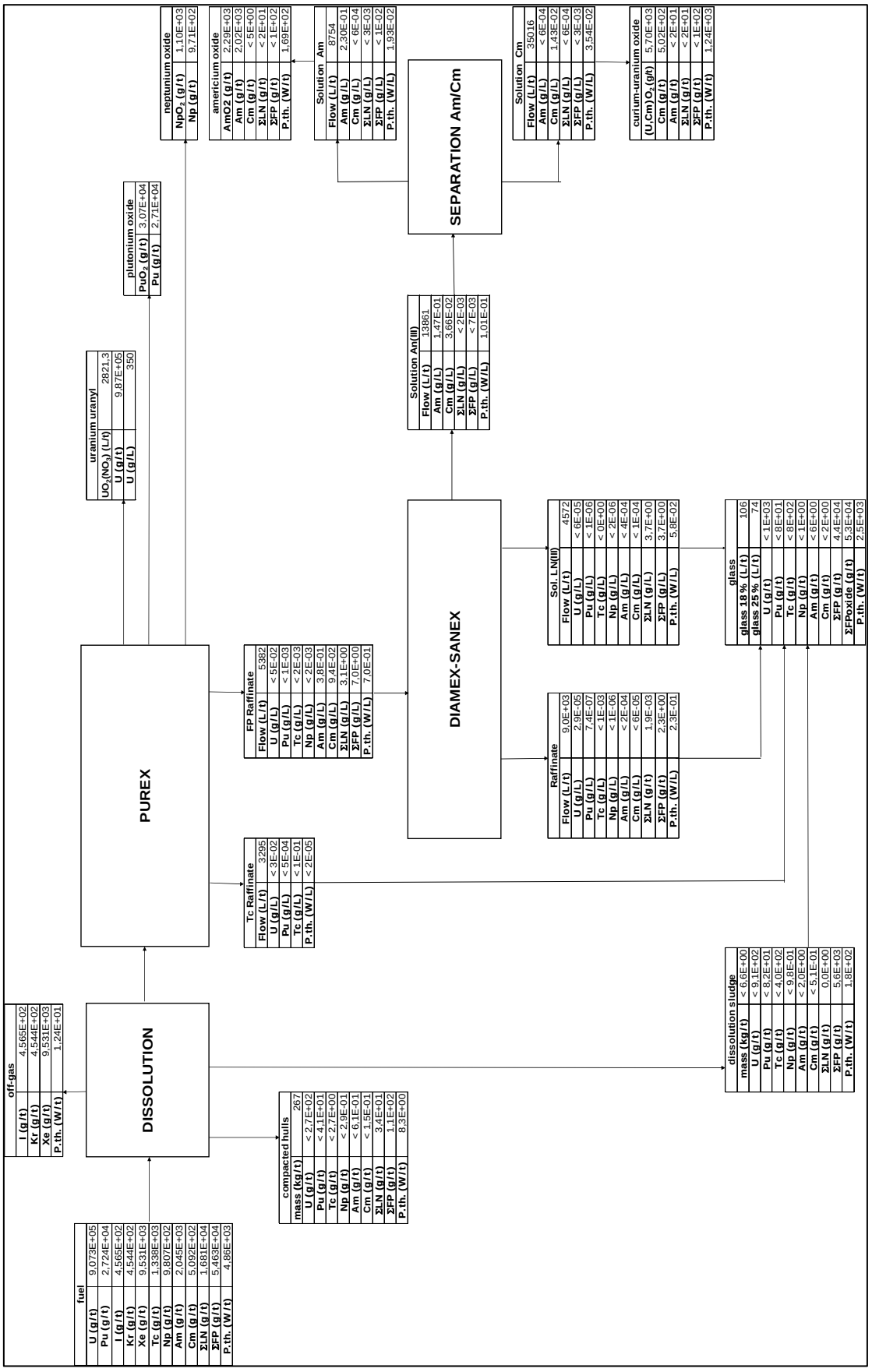

1.3. UREX+3

1.3.1. *Process description*

The model adopted for processing LWR spent fuel by means of a version of the UREX+3 flowsheet consists of the following unit steps and is shown schematically in Figure 10.

- spent fuel disassembly and dissolution;
- off-gas treatment;
- chemical separation of all actinide elements and high-heat fission products;
- conversion of low heat fission products to a vitrified waste form.

Figure 10: UREX+3 flowsheet

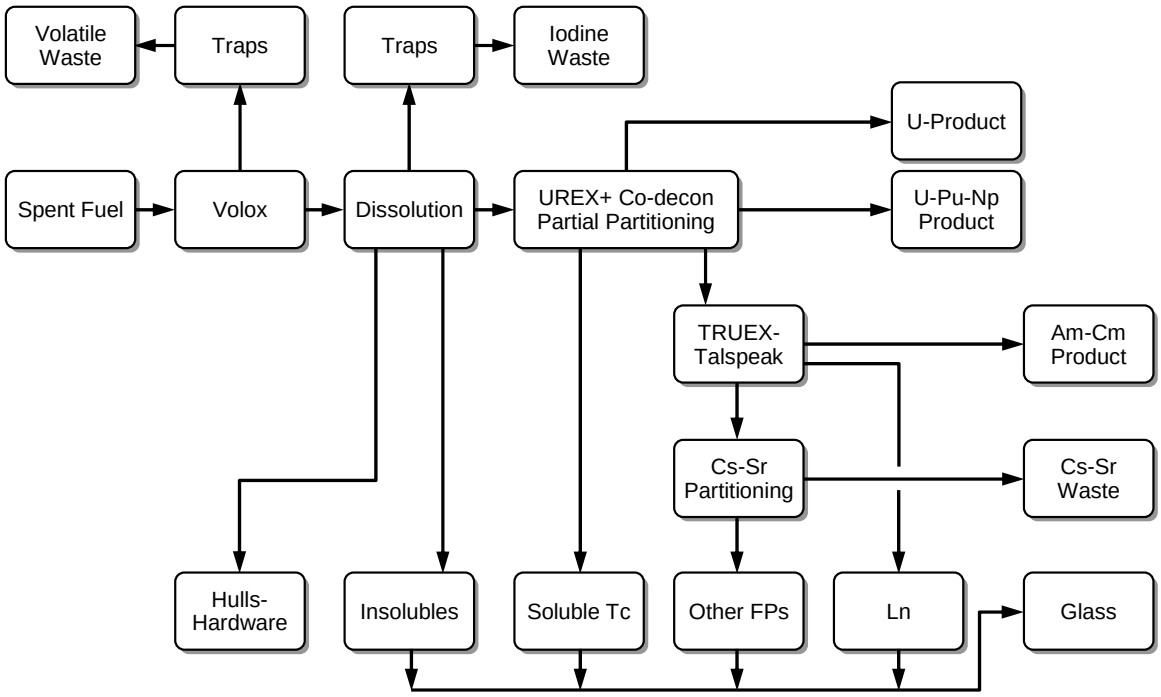

In comparison to the standard PUREX option, the UREX+3 flowsheet can utilise similar methods for spent fuel disassembly, dissolution, and disposal of waste hulls and hardware. The off-gas treatment is enhanced to include recovery and managed disposal of iodine-129, tritium, and possibly krypton-85, in addition to carbon-14. The chemical separations processes applied to the dissolved fuel components are modified and extended to provide (1) a purified uranium product for potential re-enrichment and recycle, (2) a mixed plutonium-neptunium-uranium product for conversion to mixed-oxide (MOX) recycle fuel, (3) recovered soluble technetium-99 for managed disposal, (4) a minor actinide (Am-Cm) product for use as burnable poison (and transmutation) in power reactors, (5) a high-heat generating fission product waste (Cs-Sr), likely solidified in the form of an aluminum-silicate, for managed storage and disposal, and (6) a composite vitrified waste containing all other fission products.

Since the front end process steps are similar to current industrial-scale experience, the uranium and plutonium product recoveries and compositions in waste streams are expected to be the same. In addition, the product recoveries of the minor actinides, neptunium, americium, and curium, are expected to be 99+% when the process optimisation and implementation is complete. Managed waste products containing >95% of the ^{131}I, >95% of the ^{99}Tc, and >99% of the Cs-Sr are expected.

Development of an efficient recovery process for the trivalent actinides, Am and Cm, is a topic of current R&D programmes. The current reference process uses a two-step solvent extraction. The first step is the TRUEX process which separates the group of trivalent actinides and lanthanide fission product elements from the hydrolysable zirconium and molybdenum elements, as well as the other fission products. The separation of the actinides from the lanthanides is done by means of the TALSPEAK process using the solvent, di-2-ethylhexyl phosphoric acid, and an aqueous phase containing chemical complexants at carefully controlled pH levels. For the estimated compositions of the TALSPEAK effluents, Am-Cm losses of 0.1% were assumed. Also, the Am-Cm product was assumed to contain ~250 ppm of the heavier rare earth lanthanides (Gd, Eu, Sm, Pm) and ~22 000 ppm of the lighter lanthanides (Ce, Pr, Nd, La). Optimisation studies will be required to achieve these levels of separation.

1.3.2. Flowsheet cases

Mass and heat balances for the UREX+3 process product and waste streams are provided for low-enriched uranium (LEU) spent fuel ($LEUO_2$) irradiated for 45 GWd/MT. Calculated data are provided using both 5-year decay and 30-year decay periods. The 5-year decay data are applicable to current reprocessing conditions in Europe, while the 30-year decay data are more applicable to spent fuels in the United States, where reprocessing is not likely to be started for another two decades, and large amounts of older spent fuel (>30 years) are accumulating. Recent partitioning-transmutation (P-T) studies have shown significant differences in actinide compositions during multi P-T recycling when processing the longer cooled fuels. This occurs because of the decay of ^{241}Pu (14.3-year) and ^{244}Cm (18-year) during the longer spent fuel storage periods. Moreover, the decreased heat output from fission products in older spent fuels is significant, as indicated in Table 3.

The flowsheets and composition of LEU spent fuel at different cooling times (5 and 30 years) are shown in Figures 11 and 12 and Tables 4 and 5.

Table 3: Compositions of typical spent fuels*

	5 years, Cooling tIme				30 years, Cooling tIme			
	Burn-up, 45 GWd/t Spent fuel		Burn-up, 60 GWd/t Spent fuel		Burn-up, 45 GWd/t Spent fuel		Burn-up, 60 GWd/t Spent fuel	
Component	kg/t	W/t	kg/t	W/t	kg/t	W/t	kg/t	W/t
Zr	362		362		362		362	
SS	57		57		57		57	
Inconel	21		21		21		21	
Total Clad	440		440		440		440	
Xe	7.12		9.59		7.12		9.59	
Kr	0.50	14	0.63	17.4	0.48	2.9	0.61	3.5
H-3	0.00008		0.00010		0.00002		0.00002	
C-14	0.00013		0.00019		0.00013		0.00019	
I	0.26		0.36		0.26		0.36	
Cs	3.69	493	4.76	762	3.02	79	3.87	105
Ba	2.23	474	3.05	625	2.96	266	3.94	351
Sr	1.11	106	1.41	130	0.87	57	1.03	70
Y	0.64	508	0.8	621	0.64	274	0.8	335
Zr	4.82		6.26		4.82		6.26	
Sb	0.021	11.6	0.028	15	0.017	0	0.024	0
Mo	4.60		6.06		4.60		6.06	
Tc	1.07		1.36		1.07		1.36	
Ru	2.96	1.2	4.16	1.6	2.96	0	4.15	0
Rh	0.60	190	0.73	251	0.60	0	0.73	0
Pd	1.68		2.68		1.68		2.69	
Ag	0.09		0.14	0.6	0.09		0.14	
Total NM	11.0	191	15.1	253	11.0	0	15.1	0
Gd	0.15		0.31		0.18		0.346	
Eu	0.19	60	0.26	90	0.17	7.9	0.23	11.9
Sm	1.06		1.37		1.12		1.43	
Pm	0.063	21	0.062	21	0	0	0.84	0
Total HREs	1.463	81	2.002	111	1.47	7.9	2.846	11.9
Ce	3.21	10	4.23	10	3.21	0	4.22	0
Pr	1.54	114	2.01	113	1.54	0	2.01	0
Nd	5.57		7.31		5.57		7.31	
La	1.67		2.19		1.67		2.19	
Total LREs	12.0	124	15.7	123	12.0	0	15.7	0
Total RE	13.5	205	17.7	234	13.5	8	18.6	12
Other FP	31.4	1786	42.0	2409	31.2	679	41.6	865
U	941	0.06	923	0.06	941	0.06	923	0.06
Pu	11.2	164	12.6	283	10.2	138	11.5	236
Np	0.57	0.01	0.78	0.02	0.57	0.01	0.78	0.02
Am	0.51	47	0.74	58	1.38	146	1.78	178
Cm	0.033	88	0.113	292	0.014	34	0.0497	112
Total TRUs	12.3	299	14.2	633	12.2	318	14.1	526

*NM: Noble Material, RE : Rare Earth, LRE : Light Rare Earth, HRE : Heavy Rare Earth

Figure 11: Flowsheet for $LEUO_2$ spent fuel (45 GWd/t, 5-year cooled)

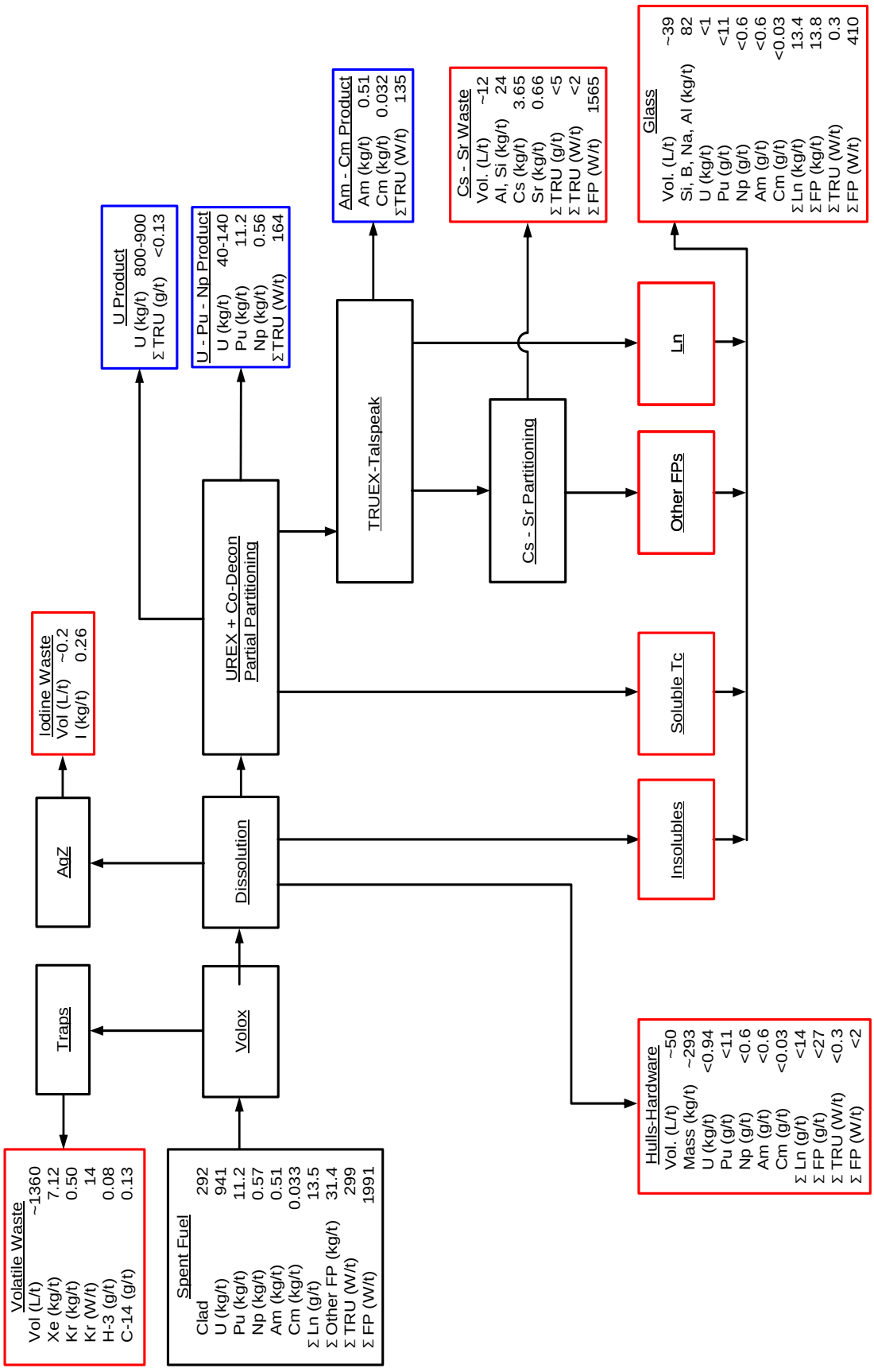

Figure 12: Flowsheet for $LEUO_2$ spent fuel (45 GWd/t, 30-year cooled)

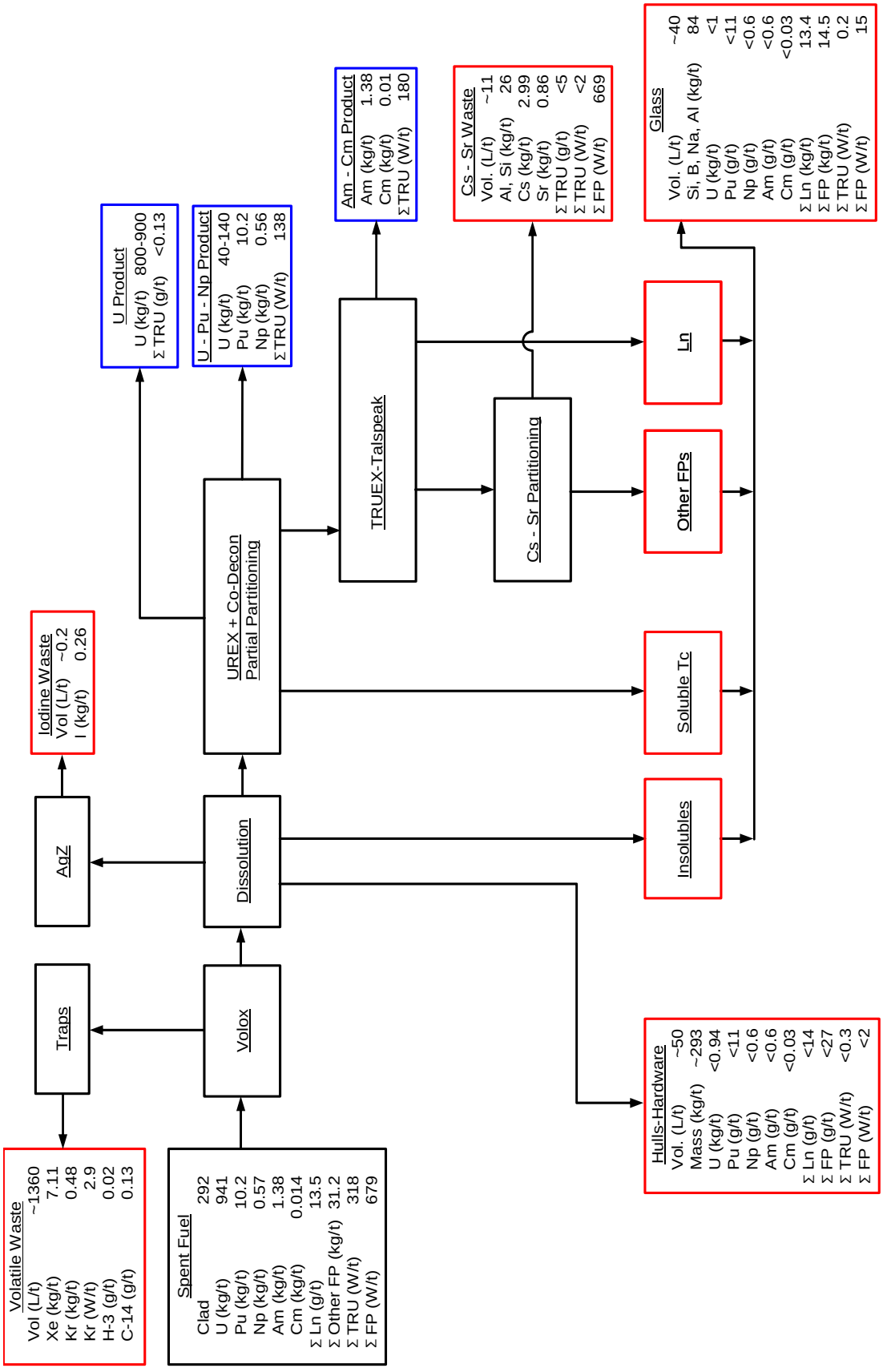

Table 4: Compositions of $LEUO_2$ spent fuel (45 GWd/t, 5-year cooled)

Component	Spent fuel		Hulls - Hardware		I Waste	Volatile wastes		Insolubles		Feed to UREX+	
	kg/t	W/t	kg/t	W/t	kg/t	kg/t	W/t	kg/t	W/t	kg/t	W/t
Zr	235		235								
Hardware	57		57								
Total clad	292		292								
Xe	7.12		<0.0071			7.11				0.00	0
Kr	0.59	14	<0.0005	<0.014		0.50	14		0	0.00	0
^{3}H	0.00008		7.6E-08			0.00008					
^{14}C	0.00013		<1.3E-07			0.00013				0.00	0
I	0.26		<0.00026		0.26					0.00	0
Cs	3.69	493	<0.0037	<0.493						3.69	493
Ba	2.23	474	<0.00223	<0.474						2.23	474
Sr	1.11	106	<0.00111	<0.106						1.11	106
Y	0.64	508	<0.00064	<0.508						0.64	507
Zr	4.82		<0.0048	0.000						4.82	0
Sb	0.021	11.6	0.0000	0.0116						0.02	12
Mo	4.60		<0.0046	0.000				0.70		3.90	0
Tc	1.07		<0.0011	0.000				0.12		0.95	0
Ru	2.96	1.2	<0.0030	0.001				1.10	0.45	1.86	1
Rh	0.60	190	<0.0006	<0.190				0.12	38	0.48	152
Pd	1.68		<0.0017	0.000				0.20		1.48	0
Ag	0.09		<0.00009	0.000				0		0.09	0
Total NM	11.0	191	<0.011	<0.191				2.24	38	8.75	153
Gd	0.15		<0.00015	0.000						0.15	0
Eu	0.19	60	<0.00019	<0.060						0.19	60
Sm	1.06		<0.0011	0.000						1.06	0
Pm	0.063	21	<0.000063	0.021						0.06	21
Total HREs	1.463	81	<0.001463	0.081						1.46	81
Ce	3.21	10	<0.0032	<0.010						3.21	10
Pr	1.54	114	<0.0015	0.114						1.54	114
Nd	5.57		<0.0056	0.000						5.56	0
La	1.67		<0.0017	0.000						1.67	0
Total LREs	12.0	124	<0.0120	<0.124						12.0	124
Total RE	13.5	205	<0.013	<0.205						13.4	205
Other FP	31.4	1786	<0.031	<1.786	0.3	7.6		2.2	38.4	21.2	1732
U	94.1	0.06	<0.94	0.000						940	0
Pu	11.2	164	<0.01	<0.164						11.2	164
Np	0.57	0.01	<0.00057	0.000						0.57	0
Am	0.51	47	<0.00051	<0.047						0.51	47
Cm	0.33	88	<0.000033	0.088						0.03	88
Total TRU	12.3	299	<0.012	<0.299						12.3	299
Inert added			0		0.42	0					
Total mass			~293		0.68	7.6					
Total Vol. (L/t)			~50		~0.2	~1360					

Table 4: Compositions of $LEUO_2$ spent fuel (45 GWd/t, 5-year cooled) (continued)

Component	U product		U-Pu-Np product		Soluble Tc		Feed to Truex-Talsp		Am-Cm product	
	kg/t	W/t	kg/t	W/t	kg/t	W/t	kg/t	W/t	kg/t	W/t
Zr										
Hardware										
Total clad										
Xe							0.0	0.0		
Kr							0.0	0.0		
^{3}H							0.0	0.0		
^{14}C							0.0	0.0		
I							0.0	0.0		
Cs							3.69	493		
Ba							2.23	474		
Sr							1.11	106		
Y							0.64	507		
Zr							4.82	0		
Sb							0.02	12		
Mo							3.90	0		
Tc					0.94	0	0.01	0		
Ru							1.86	1		
Rh							0.48	152		
Pd							1.48	0		
Ag							0.09	0		
Total NM					0.94	0	8.75	153		
Gd							0.15	0	1E-0.5	0
Eu							0.19	60	2E-0.5	0.00599
Sm							1.06	0	0.0001	0
Pm							0.06	21	6E-06	0.002
Total HREs							1.46	81	0.0001	0.01
Ce							3.21	10	0.0032	0.00999
Pr							1.54	114	0.015	0.11
Nd							5.56	0	0.0056	0
La							1.67	0	0.0017	0
Total LREs							12.0	124	0.12	0.12
Total RE	0.0	0	0.0	0	0.0	0	13.4	205	0.012	0.13
Other FP	0.0	0	0.0	0	0.9	0	20.3	1732	0.0	0
U	900		40				0.06	0.06		
Pu			11.2	164			0.01	0.16		
Np			0.56	0			0.01	0.00		
Am							0.51	47	0.51	47
Cm							0.033	88	0.03	88
Total TRU			11.7	164			0.56	135	0.54	135
Inert added										
Total mass										
Total Vol. (L/t)										

Table 4: Compositions of $LEUO_2$ spent fuel (45 GWd/t, 5-year cooled) (continued)

Component	RE waste		Feed to CsSr Sep.		CsSr waste		Other FPs		Glass	
	kg/t	W/t	kg/t	W/t	kg/t	W/t	kg/t	W/t	kg/t	W/t
Zr										
Hardware										
Total clad										
Xe			0.0	0.0					0.0	0.0
Kr			0.0	0.0					0.0	0.0
^{3}H			0.0	0.0					0.0	0.0
^{14}C			0.0	0.0					0.0	0.0
I			0.0	0.0					0.0	0.0
Cs			3.69	493	3.65	488	0.037	4.9	0.04	4.93
Ba			2.23	474	0.02	469	2.21	4.7	2.21	4.74
Sr			1.11	106	1.10	105	0.011	1.1	0.01	1.06
Y			0.64	507	0.01	502	0.63	5.1	0.63	5.07
Zr			4.82	0					0.00	0.00
Sb			0.02	12			0.02	11	0.02	11.5
Mo			3.90	0	0.039	0	3.861	0	4.56	0.00
Tc			0.01	0	1^{E}-04	0	0.0099	0	1.07	0.00
Ru			1.86	1	0.019	0.008	1.84	0.74	2.94	1.19
Rh			0.48	152	0.005	1.52	0.47	150	0.59	188
Pd			1.48	0	0.015	0	1.46	0	1.66	0.00
Ag			0.09	0	9^{E}-04	0	0.09	0	0.09	0.00
Total NM			7.81	153	0.078	1.53	7.74	151	10.9	189
Gd	0.15	0	0.0	0.0					0.15	0.00
Eu	0.19	60	0.0	0.0					0.19	59.9
Sm	1.06	0	0.0	0.0					1.06	0.00
Pm	0.06	21	0.0	0.0					0.06	21.0
Total HREs	1.46	81	0.0	0.0					1.46	81
Ce	3.20	10	0.0	0.0					3.20	9.98
Pr	1.54	114	0.0	0.0					1.54	114
Nd	5.56	0	0.0	0.0					5.56	0.00
La	1.67	0	0.0	0.0					1.67	0.00
Total LREs	12.0	124	0.0	0.0					12.0	124
Total RE	13.43	205	0.0	0.0	0.00	0.00	0.00	0.00	13.4	205
Other FP	0.0	0	20.3	1732	4.85	1565	10.62	167	13.8	205
U			0.1	0.1					0.000	0.00
Pu			0.0	0.2					0.000	0.00
Np			0.0	0.0					0.000	0.00
Am	0.0005	0.047	0.0	0.0					0.001	0.05
Cm	3^{E}-05	0.088	0.0	0.0					0.000	0.09
Total TRU	0.0005	0.13	0.1	0.2					0.001	0.13
Inert added					28				82	
Total mass					32				109	
Total Vol. (L/t)					~13				~39	

Table 5: Compositions of $LEUO_2$ spent fuel (45 GWd/t, 30-year cooled)

Component	Spent fuel		Hulls - Hardware		I Waste	Volatile wastes		Insolubles		Feed to UREX+	
	kg/t	W/t	kg/t	W/t	kg/t	kg/t	W/t	kg/t	W/t	kg/t	W/t
Zr	235		235								
Hardware	57		57								
Total clad	292		292								
Xe	7.12		<0.0071			7.11				0.00	0
Kr	0.48	2.9	<0.00048	<0.003		0.48	2.9		0	0.00	0
^{3}H	0.00002		1.9E-08			0.00002					
^{14}C	0.00013		<1.3E-07			0.00013				0.00	0
I	0.26		<0.00026		0.26					0.00	0
Cs	3.02	79	<0.0030	<0.079						3.02	79
Ba	2.96	266	<0.00296	<0.266						2.96	266
Sr	0.87	57	<0.00087	<0.057						0.87	57
Y	0.64	274	<0.00064	<0.274						0.64	274
Zr	4.82		<0.0048	0.000						4.82	0
Sb	0.017	0	0.0000	0.0000						0.02	0
Mo	4.60		<0.0046	0.000				0.70		3.90	0
Tc	1.07		<0.0011	0.000				0.12		0.95	0
Ru	2.96	0	<0.0030	0.000				1.10	0	1.86	0
Rh	0.60	0	<0.0006	<0.000				0.12	0	0.48	0
Pd	1.68		<0.0017	0.000				0.20		1.48	0
Ag	0.09		<0.00009	0.000				0		0.09	0
Total NM	11.0	0	<0.011	<0.000				2.24	0	8.75	0
Gd	0.18		<0.00018	0.000						0.18	0
Eu	0.17	7.9	<0.00017	<0.008						0.17	8
Sm	1.12		<0.0011	0.000						1.12	0
Pm	1	1	<0	<0.000						0.00	0
Total HREs	1.47	7.9	<0.00147	0.008						1.47	8
Ce	3.21	0	<0.0032	<0.010						3.21	0
Pr	1.54	0	<0.0015	0.000						1.54	0
Nd	5.57		<0.0056	0.000						5.56	0
La	1.67		<0.0017	0.000						1.67	0
Total LREs	12.0	124	<0.0120	<0.124						12.0	0
Total RE	13.5	8	<0.014	<0.008						13.4	8
Other FP	31.4	679	<0.031	<0.679	0.3	7.6		2.2	0.0	21.0	675
U	94.1	0.06	<0.94	0.000						940	0
Pu	10.2	138	<0.01	<0.138						10.2	138
Np	0.57	0.01	<0.00057	0.000						0.57	0
Am	1.38	146	<0.00138	<0.146						1.38	146
Cm	0.014	34	<0.000014	<0.034						0.01	34
Total TRU	12.2	318	<0.012	<0.318						12.2	318
Inert added			0		0.42	0					
Total mass			~293		0.68	7.6					
Total Vol. (L/t)			~50		~0.2	~1360					

Table 5: Compositions of $LEUO_2$ spent fuel (45 GWd/t, 30-year cooled) (continued)

Component	U product		U-Pu-Np product		Soluble Tc		Feed to Truex-Talsp		Am-Cm product	
	kg/t	W/t	kg/t	W/t	kg/t	W/t	kg/t	W/t	kg/t	W/t
Zr										
Hardware										
Total clad										
Xe							0.0	0.0		
Kr							0.0	0.0		
^{3}H							0.0	0.0		
^{14}C							0.0	0.0		
I							0.0	0.0		
Cs							3.02	79		
Ba							2.96	266		
Sr							0.87	57		
Y							0.64	274		
Zr							4.82	0.0		
Sb							0.02	0		
Mo							3.90	0.0		
Tc					0.94	0	0.01	0.0		
Ru							1.86	0.0		
Rh							0.48	0.0		
Pd							1.48	0.0		
Ag							0.09	0.0		
Total NM					0.94	0	7.81	0.0		
Gd							0.18	0	1.8^{E}-05	0
Eu							0.17	8	1.7^{E}-05	0.0008
Sm							1.12	0	0.00011	0
Pm							0.00	0	0	0.000
Total HREs							1.47	8	0.00015	0.00
Ce							3.21	0	0.00321	0
Pr							1.54	0	0.00154	0
Nd							5.56	0	0.00556	0
La							1.67	0	0.00167	0
Total LREs							12.0	0	0.012	0
Total RE	0.0	0	0.0	0	0.0	0	13.4	8	0.012	0
Other FP	0.0	0	0.0	0	0.9	0	20.1	674	0	0
U	900		40				0.06	0.06		
Pu			10.2	138			0.01	0.14		
Np			0.56	0			0.01	0.00		
Am							1.37	146	1.38	146
Cm							0.014	34	0.01	34
Total TRU			10.7	138			1.41	180	1.39	180
Inert added										
Total mass										
Total Vol. (L/t)										

Table 5: Compositions of $LEUO_2$ spent fuel (45 GWd/t, 30-year cooled) (continued)

Component	RE waste		Feed to CsSr Sep.		CsSr waste		Other FPs		Glass	
	kg/t	W/t	kg/t	W/t	kg/t	W/t	kg/t	W/t	kg/t	W/t
Zr										
Hardware										
Total clad										
Xe			0.0	0.0					0.0	0.0
Kr			0.0	0.0					0.0	0.0
^{3}H			0.0	0.0					0.0	0.0
^{14}C			0.0	0.0					0.0	0.0
I			0.0	0.0					0.0	0.0
Cs			3.02	79	2.99	78	0.030	0.8	0.03	0.79
Ba			2.96	266	0.03	263	2.93	2.7	2.93	2.66
Sr			0.87	57	0.86	56	0.009	0.6	0.01	0.57
Y			0.64	274	0.01	271	0.63	2.7	0.63	2.74
Zr			4.82	0.0					0.00	0.00
Sb			0.02	0.0			0.02	0	0.02	0.00
Mo			3.90	0.0	0.039	0	3.8572	0	4.56	0.0
Tc			0.01	0.0	9^{E}-05	0	0.0094	0	1.07	0.0
Ru			1.86	0.0	0.0019	0	1.84	0	2.94	0
Rh			0.48	0.0	0.005	0	0.47	0	0.59	0
Pd			1.48	0.0	0.015	0	1.46	0	1.66	0
Ag			0.09	0.0	9^{E}-04	0	0.09	0	0.09	0
Total NM			7.81	0	0.078	0	7.73	0	10.9	0
Gd	0.18	0	0.0	0.0					0.18	0.00
Eu	0.17	8	0.0	7.9					0.17	7.89
Sm	1.12	0	0.0	0.0					1.12	0
Pm	0.00	0	0.0	0.0					0	0
Total HREs	1.47	8	0.0	7.9					1.47	8
Ce	3.20	0	0.0	0.0					3.20	0
Pr	1.54	0	0.0	0.0					1.54	0
Nd	5.56	0	0.0	0.0					5.56	0
La	1.67	0	0.0	0.0					1.67	0
Total LREs	12.0	0	0.0	0.0					12.0	0
Total RE	13.43	8	0.0	7.89	0	0	0	0	13.4	7.89
Other FP	0.0	0	20.11	675	3.96	669	11.33	7	14.5	6.75
U			0.06	0.06					0.000	0.00
Pu			0.01	0.14					0.000	0.00
Np			0.01	0.00					0.000	0.00
Am	0.0014	0.145	0.0	146					0.000	0.15
Cm	1^{E}-05	0.034	0.0	34					0.000	0.03
Total TRU	0.0014	0.18	0.1	180.0					0.001	0.18
Inert added					22				84	
Total mass					26				112	
Total Vol. (L/t)					~11				~40	

1.4. Grind/Leach

1.4.1. *Process description*

The model adopted for processing TRISO-coated spent fuel by means of a mechanical grind/leach disassembly/dissolution process followed by UREX+3 separations consists of the following unit steps and is shown schematically in Figure 13.

- special mechanical disassembly, grinding and dissolution (leaching) of fuel;
- off-gas treatment;
- chemical separation of all actinide elements and high-heat fission products;
- conversion of low-heat fission products, carbon, and silicon carbide components to a graphite waste form.

TRISO-coated spent fuels differ most from LWR spent fuels in the type and amount of cladding material. The mass ratio of cladding (graphite, carbon, and silicon carbide) to fuel is 16 650 kg/tonne of fuel when the prismatic graphite block is included and 3 660 kg/tonne of fuel when the block is not included. These amounts are both much larger than the mass ratio of zirconium cladding to fuel of ~250–400 kg per tonne of fuel in LWR spent fuels. Moreover, the large amounts of carbon in TRISO-coated spent fuel cladding contain significant amounts of the radioisotope, carbon-14, produced by activation of nitrogen impurities in the carbon and graphite.

In early process development work, the carbon/graphite was removed from the fuel by burning and the carbon dioxide produced was captured by scrubbing to prevent release of the radioactive ^{14}C. However, the resulting metal carbonate waste produced was even greater in volume. Therefore, current process development is patterned after the commercial process used to produce high purity nuclear-grade graphite by means of grinding the graphite to small particle size (~50 µm), followed by leaching in acid to remove the impurities.

The first step in the disassembly process is to remove the fuel sticks (columns of fuel/carbon compacts) from the prismatic block by cutting the top and bottom seal plugs off of the block and removing the fuel/carbon compacts by pushing them out. Experience with Fort St. Vrain irradiated fuel, showed that a relatively low pressure is required to push the compacts out. This was possible because the fuel/carbon compacts had been sintered prior to loading into the block during the fuel manufacture. If sintering of the block and compacts had been done together, the compacts would have been bound to the block and subsequent removal would require a more difficult coring operation.

The second step in the disassembly process is to crush and grind the fuel/carbon compacts by a series of operations which include jaw crushing, roll crushing, and jet milling to reduce the particle size to ~50 µm. The resulting particles can be leached in nitric acid, using a stirred-tank reactor, to dissolve the fuel components. Previous tests, without grinding, recovered ~95% of the fuel; with grinding, the goal is a recovery of 99+%.

The final disassembly/dissolution process is a solid-liquid separation by filtration. The use of a continuous belt filter, similar to that used in the industrial process for making nuclear-grade graphite, is assumed (process development is still in progress).

Because of the large volume of cladding waste, waste treatment and encapsulation is a very important step. Following the UREX+3 separations of uranium, actinide elements, and selected fission products, process development plans are to combine the low-heat fission product waste stream (normally encapsulated in a vitrified glass form) with the carbon-containing cladding waste (leached solids from fuel/carbon compacts). The mixture will then be re-compacted and converted to graphite-based waste compacts which can be encapsulated into the original prismatic block for disposal in the repository.

To increase the efficiency of this waste disposal process, the low-heat fission product waste from an additional ~20 MT of LWR spent fuel could be added to that from each metric ton of TRISO-coated spent fuel and converted to graphite-based waste compacts for encapsulation in the same prismatic block.

The flowsheets and composition of 14% LEU TRISO-coated spent fuel of 100 GWd/t and 5-year cooled are shown in Figure 14 and Table 6.

Figure 13: Schematic diagram of mechanical Grind/Leach – UREX+3 flowsheet

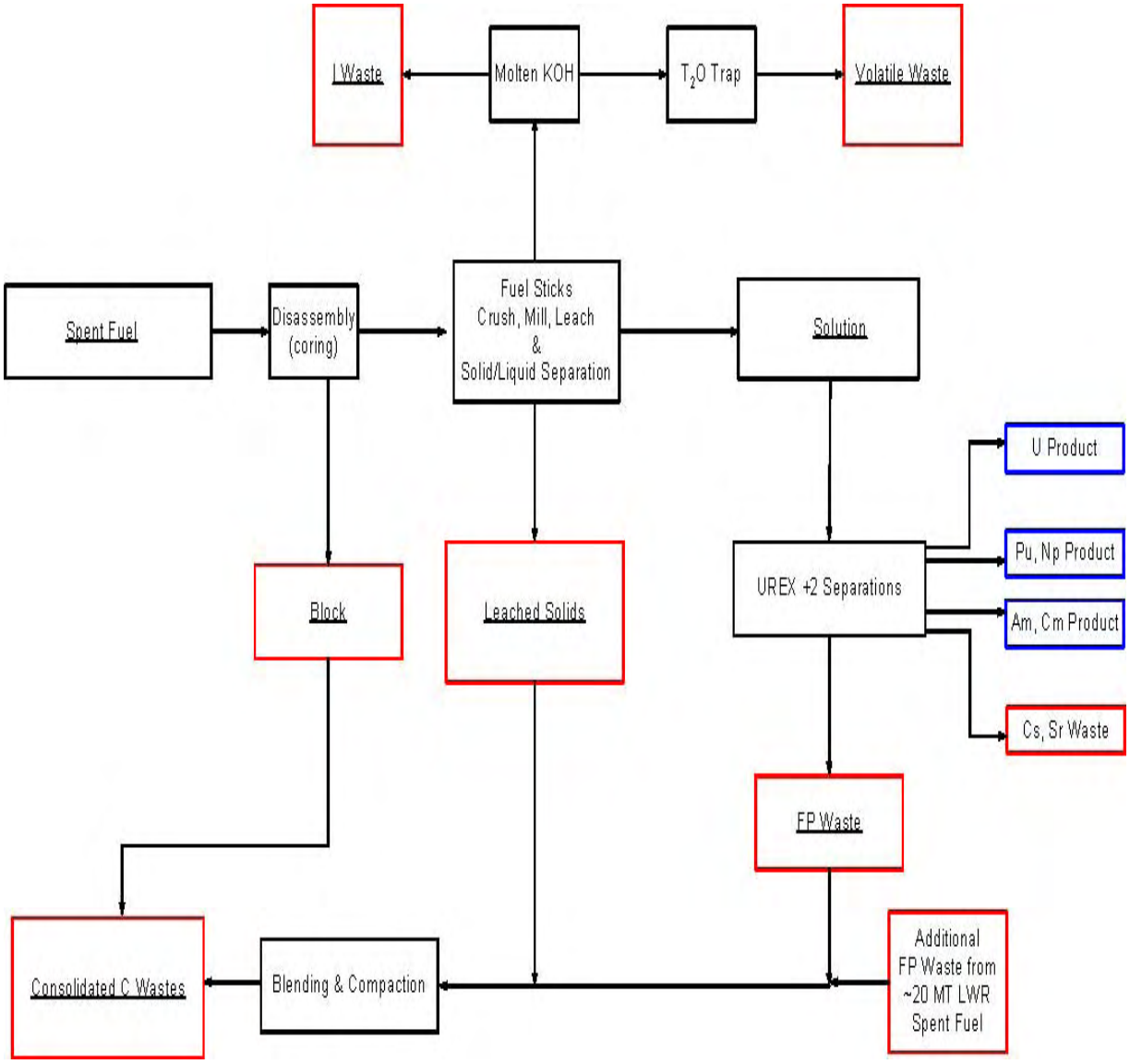

Figure 14: Flowsheet of 14% LEU TRISO-coated spent fuel (100 GWd/t and 5-year cooled)

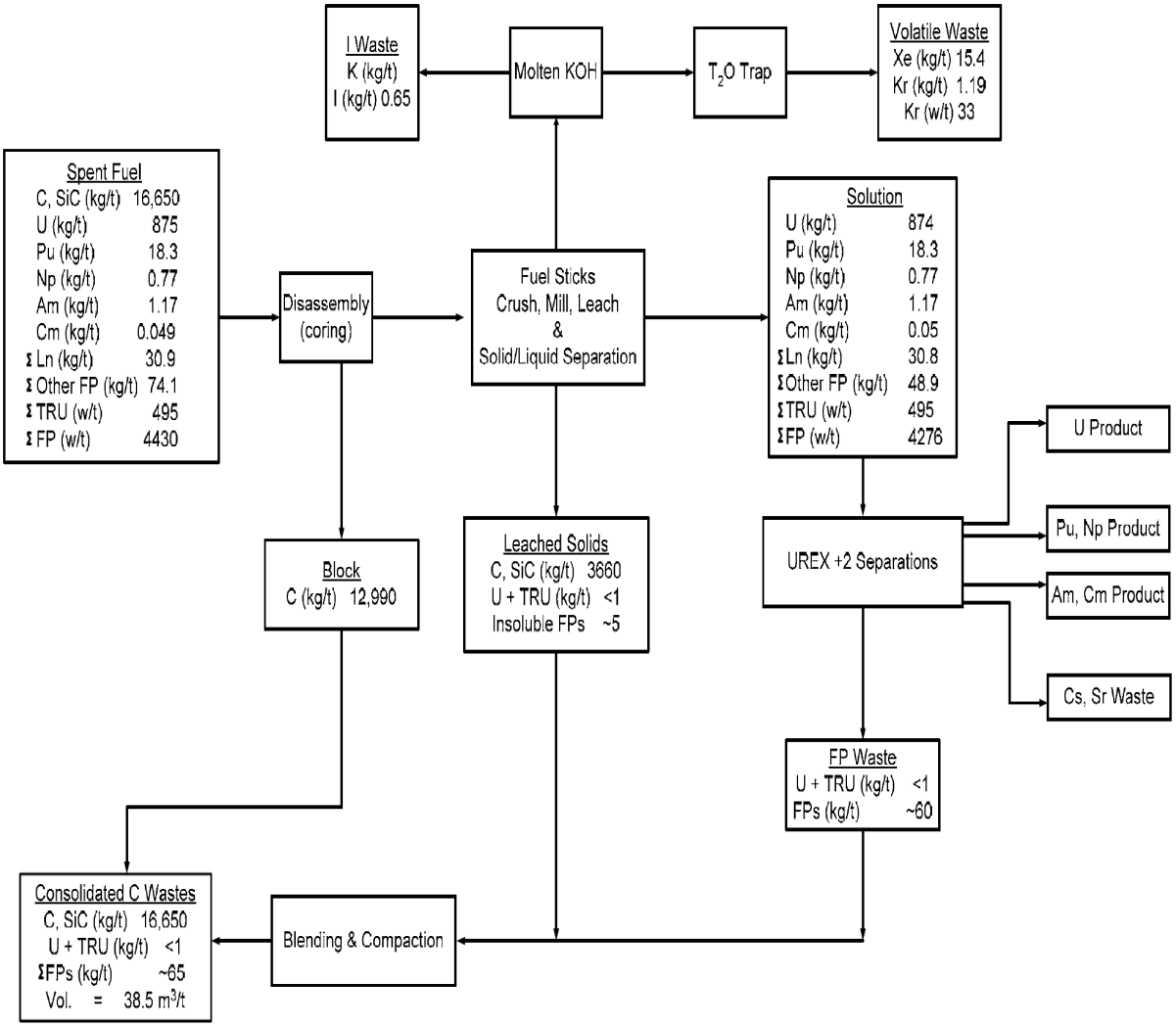

Table 6: Composition of 14% LEU TRISO-coated spent fuel (100 GWd/t, 5-year cooled)

Component	Spent fuel		Graphite block		I-C waste	Volatile wastes		Leached solides		Feed to 1st St. SX	
	kg/t	W/t	kg/t	W/t	kg/t	kg/t	W/t	kg/t	W/t	kg/t	W/t
C, SiC	16 650		12 990					3 660			
Xe	15.4		0.0			15.38				0.00	0
Kr	1.19	33	0.0	0.0		1.19	33.0			0.00	0
^{3}H	0.0012		0.0			0.0012					
^{14}C	0.0028		0.002					8E-04		0.00	0
I	0.65		0.0		0.65					0.00	0
Cs	8.91	869	0.0	0.0				0.009	0.87	8.89	868
Ba	4.87	1 065	0.0	0.0				0.005	1.07	4.86	1 064
Sr	2.78	253	0.0	0.0				0.003	0.25	2.77	253
Y	1.54	1 212	0.0	0.0				0.002	1.21	1.54	1 211
Zr	11.6		0.0	0.0				0.012	0	11.58	0
Sb	0.03	25	0.0	0.0				3E-05	0.025	0.03	25
Mo	10.4		0.0	0.0				1.58		8.81	0
Tc	2.52		0.0	0.0				0.282		2.24	0
Ru	6.24	91	0.0	0.0				2.32	34	3.91	57
Rh	1.55	418	0.0	0.0				0.31	84	1.24	334
Pd	3.28		0.0	0.0				0.39		2.89	0
Ag	0.21		0.0	0.0				0		0.21	0
Total NM	24.2	509	0.0	0.0				4.88	117	19.29	392
Gd	0.2		0.0	0.0				2E-04	0	0.2	0
Eu	0.34	91	0.0	0.0				3E-04	0.091	0.34	91
Sm	2.62		0.0	0.0				0.003	0	2.61	0
Pm	0.17	56	0.0	0.0				2E-04	0.056	0.17	56
Total HREs	3.33	147	0.0	0.0				0.003	0.15	3.32	147
Ce	7.51	28	0.0	0.0				0.008	0.03	7.49	28
Pr	3.56	314	0.0	0.0				0.004	0.31	3.55	314
Nd	12.6		0.0	0.0				0.013	0	12.57	0
La	3.85		0.0	0.0				0.004	0	3.84	0
Total LREs	27.5	342	0.0	0.0				0.028	0.34	27.5	342
Total RE	30.9	489	0.0	0.0				0.031	0.49	30.85	489
Other FP	71.1	3 941	0.0	0.0	0.6	16.6		4.9	121	48.9	3 787
U	875	0.06	0.0	0.0				0.875	6E-05	874	0
Pu	18.3	258	0.0	0.0				0.018	0.258	18.3	258
Np	0.77	0.01	0.0	0.0				8E-04	1E-05	0.77	0
Am	1.17	108	0.0	0.0				0.001	0.108	1.17	108
Cm	0.049	129	0.0	0.0				5E-05	0.129	0.05	129
Total TRU	20.3		0.0	0.0				0.020	0.50	20.2	495

Table 6: Composition of 14% LEU TRISO-coated spent fuel (100 GWd/t, 5-year cooled) (continued)

Component	Feed to CsSr Sep.		CsSr waste		Other FPs		FP waste		U product		Pu-Np product	
	kg/t	W/t	kg/t	W/t	kg/t	W/t	kg/t	W/t	kg/t	W/t		
Total clad												
Xe	0.0	0.0					0.0	0.0				
Kr	0.0	0.0					0.0	0.0				
^{3}H	0.0	0.0					0.0	0.0				
^{14}C	0.0	0.0					0.0	0.0				
I	0.0	0.0					0.0	0.0				
Cs	8.89	868	8.80	859	0.089	8.7	0.1	8.7				
Ba	4.86	1 064	0.05	1 053	4.81	10.6	4.8	10.6				
Sr	2.77	253	2.75	250	0.028	2.5	0.0	2.5				
Y	1.54	1 211	0.02	1 199	1.52	12.1	1.5	12.1				
Zr	0.0	0.0					11.6	0.0				
Sb	0.03	25			0.03	25	0.0	25				
Mo	0.00	0.0	0	0	0	0	8.8	0.0				
Tc	0.00	0.0	0	0	0	0	2.2	0.0				
Ru	3.91	57.1	0.039	0.571	3.87	56.58	3.9	57				
Rh	1.24	334	0.012	3.34	1.23	331	1.2	331				
Pd	2.89	0.0	0.029	0	2.86	0	2.9	0.0				
Ag	0.21	0.0	0.002	0	0.21	0	0.2	0.0				
Total NM	8.25	392	0.082	3.92	8.16	388	19.2	388				
Gd	0.0	0.0					0.2	0				
Eu	0.0	0.0					0.3	91				
Sm	0.0	0.0					2.6	0				
Pm	0.0	0.0					0.2	56				
Total HREs	0.0	0.0					3.32	147				
Ce	0.0	0.0					7.5	28				
Pr	0.0	0.0					3.5	313				
Nd	0.0	0.0					12.6	0				
La	0.0	0.0					3.8	0				
Total LREs	0.0	0.0					27.4	341				
Total RE	0.0	0.0	0.0	0.0	0.0	0.0	30.8	488	0.0	0	0.0	0
Other FP	26.31	3787	11.70	3366	14.61	422	37.2	422	0.0	0.	0.0	0
U	0.0	0.0					0.44	0.06	874			
Pu	0.0	0.0					0.02	0.26			18.2	257
Np	0.0	0.0					0.01	0.00			0.76	0
Am	0.0	1.0					0.00	0.11				
Cm	0.0	1.2					0.00	0.13				
Total TRU	0.0	2.1					0.027	0.49	0.13		19.0	257

Table 6: Composition of 14% LEU TRISO-coated spent fuel (100 GWd/t, 5-year cooled) (continued)

Component	Soluble Tc		Feed to 2nd St. SX		Zr-Mo waste		Am-Cm product		RE waste	
	kg/t	W/t	kg/t	W/t	kg/t	W/t	kg/t	W/t	kg/t	W/t
Total clad										
Xe			0.0	0.0						
Kr			0.0	0.0						
^{3}H			0.0	0.0						
^{14}C			0.0	0.0						
I			0.0	0.0						
Cs			8.89	868						
Ba			4.86	1 064						
Sr			2.77	253						
Y			1.54	1 211						
Zr			11.58	0.0	11.58	0.0				
Sb			0.03	25						
Mo			8.81	0.0	8.81	0.0				
Tc	2.21	0	0.02	0.0	0.02	0.0				
Ru			3.91	57.1						
Rh			1.24	334						
Pd			2.89	0.0						
Ag			0.21	0.0						
Total NM	2.21	0	17.08	392	8.83	0.00				
Gd			0.20	0			2^{E}-05	0	0.2	0
Eu			0.34	91			3^{E}-05	0.0091	0.34	91
Sm			2.61	0			0.000.	0	2.61	0
Pm			0.17	56			2^{E}-05	0.006	0.17	56
Total HREs			3.32	147			0.0003	0.01	3.32	147
Ce			7.49	28			0.0075	0.028	7.49	28
Pr			3.55	314			0.0036	0.31	3.55	313
Nd			12.57	0			0.0126	0	12.56	0
La			3.84	0			0.0038	0	3.84	0
Total LREs			27.5	342			0.027	0.34	27.4	341
Total RE	0.0	0	30.8	489	0.0	0	0.028	0.36	30.76	488
Other FP	2.2	0	46.7	3787	20.4	0	0.0	0	0.0	0
U			0.44	0.06	0.44	0.06				
Pu			0.02	0.26	0.02	0.26				
Np			0.01	0.00	0.01	0.00				
Am			1.17	108			1.16	107	0.0012	0.1079
Cm			0.049	129			0.05	128	5^{E}-05	0.129
Total TRU			1.24	237	0.03	0.26	1.20	234	0.0012	0.24

Chapter 2: Pyrometallurgy process

2.1. Pyroprocess (CRIEPI - Japan)

CRIEPI's pyrochemical process mainly consists of (1) voloxidation of oxide fuels, (2) electrowinning of uranium oxide, (3) electrochemical reduction of residual actinide oxide to metal form, (4) electrorefining of reduced metal and (5) removal of salt or cadmium from cathode deposits by distillation. Introduction of oxide-electrowinning step prior to electrochemical reduction is the specific feature of CRIEPI process. It drastically reduces the amount of fuel to be treated in the latter steps, and consequently reduces the fuel cycle cost.

Partial or integral experimental validations are being carried out to optimise the flowsheet parameters. The recovery of uranium oxide by electrowinning in LiCl-KCl electrolyte was verified using UO_2[1]. The material balance from the reduction step to electrorefining step was experimentally measured with UO_2, PuO_2 and MOX fuels, respectively. In the PuO_2 test, high material balance was achieved but the existence of anode residue was predicted [2]. In the MOX test, dissolution of actinide from anode residue was demonstrated by adding K_2LiCl_4 as oxidant.[3] As for the reductive extraction process which recovers actinides from molten salt by keeping the separation between actinides and lanthanides, a high recovery ratio was obtained through experiments with multi-reduction steps. The result agreed well with the calculation based on thermodynamic properties [4]. Based on these experimental results, material balances of main processes are determined as shown in Figures 15 through 18 with different input fuel characteristics. The composition of the recovered products is shown in Table 7.

References

[1] M. Kurata *et al.* (2005), "Preliminary examination of electrochemical recovery for high pure UO_2", AESJ, September 2005, Hatchinohe, Japan, p.510.

[2] T. Koyama *et al.* (2007), "Integrated experiments of electrochemical pyroprocessing using plutonium oxide", *J. Nucl. Sci. Technol.* 44(3), 1-11.

[3] M. Kurata *et al.* (2006), "Series process test including "re-work" of various residues generated from metal pyro-processing", 3rd RRTD International Workshop on Development of Spent Fuel Management for increasing Nuclear Power Plants rapidly, 8-9 December 2006, Fukuoka, Japan, p.63.

[4] K. Kinoshita *et al.* (1999), *J. Nucl. Sci. Technol.*, 36, 189.

Figure 15: Flowsheet calculation result of 1 000 kg LWR spent fuel processing - Spent UO_2 fuel, 45 GWd/t burn-up, 5 years' cooling

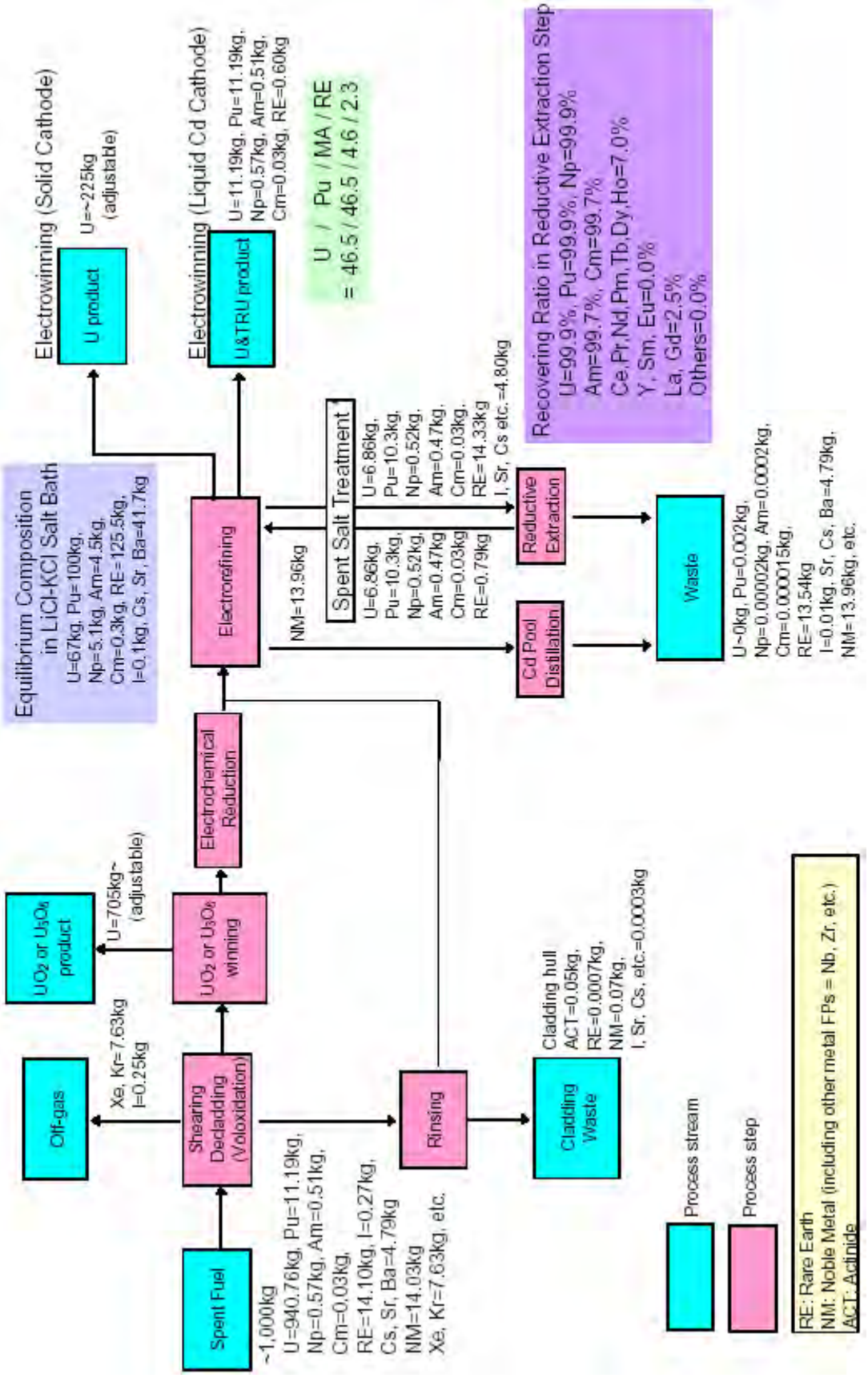

Figure 16: Flowsheet calculation result of 1 000 kg LWR spent fuel processing - Spent UO_2 fuel, 60 GWd/t burn-up, 5 years' cooling

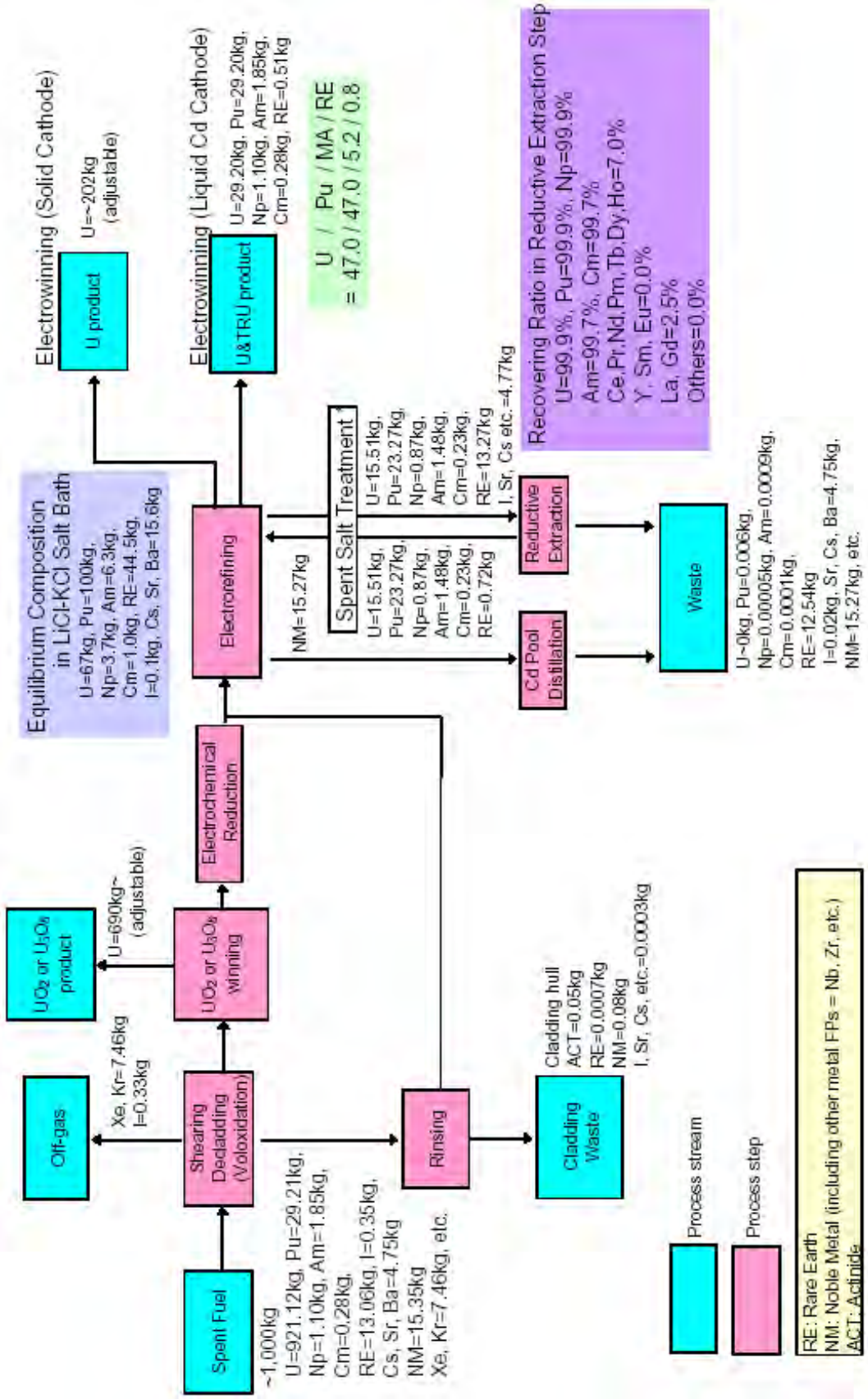

Figure 17: Flowsheet calculation result of 1 000 kg LWR spent fuel processing - Spent MOX fuel, 45 GWd/t burn-up, 5 years' cooling

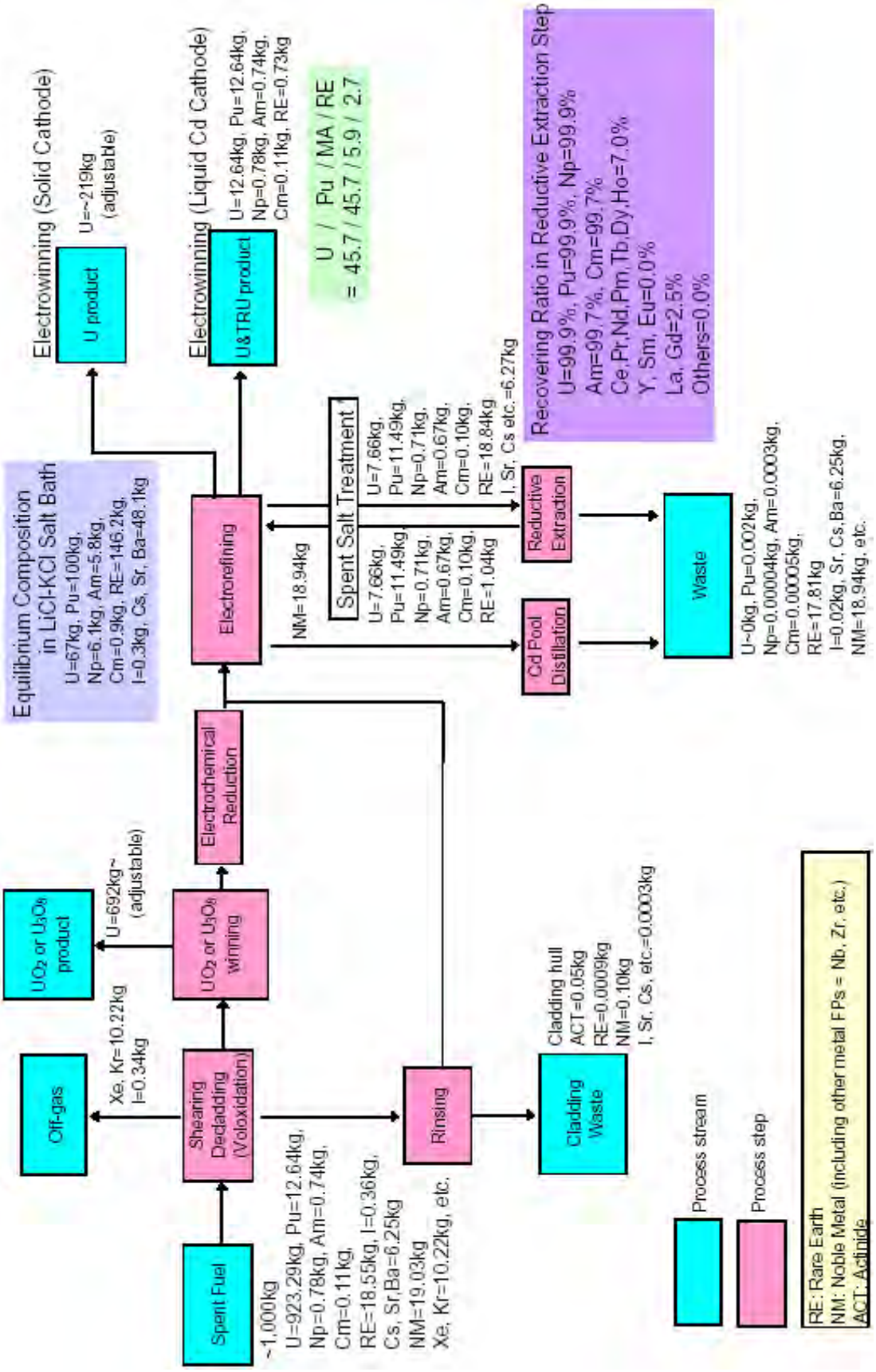

Figure 18: Flowsheet calculation result of 1 000 kg LWR spent fuel processing - Spent MOX fuel, 60 GWd/t burn-up, 5 years' cooling

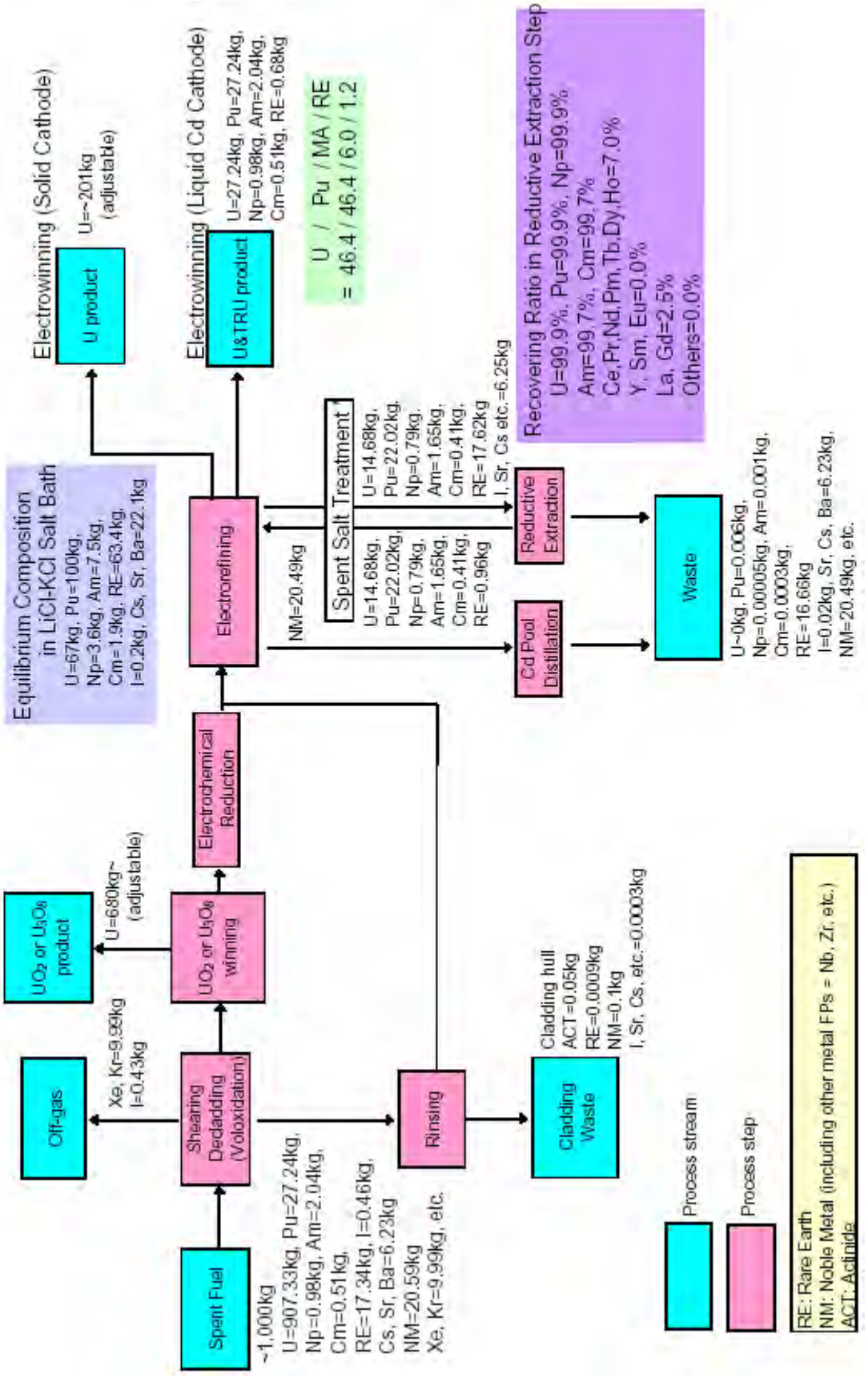

Table 7: Recovered U-Pu-Mas-REs alloy products

Spent fuel	Uranium (wt%)	Plutonium (wt%)	Minor actinides (wt%)	Rare earths (wt%)
UO_2, 45 GWd/t	46.5	46.5	4.6	2.3
UO_2, 60 GWd/t	45.7	45.7	5.9	2.7
MOX, 45 GWd/t	47.0	47.0	5.2	0.8
MOX, 60 GWd/t	46.4	46.4	6.0	12.

2.2. 4-group partitioning process

2.2.1. Outline of the 4-group partitioning process

The 4-group partitioning process was developed in the Japan Atomic Energy Research Institute (JAERI), presently the Japan Atomic Energy Agency (JAEA). The process was developed for concentrated HLLW to separate the elements in HLLW into four groups: transuranium elements (TRU), Tc - platinum group metals (PGM), Sr - Cs and the other elements [1], [2]. The flowsheet is shown in Figure 19. TRU are separated by extraction with diisodecylphosphoric acid (DIDPA). Tc and PGM are separated by precipitation through denitration. Sr and Cs are separated by adsorption with inorganic ion exchangers of titanic acid and zeolite.

DIDPA is an acidic extractant of a phosphoric ester. Figure 20 shows the separation process for all the actinides with DIDPA [3]. Trivalent actinides, Am and Cm, and lanthanides can be extracted with DIDPA from a solution whose nitric acid concentration is about 0.5M. The denitration method has been developed to reduce the nitric acid concentration in HLLW, where formic acid is used as an agent for the denitration. Trivalent actinides and lanthanides are stripped with 4 M nitric acid, and they are separated from each other in the second extraction cycle by selective stripping of the actinides with diethylenetriaminepentaacetic acid (DTPA), which is a similar method to the TALSPEAK process developed in the United States. Tetravalent and hexavalent actinides, Pu and U, have a very high distribution ratio in the DIDPA extraction in a wide range of nitric acid concentration. Neptunium initially in the pentavalent state can be extracted accompanying the reduction to Np(IV) in the presence of hydrogen peroxide. Tetravalent actinides, Np(IV) and Pu(IV), are stripped with oxalic acid and hexavalent U is stripped with sodium carbonate.

At the separation step for Tc-PGM, the raffinate from the DIDPA extraction step is denitrated with formic acid to increase the solution pH to a neutral region and then Tc and PGM (Ru, Rh and Pd) are precipitated. From the precipitate, Tc can be selectively dissolved with hydrogen peroxide. No secondary waste is produced at this step.

The filtrate of the above precipitation step has already been neutralised and can be directly fed to the adsorption step for Sr with titanic acid and for Cs with zeolite (natural mordenite). The titanic acid and mordenite which adsorbed Sr and Cs respectively can be converted to a very stable material by calcination. No secondary waste is produced at the adsorption step, either.

2.2.2. Demonstration test of the 4-group partitioning process

To demonstrate the 4-group partitioning process by the test with real HLLW, the Partitioning Test Facility [4] was constructed and installed in a hot cell at NUCEF (Nuclear Fuel Cycle Safety Engineering Research Facility) in JAERI Tokai. Partitioning tests at NUCEF were started from the cold test using simulated HLLW, whose composition corresponds to a concentrated HLLW. The behaviours of all the elements added were examined. In 1997, the semi-hot test was carried out to examine the behaviour of radionuclides, particularly Am and Tc, in the condition of high element concentration.

Then the first hot test was performed with real HLLW in 1998 [5]. Finally, a demonstration test of the 4-group partitioning process was carried out in 1999-2000 with the concentrated real HLLW [6], [7]. In the demonstration test, about 12.5 L (5 TBq) of the raffinate from the co-decontamination cycle of the PUREX process were used after the concentration to about 2.5 L by evaporation and denitration and the adjustment of nitric acid concentration to 0.49 M in the pre-treatment step [6]. At the pre-treatment step before the extraction step, Zr, which forms colloid in HLLW, was separated in a yield of more than 99%.

Table 8 summarises separation yields for objective elements at each step obtained in the demonstration test and their evaluation [8]. In the extraction step, all the actinides were separated as expected. The extraction yields for Am and Cm were higher than the objective value. The ratio of Np extracted was 95.9%, but it will be improved if the extraction condition is optimised. In the tracer experiments with simulated HLLW, more than 99.95% of Np was extracted with sixteen extraction stages and proper addition of hydrogen peroxide [9], [10]. No difference was found for Np behaviour between the tracer experiment and the tests with real HLLW [5]. The yields of stripping with 4 M nitric acid for Am and Cm were a little lower than the objective value, but must be improved by increasing the number of stages. Stripping with oxalic acid gave a sufficient result.

The second cycle of the DIDPA extraction step which includes selective stripping of Am and Cm with DTPA was not examined in the demonstration test, but a cold experiment with lanthanides and a tracer experiment with Am showed that the separation behaviours of these elements can be predicted by simulation calculation using distribution ratios obtained in batch experiments. In an optimised process, it would be possible to separate Am and Cm from lanthanides in a yield of 99.99% and with a purity of 75 wt% [11].

At the precipitation step for Tc-PGM, more than 90% of Rh and more than 97% of Pd were precipitated by denitration. About half of Ru remained in the denitrated solution, but the remaining Ru was quantitatively precipitated by neutralisation of the denitrated solution to pH 6.7. Tc could not be detected in the demonstration test, but in the semi-hot test, 96.2% of Tc was precipitated.

At the adsorption step for Sr-Cs, an analysis of the effluent showed a complete adsorption of Sr and Cs. Decontamination factors for Sr and Cs were more than 10^4 and 10^6 respectively in all effluent samples.

Thus, in the demonstration test of the 4-group partitioning process with concentrated real HLLW, objective elements were separated with an expected yield. We found no difficulty in operation and no difference in separation behaviours of elements between simulated and real HLLW. The test demonstrated a good performance of the 4-group partitioning process in separation of objective elements.

2.2.3. Evaluation of the 4-group partitioning process

From various experiments on the 4-group partitioning process including the demonstration test, we can evaluate separation yields for various elements at each separation step. Figure 21 shows the separation steps in the 4-group partitioning process and separation yield for each step as K*i* (i=1 - 16). Table 9 shows the values of K*i* evaluated for the optimised condition of the process. Using these values, products and secondary waste from the 4-group partitioning process were evaluated to elucidate the benefit and effect of implementing the partitioning of HLLW [8], [12-14].

Table 10 shows properties of the products (=separated fractions: TRU, U, Tc, PGM) and the wastes (= “Sr-Cs” and “other elements” group) from the 4-group partitioning process. The values were calculated on the basis of HLLW from 1 tonne of 45 GWd/t LWR spent fuel [14]. Wastes are listed in the three right-hand columns; 71.9 kg or 22.1 L of calcined Sr-Cs fraction are generated. The “other elements” fraction is assumed to be vitrified into

38.7 L of waste form with the waste loading of 30 wt%. This high loading, 30 wt%, is possible in vitrified waste mainly because of removal of the heat emitters from the HLW: Sr and Cs. The total volume of the high-level waste form after the partitioning is 22.1+38.7 = about 60 L. This volume is about a third of that in the current Japanese-type glass waste form of HLLW, with a 12 wt% loading (170 L).

Table 11 shows amounts and properties of the secondary wastes generated in the 4-group partitioning process [14]. The secondary wastes are typically of two types. One is used or spent solvent, DIDPA-TBP-dodecane and the other type is sodium salt solutions, sodium carbonate and sodium nitrate. These wastes are stabilised into calcium phosphate ($Ca_2P_2O_7$) and sodium nitrate ($NaNO_3$) pellets, respectively, as their waste forms. These waste forms are the same as those planned for the Rokkasho reprocessing plant, and therefore it is assumed that these will be solidified into a cemented waste form. As listed in Table 11, the amounts of these secondary wastes are not high. For instance, the volume of the used solvent waste is about 40% of that generated from the Rokkasho reprocessing plant. The radioactivity of the secondary wastes is fairly low. Based on radioactivity, these wastes can be disposed of at the low-level waste site.

Based on the evaluation of the separated HLW, impact on the HLW disposal was estimated from aspects of repository saving and cost reduction of the disposal [14]. A preliminary cost estimation for the partitioning and transmutation system was also conducted taking into account the cost benefit in the disposal [15].

References

[1] M. Kubota *et al.* (1993), "Development of a Partitioning Process for the Management of High-Level Waste", *Proc. of Int. Conf. on Future Nuclear Systems: Emerging Fuel Cycles and Waste Disposal Options* (GLOBAL'93), Seattle, Washington, 12-17 September 1993, p.588.

[2] M. Kubota *et al.* (1997), "Preliminary Assessment on Four Group Partitioning Process Developed in JAERI", *Proc. of Int. Conf. on Future Nuclear Systems: Challenge Towards Second Nuclear Era with Advanced Fuel Cycles* (GLOBAL'97), Yokohama, Japan, 5-10 October 1997, p.458.

[3] Y. Morita *et al.* (1995), "Diisodecylphosphoric Acid, DIDPA, as an Extractant for Transuranium Elements", *Proc of Int. Conf. on Evaluation of Emerging Nuclear Fuel Cycle Systems* (GLOBAL'95), Versailles, France, 11-14 September 1995, p.1163.

[4] Y. Morita *et al.* (1997), "Partitioning Test Facility Constructed in NUCEF", *Proc of 4th Int. Information Exchange Meeting on Actinide and Fission Product Partitioning and Transmutation*, Mito, Japan, 11-13 September 1996, p.375, OECD/NEA.

[5] Y. Morita *et al.* (1999), "The First Test of 4-Group Partitioning Process with real High-Level Liquid Waste", *Proc. of Int. Conf. on Future Nuclear Systems* (GLOBAL'99), Jackson Hole, USA, 30 August – 3 September 1999, (CD-ROM).

[6] Y. Morita *et al.* (2000), "A Demonstration Test of 4-Group Partitioning Process with Real High-Level Liquid Waste", *Proc. Int. Conf. ATALANTE 2000*, 24-26 October 2000, Avignon, France, Paper No. P3-37, (www.cea.fr/conferences/atalante2000/index.htm).

[7] Y. Morita *et al.* (2005), "Accomplishment of 10 Year Research in NUCEF and Future Development - Process Safety and Development Research", *Proc. Int. Symp. NUCEF2005*, 9-10 February 2005, Tokai, Japan, JAERI-Conf 2005-007, p.25.

[8] H. Oigawa *et al.* (2005), "Status and Future Plan of Research and Development on Partitioning and Transmutation Technology for Long-lived Nuclides in JAERI", JAERI-Review 2005-043, (in Japanese).

[9] Y. Morita *et al*. (1992), "Separation of Neptunium from High-Level Waste by extraction with Diisodecyl phosphoric Acid", T. Sekine Ed. "Solvent Extraction 1990", *Proc. Int. Solvent Extraction Conf*. (ISEC'90), 18-21 July 1990, p.585, Elsevier, The Netherlands.

[10] Y. Morita *et al*. (1991), "Separation of Transuranic Elements from High-Level Waste by extraction with Diisodecyl phosphoric Acid", *Proc. of 3rd Int. Conf. on Nuclear Fuel Reprocessing and Waste Management* (RECOD'91), Sendai, Japan, 14-18 April 1991, p.348.

[11] Y. Morita *et al*. (2005), "Research and Development on Partitioning in JAERI –Review of the Research Activities until the Development of 4-Group Partitioning Process", JAERI-Review 2005-041, (in Japanese).

[12] H. Oigawa *et al*. (2005), "Parametric Survey on Possible Impact of Partitioning and Transmutation of High-level Radioactive Waste", *Proc. of GLOBAL 2005*, 9-13 October 2005, Tsukuba, Japan, Paper No.266 (CD-ROM).

[13] S. Nakayama *et al*. (2005), "Geologic Disposal of Radioactive Waste Produced by Application of Partitioning - Transmutation Technology to Nuclear Fuel Cycle", *Proc. of GLOBAL 2005*, 9-13 October 2005, Tsukuba, Japan, Paper No.522 (CD-ROM).

[14] S. Nakayama *et al*. (2004), "Partitioning-Transmutation Technology: A Potential Future Nuclear Waste Management Option", *Proc. 8th OECD/NEA Int. Information Exchange Meeting on Actinide and Fission Product Partitioning and Transmutation*, 9-11 November 2004, Las Vegas, USA, p.347.

[15] H. Oigawa *et al*. (2005), "Present Status and Future Perspective of Research and Development on Partitioning and Transmutation Technology at JAERI", *Proc. of GLOBAL 2005*, 9-13 October 2005, Tsukuba, Japan, Paper No.272 (CD-ROM).

Table 8: Results of the demonstration test of the 4-group partitioning process with real HLLW and their evaluation

Separation step	Item	Element	Result	Objective value	Evaluation
Separation of TRU (DIDPA extraction)	Yield of extraction	Am	>99.998%	>99.995%	The object was achieved.
		Cm	>99.999%	>99.995%	
		Pu	-	>99.995%	The higher extraction yield than Am.
		Np	98.2%	>99.95%	The same result as obtained in the tracer experiment under the same condition. Extraction yield >99.95% was obtained in the tracer experiments.
	Yield of stripping with 4M nitric acid	Am	99.986%	>99.99%	As expected. The increase of stage would give >99.99% stripping.
		Cm	99.984%	>99.99%	
		Pu	-	-	Not back-extracted with 4M nitric acid.
		Np	0.3%	-	
	Yield of stripping with oxalic acid	Am	99.985%	-	Am which was not stripped with 4M nitric acid can be recovered with oxalic acid.
		Cm	99.996%	-	
		Pu	>99.98%	>99.99%	Under detection limit. The object must be achieved.
		Np	>99.93%	>99.98%	
Separation of Tc-PGM (Precipitation through denitration)	Yield of precipitation after denitration (pH2.8)	Ru	42%	-	Neutralisation is required, but the addition of alkaline elements had been minimised.
		Rh	90%	-	
		Pd	97%	-	
	Yield of precipitation after neutralisation (pH6.7)	Ru	>99%	>95%	The object was achieved.
		Rh	>99%	>95%	
		Pd	>99%	>95%	
	Yield of precipitation after denitration	Tc	96.6%	>95%	This is the result of semi-hot test. The object was achieved.
Separation of Sr-Cs (Adsorption)	Yield of adsorption	Sr	>99.99%	>99.99%	The object was achieved.
		Cs	>99.99%	>99.99%	

Table 9: Separation yields (Ki) used for the evaluation of the 4-group partitioning process (Ki is shown in Figure 21)

element	To HLW	To precipitate	Raffinate	To precipitate	Cs Adsorption	Sr adsorption	Strip1	Strip2	Strip3	Re-extraction	Strip4	Strip5	Sr dissolution	Tc dissolution	Np refining	U refining
	K1	K2	K3	K4	K5	K6	K7	K8	K9	K10	K11	K12	K13	K14	K15	K16
Sr	1	0.00005	0.9998	0.5	0.00005	0.99999	0.9999	0.999	0.999	0.0002	0.00001	0.9999	0.98	0.99	0.1	0.99
Y	1	0.00005	0.00005	0.99	0.00005	0.999	0.05	0.005	0.99	0.99995	0.00005	0.05	0.9	0.0001	0.01	0.99
Zr	1	0.99	0.0001	0.99	0.00005	0.99	0.03	0.8	0.999	0.9999	0.00001	0.03	0.00005	0.0001	0.99	0.99
Mo	1	0.95	0.95	0.99	0.00005	0.001	0.99	0.8	0.999	0.99	0.00001	0.05	0.00005	0.99	0.99	0.99
Tc	1	0.002	0.99995	0.98	0.00005	0.00005	0.999	0.1	0.999	0.00005	0.00001	0.999	0.00005	0.98	0.99	0.99
Ru	1	0.4	0.99	0.9	0.00005	0.5	0.3	0.1	0.9	0.01	0.00001	0.3	0.00005	0.0001	0.99	0.99
Rh	1	0.001	0.995	0.95	0.00005	0.9	0.99	0.1	0.9	0.005	0.00001	0.99	0.00005	0.0002	0.99	0.99
Pd	1	0.001	0.99	0.98	0.00005	0.9	0.5	0.1	0.9	0.01	0.00001	0.5	0.00005	0.002	0.99	0.99
Te	1	0.95	0.99995	0.99	0.00005	0.00005	0.999	0.1	0.999	0.00005	0.00001	0.999	0.1	0.0001	0.99	0.99
Cs	1	0.00005	0.99995	0.001	0.99999	0.00005	0.9999	0.999	0.999	0.00005	0.00001	0.9999	0.999	0.999	0.99	0.99
Ba	1	0.00005	0.9998	0.5	0.00005	0.99999	0.9999	0.999	0.999	0.0002	0.00001	0.9999	0.98	0.99	0.1	0.99
La	1	0.00005	0.0001	0.99	0.00005	0.999	0.9999	0.8	0.999	0.9999	0.00019	0.9999	0.9	0.0001	0.01	0.99
Ce	1	0.00005	0.0001	0.99	0.00005	0.999	0.999	0.8	0.999	0.99997	0.00179	0.999	0.9	0.0001	0.01	0.99
Pr	1	0.00005	0.0001	0.99	0.00005	0.999	0.9999	0.8	0.999	0.99995	0.00526	0.9999	0.9	0.0001	0.01	0.99
Nd	1	0.00005	0.0001	0.99	0.00005	0.999	0.9999	0.8	0.999	0.99999	0.0179	0.9999	0.9	0.0001	0.01	0.99
Pm	1	0.00005	0.0001	0.99	0.00005	0.999	0.9995	0.8	0.999	0.99999	0.027	0.9995	0.9	0.0001	0.01	0.99
Sm	1	0.00005	0.0001	0.99	0.00005	0.999	0.999	0.8	0.999	0.99999	0.0323	0.999	0.9	0.0001	0.01	0.99
Eu	1	0.00005	0.0001	0.99	0.00005	0.999	0.9985	0.8	0.999	0.99999	0.0278	0.9985	0.9	0.0001	0.01	0.99
Gd	1	0.00005	0.0001	0.99	0.00005	0.999	0.998	0.8	0.999	0.99999	0.0182	0.998	0.9	0.0001	0.01	0.99
Fe	1	0.1	0.02	0.5	0.00005	0.999	0.005	0.998	0.999	0.98	0.00001	0.005	0.1	0.7	0.99	0.99
Cr	1	0.001	0.999	0.95	0.00005	0.999	0.999	0.999	0.999	0.001	0.00001	0.999	0.1	0.3	0.99	0.99
Ni	1	0.0001	0.995	0.5	0.00005	0.999	0.999	0.999	0.999	0.005	0.00001	0.999	0.99	0.9	0.99	0.99
U	0.005	0.0001	0.00005	0.9	0.00005	0.99	0.00005	0.00005	0.999	0.99999	0.001	0.00005	0.9	0.01	0.1	0.00005
Np	1	0.0001	0.0005	0.9	0.00005	0.99	0.00005	0.9998	0.999	0.95	0.001	0.00005	0.9	0.01	0.0001	0.01
Pu	0.005	0.02	0.00005	0.99	0.00005	0.999	0.00005	0.9999	0.999	0.99999	0.001	0.00005	0.2	0.0001	0.0001	0.00005
Am	1	0.00005	0.00005	0.99	0.00005	0.999	0.9999	0.9998	0.999	0.99999	0.9999	0.9999	0.9	0.0001	0.01	0.99
Cm	1	0.00005	0.00005	0.99	0.00005	0.999	0.9999	0.9998	0.999	0.99999	0.9999	0.9999	0.9	0.0001	0.01	0.99

Table 10: Products and wastes from 1 tonne of 45 GWd/t LWR spent fuel by the 4-group partitioning [14]

	Np, Pu, Am, Cm	U	Tc	PGM	Waste		Non-partitioned vitrified waste
					Sr-Cs	Others	
Weight of elements (kg/MTU)	1.51	4.71	1.33	4.36	7.88	25.41	45.86
Weight of oxide (kg/MTU)	1.68	5.34	1.95	5.18	8.42	30.97	54.38
Purity (wt%)	88.4	99.9	75.6	93.8	92.6	-	-
α activity (Bq/MTU)	2.24E+14	4.51E+08	1.22E+05	1.14E+09	1.00E+10	5.66E+10	2.24E+14
$\beta\gamma$ activity (Bq/MTU)	9.21E+13	1.22E+11	6.44E+13	1.03E+15	1.74E+16	4.15E+15	2.28E+16
Total activity (Bq/MTU)	3.16E+14	1.23E+11	6.44E+13	1.03E+15	1.74E+16	4.15E+15	2.30E+16
Heat emission from FP (W/MTU)	2.3	0.0122	5.84	130	1683	292	2114
Heat emission from An (W/MTU)	207.6	0.0004	1.12E-07	0.0011	0.0093	0.052	208
Total heat emission (W/MTU)	20.99	0.0126	5.84	130	1683	292	2321
Chemical form or waste form	Oxide	Oxide	Metal	Metal + Oxide	Calcined	Vitrified (30 wt%)	Vitrified (12 wt%)
Weight (kg/MTU)	1.69	5.34	1.33	4.97	71.9	103.2	453.2
Density (kg/L)	10	10.412	11.5	8	4.2	2.67	2.67
Volume (L/MTU)	0.169	0.513	0.116	0.621	22.1	38.7	169.7
Radioactivity in the products (separated fractions) or wastes							
α activity (Bq/ton)	1.32E+17	8.45E+10	9.12E+07	2.30E+11	1.40E+11	5.48E+11	4.93E+14
$\beta\gamma$ activity (Bq/ton)	5.44E+16	2.29E+13	4.82E+16	2.08E+17	2.43E+17	4.02E+16	5.03E+16
Total activity (Bq/ton)	1.86E+17	2.30E+13	4.82E+16	2.08E+17	2.43E+17	4.02E+16	5.08E+16
Heat density (W/L)	1240	0.024	50.4	208.5	76.3	7.53	13.7

Table 11: Secondary wastes by the 4-group partitioning after reprocessing of 1 tonne of 45 GWd/t LWR spent fuel [14]

	Used solvent	Na waste
Solid waste weight (kg/MTU)	7.90	288.2
	($Ca_2P_2O_7$)	($NaNO_3$)
Solidification	Cement	Cement
Cemented waste form		
Weight (kg/MTU)	79.0	576.3
Density (kg/L)	1.7	2.0
Volume (L/MTU)	46.5	288.2
Radioactiviy		
α activity (Bq/ton)	6.89E+06	7.73E+06
$\beta\gamma$ activity (Bq/ton)	5.32E+11	2.06E+13
Total activity (Bq/ton)	5.32E+11	2.06E+13
Heat density (W/L)	8.68E-05	4.19E-03

Figure 19: Flowsheet of the 4-group partitioning process

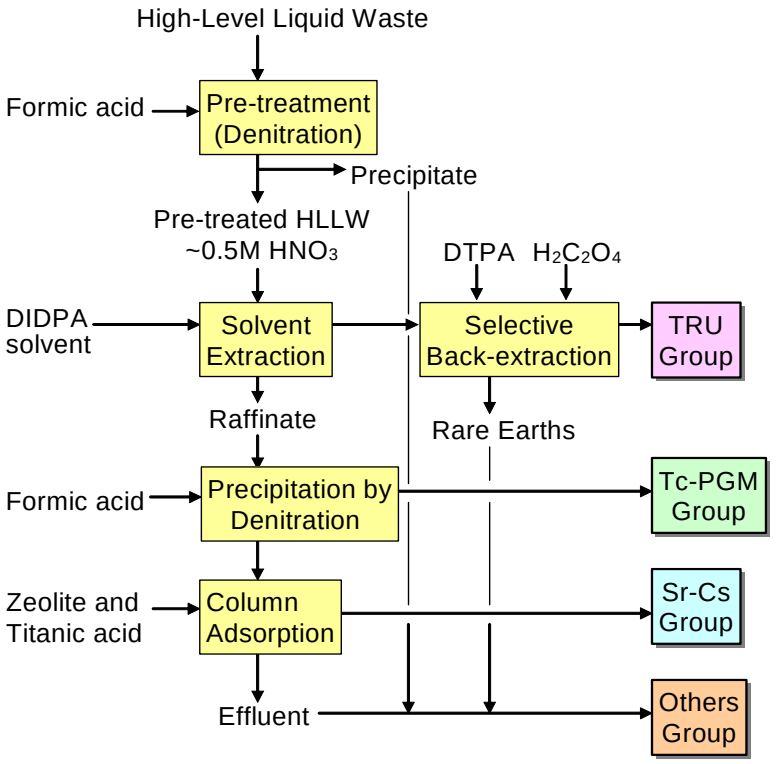

Figure 20: Flowsheet of the DIDPA extraction step

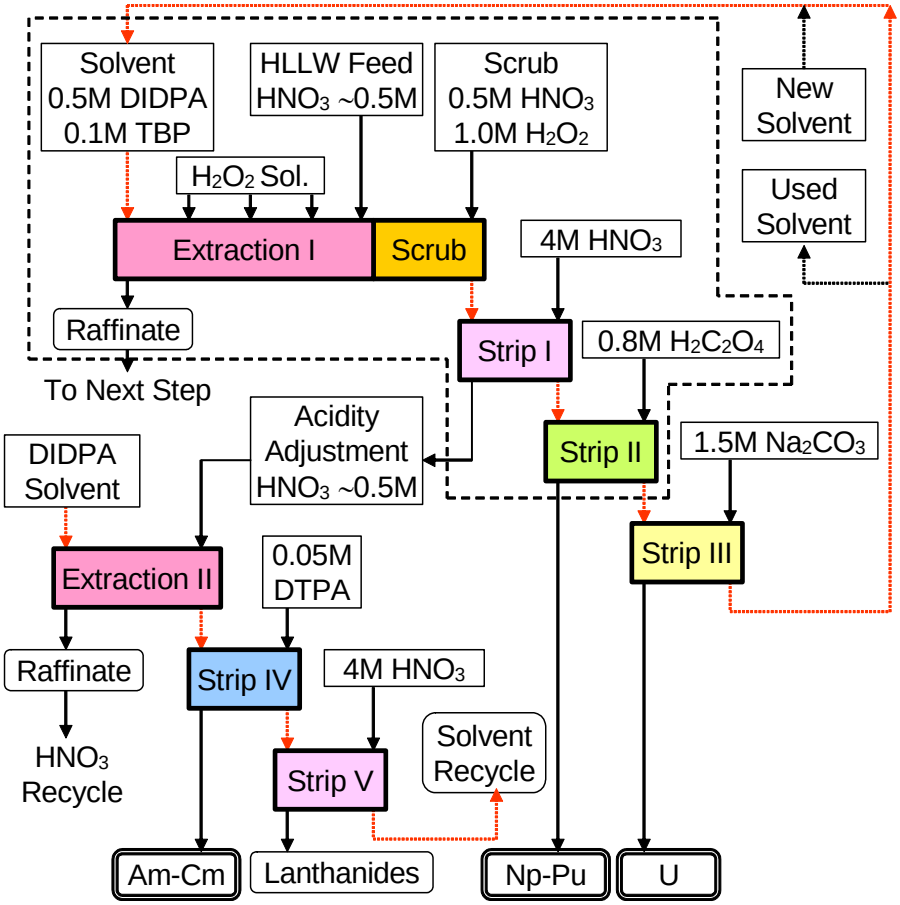

Figure 21: Separation steps in the 4-group partitioning process and separation yield (Ki) for each step

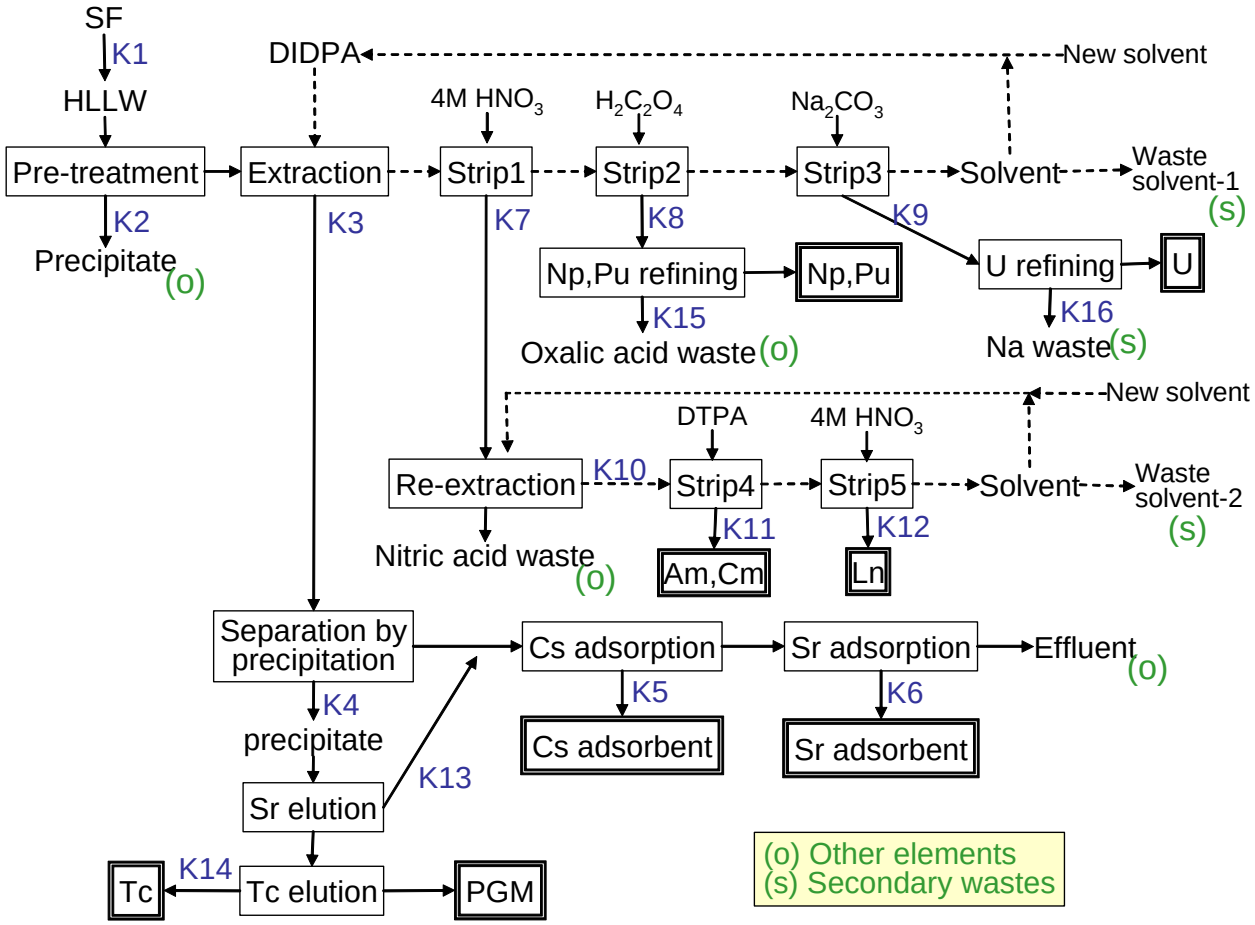

2.3. Pyroprocess (KAERI - Korea)

2.3.1. Pyroprocessing flowsheet in Korea

Next generation nuclear fuel cycles require innovative features such as an environmental load reduction, safety, efficient recycle of resources, nuclear proliferation resistance and economics, etc. From these viewpoints, a pyrometallurgical processing of spent fuel is now considered to be one of the most promising options for future nuclear systems in Korea. KAERI has been developing pyroprocessing technologies, which could reduce the increasing amount of spent nuclear fuel and dramatically decrease the disposal load, through recycling and destroying toxic waste such as the long-life fission products in spent nuclear fuels.

In Korea, an integrated pyroprocessing system is under consideration to process the spent oxide fuels discharged from PWRs and fabricate metallic fuels containing TRU (transuranic element) for a future SFR (sodium-cooled fast reactor). A flowsheet study for a pyroprocess of an oxide to a metal is based on 10 MTHM(defined by a mass of the spent fuels). In this flowsheet study, a reference spent fuel with a ^{235}U enrichment of 4.5 wt% in fresh fuel,

an averaged fuel burn-up of 45 GWd/t and a cooling time of five years, which was discharged from PWRs in Korea was selected. The integrated pyroprocessing system is composed of the following seven principal processes; (1) fuel-element chopping and decladding, (2) high temperature voloxidation, (3) electrolytic reduction, (4) electrorefining, (5) electrowinning, (6) salt purification and (7) fuel fabrication. A tentative flowsheet for the Korean integrated pyroprocessing system under consideration is shown in Figure 22.

In order to recover the actinide elements, the spent PWR fuel is first disassembled and chopped into an appropriate size to obtain spent UO_2 pellets, followed by an air-voloxidation process in which the UO_2 pellet is converted and pulverised into U_3O_8 powder. The produced U_3O_8 powder is introduced into a LiCl molten salt bath for a conversion of the spent oxide powder to a metallic powder. During the electrochemical reduction process, the oxide powder is easily reduced into a metal form which normally contains most of the transition elements, all of the actinides and a certain fraction of rare earths. The metal mixture is then transferred to the electrorefining process with LiCl-KCl eutectic salt in order to recover the pure uranium on the solid cathode and to collect the mixture of actinide and some rare earth elements at the liquid cadmium cathode. The cathode deposits are recovered after the desired amount of material has been collected and then sent to a cathode processor. The eutectic salt occluded in the uranium deposits and the cadmium in the LCC-actinide mixture alloy is distilled by the cathode processors such as a cathode forming unit to produce an uranium ingot and a Cd distillation unit for recovery of a TRU alloy, respectively. The latter is sent to a fuel fabrication process to prepare it as a fuel for a transmutation of long-life radionuclides, whereas the former, the pure uranium can be stored as a low-level waste or recycled as a fresh fuel material, by blending it with an actinide mixture.

2.3.2. Unit process and material balance description

Chopping and decladding

- Function

The function of the chopping and decladding process provides a possible means to recover spent fuel materials from fuel rods. A high recovery ratio of fuel is required to reduce a loss of spent fuel material, which has a common target level of over 99% of a fuel recovery ratio. Several decladding techniques can be adopted. In the oxidative decladding process, the fuel expands and disintegrates into interfine powder, and separates it from the cladding tube.

- Process description

After pulling the fuel rods from the fuel assembly, cladding tubes are sheared axially and cut into several pieces with a length of about 10 inch. In the oxidative decladding process, after the fuel species are placed in a furnace and heated them, the fuel pellets are pulverised into powders through an oxidation from UO_2 to U_3O_8 at 500°C under an air atmosphere. During this oxidation step, volatile fission gases such as I, Kr, C-14 are evolved except for a complete removal of tritium. After oxidation, a separation step of the pulverised fuel and cladding is required. Separation of the fuel materials as fragment shapes from the cladding tube is also required.

- Material balance

The efficiency of the decladding process is determined by the recovery ratio of the spent fuel materials from the fuel rods. The recovery ratio of all the spent fuel elements is found to be 0.9999 based on the results of a DUPIC system operation, which can be obtained by measuring the fuel weights before and after this process, and confirmed from the residual uranium amount deposited on the cladding by a chemical analysis or non-destructive analysis. A very small amount of fissile material adhered to the inside of the cladding tube is nearly all removed during the course of a reactive rinsing with molten salt (refer to the section of “2.8 Metal Waste Treatment”).

High-temperature voloxidation

- Function

The objective of the advanced voloxidation process is to provide a means to recover fuel from the cladding, and to simplify the downstream processes by removing volatile and semi-volatile fission products prior to the following pyroprocessing. During this process carried out at an elevated temperature, a substantial amount of volatile and semi-volatile fission products are released from the spent fuel.

- Process description

Pulverised powder recovered from the decladding process is placed into a high-temperature voloxidizer. Operating parameters include the temperature, oxidant, oxidant flow rate and vibration, etc. An advanced voloxidation process to increase the removal ratio of volatile and semi-volatile fission products which possibly includes I, Cs, Tc, Ru, Te, Mo should be operated at 1 250°C for 10 hrs under an oxygen gas flow. Proper adsorbents and techniques to trap and recover the fission products evolved from the voloxidation process should be applied.

- Material balance

Removal efficiency of the target fission products depends on the voloxidation temperature and time. Assuming that the voloxidation temperature is 1 250°C under an oxygen atmosphere, volatile and semi-volatile fission products are removed within a level of Table 12.

Table 12: Removal rate of target fission products by voloxidation (%)

Voloxidation temperature	H-3	C-14	Kr-85	I-129	Cs	Tc	Ru	Rh	Te	Mo
1 250^{0}C	100	100	100	100	98	100	100	80	90	80

Electrolytic reduction

- Function

In an electrolytic reduction process which includes an oxide reduction and a cathode consolidation step, PWR spent fuel is electrochemically reduced to a metallic powder form, which is smelted into an ingot to be treated in the next process.

- Unit process description

The vol-oxidised oxide powder is charged into an integrated cathode with a MgO basket and converted to a metallic powder form by an electrochemical method in a LiCl-3 wt% Li_2O molten salt. The salt-soluble FPs such as a small amount of alkali and alkali earth elements with a high radioactivity are dissolved in the form of chloride and transferred from the integrated cathode containing the spent oxide fuel to a LiCl-L_2O molten salt during an oxide reduction step. U/TRU/RE/NM oxides are reduced electrochemically at the ceramic cathode basket to their metal forms, and oxygen gas is evolved at the anode. Accordingly, all the materials except for the alkali and alkali earth elements remain in the integrated cathode, whereas the alkali and alkali earth elements are transferred to the bulk of the molten salt as a chloride form. The reactions in the oxide reduction step are as follows:

At the cathode,

$$Li^+ \rightarrow Li + e^-$$

$$M_xO_y + 2yLi \rightarrow xM + yLi_2O$$

At the anode,

$$O^{2-} \rightarrow 1/2O_2 + 2e^-$$

The fuel reduced in the oxide reduction step is prepared as a metal ingot in the next step of a cathode consolidation, where the unreacted U/TRU/RE oxides are recycled for a further reaction.

- Material balance

The assumptions in the electrolytic reduction process for a material balance are as follows: reduction conversion and recovery yield in the oxide reduction step reach higher than 99.5%. In the cathode consolidation step, unreacted oxides are removed from the metal ingot and recycled in the oxide chlorination step to dissolve the TRU and rare earth oxides. The resulting uranium oxide is transferred to an electrolytic reduction step in order to reduce the uranium oxide to metal. The remaining salt containing TRU and rare earth chlorides is introduced to an electrowiner in order to recover TRU (refer to the section of "2.4 Electrorefining process"). During the cathode consolidation, the molten salt is fully recycled for an oxide reduction. Accordingly, no elements are lost during this process.

Uranium electrorefining

- Function

The electrorefining process separates the uranium from the metallic form which is a product of the reduction process of the PWR spent fuel. All the metallic elements are oxidised and dissolved into the salt solution at the anode, whereas more noble elements remain in the anode basket. At the solid cathode the uranium including the salt deposits simultaneously. The adhered salt in the recovered uranium deposit is distilled by the cathode process, and subsequently a pure uranium ingot is obtained.

- Process description

The electrolyte salt is a eutectic mixture of LiCl and KCl containing ~9 wt% of UCl_3. Pure uranium in the salt is deposited at the solid cathode. The transition metal fission products are unable to be oxidised and remain in the anode basket as metallic elements. The rare earth fission products and transuranic elements are not allowed to deposit at the solid cathode under a general electrorefining condition which is normally 0.5~1 V of a cell potential and 500°C of the temperature. The chlorides of the transuranic elements and the rare earth fission products are more stable than uranium chloride so that these elements cannot deposit at the solid cathode as long as the uranium concentration in the electrolyte salt is sufficient enough to preserve the following reaction.

$$UCl_3 + TRU(RE) \rightarrow U + TRU(RE)Cl_3$$

The adhered salt in the uranium deposit is normally removed by the cathode process under the condition of 1 300°C and ~0.2 Torr. Pure uranium ingot is subsequently obtained after a distillation of salt in the same cathode processor. Part of the pure uranium is transferred to the chlorination process in which the RE/TRU oxide dross generated from the cathode consolidation process reacts with the transferred uranium. The following reaction balances the amount of uranium for the chlorination of the RE/TRU dross:

$$RE_2O_3 + 2UCl_3 \rightarrow 2RECl_3 + UO + UO_2,$$

$$TRUO_2 + UCl_3 \rightarrow TRUCl_3 + UO_2$$

- Material balance

The inputs to the electrorefiner are mainly composed of the fuel and dross from the cathode consolidation process, rinsed elements of the clad hull and the initial loading of uranium as UCl_3. In the electrorefiner, most transition elements remain in the anode basket at ~99.7% of an uranium dissolution efficiency. This anode sludge is transferred to the metal waste processing step and returned back to the electrorefiner as UCl_3 (31.779 kgU). In the cathode process, 30% of the salt which is adhered to the uranium deposit is completely recycled to the electrorefining process. The amount of uranium for the chlorination of the RE/TRU dross depends on the quantity of the dross. Hence, part of the uranium product (179 kgU) is transferred to the RE/TRU chlorination process and most of the dissolved rare earth fission products (126.867 kg) are delivered to the electowinning process with TRU as a chloride form.

TRU Electrowinning

- Function

In the electrowinning process, TRU, uranium and small amounts of the rare earth fission products are recovered by the use of a liquid cadmium cathode (LCC) after electrorefining operation in the case of the treatment of the PWR spent oxide fuels. When the TRU is electrodeposited in the liquid cadmium cathode its chemical activities are reduced owing to a formation of intermetallic compounds such as $PuCd_6$. Accordingly, the TRU is co-deposited with some uranium and lanthanide elements in the LCC of the electrowinner. This electrowinning process also includes cadmium distillation and TRU drawdown steps in order to recover the TRU product from a cadmium-TRU alloy in a LCC and to convert it into an ingot and to completely recover the TRU elements from the LiCl-KCl salt, which is discharged from an electrowinner before the fission products are removed from the salt in the salt purification system.

- Process description

Molten salt electrowinning is an electrolysis process in which the material to be recovered is present as a metal halide compound in an electrolyte salt. The molten salt containing the dissolved spent fuel constituents is placed in an electrowinning cell, with a potential applied between the anode and cathode. At an appropriate decomposition potential, which depends on the species to be recovered, actinides can be deposited in the LCC.

TRU and rare earth fission products are accumulated in the electrolyte salt by increasing the number of batches operated in the electrorefiner. When the U/TRU ratio or the level of decay heat in the salt reaches the limiting value, deposition of uranium is completed and the salt is transferred to the electrowinner. The LCC in the electrowinner consists of a small amount of liquid cadmium contained in a ceramic crucible suspended in the electrolyte salt. At the LCC, TRU ions are reduced to their metallic forms by combining them with electrons and an alloying with Cd to form cadmium intermetallic compounds such as $PuCd_6$. In the liquid cadmium cathode, the Gibbs free energy for a formation of uranium, TRU and some rare earths chlorides are very close to each other. As a result, TRU cannot be selectively separated from the rare earths. A certain amount of the rare earths and uranium will be recovered together with TRU. Selective separation of plutonium in TRU is not possible as the standard potentials among the TRU are very close to each other in the liquid cadmium metal.

The cadmium-TRU alloys in a liquid cathode of the electrowinner are transferred to a cadmium distillation unit after a desirable amount (up to about 10 wt% of cadmium) of TRU material has been collected. The cadmium is distilled selectively from the cadmium-TRU alloys due to its lower melting point than other TRU metals. As a result, TRU, U and some of the rare earths are consolidated after distilling the cadmium. The cadmium metal is recovered for a recycling. The TRU, U and some of the rare earth metals are

converted into ingots for a transfer to the fuel fabrication system. The small amount of actinide metal (U and TRU) remaining in the salt used in the electrowinning process is treated by a drawdown step to remove it from the salt before being transferred to the salt purification process.

- Material balance

The material balance in the electrowinner is estimated by calculating the distributions of U, TRU and rare earths between the molten salt and cadmium phase based on an electrochemical equilibrium. The recovery yields of TRU and rare earths are about 98.3% and 1.1% in the LCC, respectively, while U is entirely recovered from the salt phase at a cathode potential of -1.6 V (vs. Ag/AgCl) in the electrowinning process. The salt including TRU and rare earths discharged from an electrowinner is injected into the drawdown unit, where TRU is recovered to be returned it to the electrorefining step and the TRU-free salt is transferred to the salt purification process. About 10% of rare earths in the salt are contained in the TRU stream to be recycled to the electrorefiner. Then fraction of TRU recovered from the total TRU contained in the spent fuel eventually reaches 0.9995.

Fuel fabrication

- Function

As a result of the pyroprocessing of the spent oxide fuels discharged from PWRs, TRU alloy products are obtained from the electrowinning process. The fuel fabrication process, which uses an injection casting method, produces the metallic fuel rods containing TRU (U-TRU-Zr-RE metal alloy) to transmute long-lived nuclides in the generation IV candidate SFR.

- Process description

The main equipment in the fuel fabrication process consists of the injection casting machine, the pin processor, and the assembly fabrication, etc. TRU alloys are sent to the fuel fabrication process to prepare fuel pins and assemblies for transmuting the long-life radionuclides. Uranium ingots recovered from an electrorefining step are blended with the TRU alloy in the injection casting step.

- Material balance

The metallic fuel contains U, TRU, Zr and rare earths. It is assumed that the ratio of U:TRU:Zr is 65:20:10 and the loading of the rare earths is less than 5%. To satisfy this fuel specification, recycled U and Zr are added to the TRU product.

Salt purification

- Function

For the reduction of the amount of waste generated from both an electrolytic reduction (LiCl) and an electrowinning (LiCl-KCl eutectic) process, the FPs involved in both waste salts such as Cs, Sr and rare-earth elements with a trace amount of TRU are separated from the waste salt by using a zeolite ion-exchange, a carbonation and a precipitation method, respectively. Pure salts recovered via the salt purification process are reused in the main pyroprocesses. The separated FPs are treated for the fabrication of the final waste form: a ceramic waste form (Cs case) and vitrified waste forms (Sr and RE/TRU cases).

- Process description

The waste LiCl salt from the electrolytic reduction process contains Sr and Cs. First, Sr is precipitated into the form of a carbonate ($SrCO_3$) by the addition of Li_2CO_3. Then $SrCO_3$ separated from the molten LiCl salt is converted into its oxide form (SrO) through thermal decomposition. Finally, SrO is fabricated to a vitrified waste form.

$SrCl_3+Li_2CO_3 \rightarrow SrCO_3+2LiCl$

$SrCO_3 \rightarrow SrO + CO_2(g)$

In the case of Cs, a substantial amount of Cs is released from the high-temperature voloxidation process, but a small amount of Cs still remains in the LiCl salt. By applying an ion-exchange process with an inorganic material such as zeolite, a small amount of Cs is removed from the waste LiCl salt and then fabricated to a ceramic waste form with the addition of a solidification agent (such as glass frit). After separating Cs and Sr from the waste salt, the cleaned LiCl is recycled to the electrolytic reduction process. Cs, which is released from the high-temperature voloxidation process, is captured by a fly-ash media and is then fabricated to a ceramic waste form.

The waste LiCl-KCl salt from the electrowinning process contains a considerable amount of rare-earth elements and a very small amount of TRU. Rare earth and TRU elements are precipitated into their oxide or oxychloride forms via a reaction with oxygen gas. When the precipitates are fully settled, the upper layer, which is mainly composed of a pure LiCl-KCl salt, is separated from the precipitate part containing the rare earth elements. The remaining salts in the precipitate phase, which is a mixture of the precipitates and eutectic salt residue, are separated and recovered from the precipitates by using a vacuum distillation/condensation method. Finally, the remaining rare-earth precipitates are converted into stable oxides by a simultaneous dechlorination and oxidation reaction.

$RECl_3+0.5O_2 \rightarrow REOCl+Cl_2(g)$ or $RECl_3+O_2 \rightarrow REO_2+1.5Cl_2(g)$

$REOCl+0.25O_2 \rightarrow 0.5RE_2O_3+0.5Cl_2(g)$

- Material balance

Over 99.6% of a conversion efficiency of $SrCl_2$ into a carbonate form was obtained at an operation condition of a $Li_2CO_3/SrCl_2$ molar ration of 3 or more. In the conditions of 650^0C of a molten salt temperature, 420 min of an oxygen sparging time, the conversion to a precipitate of the rare-earth elements exceeded 99.9%. The Sr elements in the waste LiCl salt are carbonated by adding 9 kg of Li_2CO_3 and then converted into 12.6 kg of SrO in a high-temperature condition, over 700^0C. A small amount of Cs is ion-exchanged by an inorganic material (zeolite), where the required amount of the zeolytic material is about 40 times that of Cs on a weight base. The inorganic materials containing Cs and some free salt residue are fabricated into a ceramic waste form by the addition of 51 kg of a solidification agent and 34.5 kg of a glass frit. The fly-ash media used for capturing Cs from the voloxidation process is mixed with a glass frit to produce another Cs-contained ceramic waste form.

About 139 kg of the rare-earth elements involved in the waste LiCl-KCl eutectic molten salts are precipitated by the reaction with oxygen gas and then finally converted into 162 kg of oxides (RE_2O_3). To fabricate vitrified waste forms, each stream of strontium oxides and rare earth oxides is mixed with the glass frit (4 times the total weight of each oxides stream). Eventually the total weight of the wastes requiring a final disposal, when treating 10 MTHM of oxide fuel, is 735 kg of the ceramic waste form and 875 kg of the vitrified waste form.

Metal waste treatment

- Function

Metal wastes are divided into two large groups; cladding hull and insoluble noble metal fission products from the electrorefiner. In this step, these materials are rinsed to get rid of the adhered fissile materials and melted to produce a corrosion-resistant metal alloy.

- Process description

The fissile materials remaining as a hull or insoluble noble metal are dissolved in a LiCl-KCl salt by using zirconium chloride as follows:

$$1.5ZrCl_4+RE_2O_3 \rightarrow 1.5ZrO_2+2RECl_3,\ ZrCl_4+UO_2 \rightarrow ZrO_2+UCl_4$$

The noble metal fission products containing a small amount of actinides left behind in the anode basket after the electrorefining process are also rinsed to remove the actinide elements by the aforementioned dissolution reaction.

The actinide and fission product chlorides are transferred to the electrorefiner and the residual metallic fission products are melted together with the cladding hull and an additional stainless steel to produce a corrosion-resistant metal alloy at a moderate temperature.

- Material balance

Cladding hull contains ~0.01% of the actinides and fission products after chopping and decladding. Also, anodic dissolution yield of the uranium is limited below ~99.7 % to retain the noble metal fission products (e.g. Rh, Te, Mo and Pd) at the anode basket as much as possible. So, anode sludge contains all the noble metal fission products and ~0.3% of uranium. In the partial dissolution and rinsing step, ~99% of the actinides and fission products are dissolved and return back to the electrorefiner. The recovered noble metal fission products and cladding hull are melted together with an additional stainless steel to decrease the casting temperature and to enhance the corrosion resistance. Accordingly, 10^{-4} % of the actinides remain in the metal waste.

Trapping of fission gases arising from voloxidation process

- Function

Trapping of the volatile and semi-volatile fission products released from the high-temperature voloxidiation process is necessary to safely operate the pyroprocess and to minimise the emission of the evolved fission products to the environment. Target fission products to be trapped are chosen based upon their radioactivity, environmental toxicity, and on the basis of the release rates of the volatile and semi-volatile fission products.

- Process description

The off-gas treatment system for trapping the volatile and semi-volatile fission products is designed based on the estimated amount of fission products evolving from the voloxidation process of the spent fuel. The unit process in the trapping system is arranged to effectively remove an individual fission product by considering the thermo-chemical properties of the target fission products to be trapped. Semi-volatile fission products such as Cs, Rh, Tc, Mo, Te have easy condensation properties on the process line if the temperature is below its melting point. These fission products are trapped in front of the off-gas trapping system near the exit of the voloxidizer. Fission products group I are Cs, Rh, which are trapped on a fly-ash filter at around 800°C, and group II of Tc, Mo, Te on an alumino-silicate adsorbent at about 600°C. Volatile fission gases of I, H-3 and C-14 are trapped in series on each trapping unit, and an emission of Kr-85 noble gas is controlled by using a decay tank.

- Material balance

Volatile and semi-volatile fission products in a gas stream are transferred to solid adsorbent phases. Trapping efficiency criteria for removing the target fission products may affect the amount of adsorbent waste generation from the off-gas trapping system. It is a general consideration that the decontamination factor of the whole trapping process should be established for a safe operation level and a maximum allowable emission concentration to the environment. Development of an innovative off-gas trapping system is required to minimise the waste amount of adsorbents.

2.3.3. Summary

The total weight of the final waste form generated when treating 10 MTHM from PWR spent oxide fuel (4.5 wt% ^{235}U enrichment, 45 000 MWD/MTU and 5-year cooling), except for the metal waste, is about 1 610 kg, i.e. 735 kg of the ceramic waste form (CWF) and 875 kg of the vitrified waste forms (VWF), which is about 16 wt.% of 10 MTHM. As described in Section 2.7, the VWF is divided into two groups, one for Sr (63 kg) and the other for RE and a trace amount of TRU (812 kg). The characteristics of each final waste form such as its weight, volume, specific decay heat and α-activity are summarised in Table 13.

Table 13: Characteristics of final waste

Waste form / Characteristic	LLW			HLW
	MWF[3]	CWF	VWF[3]	VWF[4]
Weight [kg]	3100	735	63	812
Volume [m^3][1]	0.41	0.32	0.03	0.33
Decay heat [W/m^3]	9.08×10^{-2}	1.97×10^{4}	3.63×10^{4}	7.78×10^{4}
α-activity [Bq/g][2]	1.53×10^{4}	0	0	4.58×10^{5}

[1] Density of waste forms: 7.6 (metal), 2.3 (ceramic), 2.5 (vitrified)

[2] Considered α-emitting nuclides: U and TRU

[3] VWF for Sr involved in waste LiCl salt

[4] VWF for RE and TRU involved in waste LiCl-KCl salt

If we consider the Korean criteria for the HLW category (over 2 000 W/m^3 of total heat generation and over 4 000 Bq/g of α-emitting nuclides), among the final waste forms produced from the pyroprocessing of spent oxide fuel, only the vitrified waste form for RE and a trace amount of TRU will be classified as an HLW category, which accounts for 8.1 wt% of 10 MTHM.

Figure 22: Flowsheet and mass balance for treatment of 10 MTHM of oxide fuel with 4.5 wt% ^{235}U, 45 000 MWD/MTU, 5-year cooling

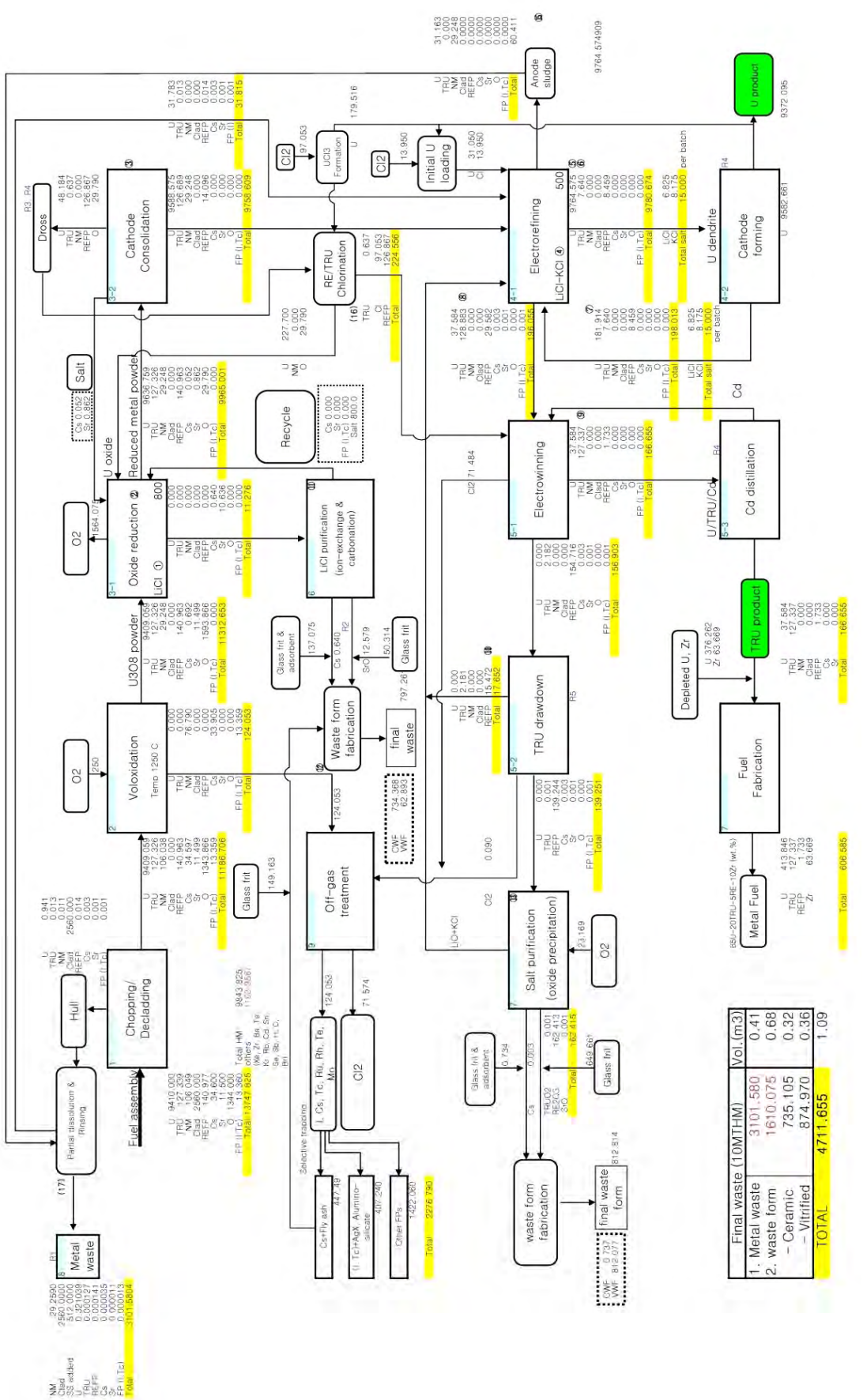

2.4. Direct electrochemical processing of metallic fuel

2.4.1. Introduction

Pyrochemical processing technologies are being developed and demonstrated at US Argonne National Laboratory for the treatment of spent nuclear fuel with the objective of recovering the actinides for recycle to advanced fast spectrum reactors and encapsulating the fission products in durable leach resistant waste forms suitable for decay storage or disposal in a high-level waste repository. Process development builds on the extensive experience gained from past fuel recovery programmes at Argonne such as the Integral Fast Reactor Programme (1), Electrometallurgical Treatment Programme (2) and numerous Experimental Breeder Reactor II fuel recycle demonstrations (3), (4). This report provides a conceptual flowsheet for the treatment of spent light-water reactor (LWR) fuel and spent fast reactor (FR) fuel and a theoretical material balance for each flowsheet that indicates the disposition of the actinides and fission products.

2.4.2. LWR Fuel

The conceptual flowsheet for the treatment of spent LWR fuel is shown in Figure 1. The flowsheet consists of a combination of electrochemical processes to achieve the desired oxide to metal conversion, and actinide and fission product separations. Products from the treatment process include uranium and a uranium - transuranic (TRU) alloy intended for recycle to an advanced FR, a ceramic waste material destined for decay storage (i.e. Cs/Sr product) and two high-level waste forms destined for geologic storage, lanthanide borosilicate glass and a metal alloy, which contains Tc and other noble metals. A brief description of each of the process steps needed for treatment of spent LWR fuel is provided.

Process descriptions

- Fuel chopping: Spent light-water reactor fuel assemblies are chopped by conventional methods to produce fuel segments approximately one to two inches in length. The fuel segments and ceramic fine materials produced during chopping are collected and transferred to the voloxidation process. Fuel assembly hardware (e.g. endplates) is transferred to metal waste processing.
- Voloxidation: LWR fuel is subjected to a low temperature, less than 500°C, oxidation process to release and recover tritium and noble gases present in the fuel matrix. Tritium can be collected as tritiated water and held in decay storage or sent to grout. Noble gases can be collected by distillation techniques and held in decay storage. Uranium dioxide present in the spent fuel is converted to U_3O_8 while the other actinide oxides are converted to their dioxide or sesquioxide form, whichever is the more stable oxide at the process conditions. The bulk of the noble metal fission products are oxidised to produce noble metal oxides. Alkali metal, alkaline earth and lanthanide oxides are unaffected in this process. Although the bulk of the oxides are effectively removed from the cladding by this process, residual oxide contamination remains on the cladding and must be removed prior to discharging the cladding as waste.
- Electrolytic reduction: The oxide material produced in the voloxidation process is converted to its metallic form by an electrolytic reduction process (5). The oxides, placed in a basket, function as the cathode of the electrochemical cell. An inert material such as platinum or a conductive ceramic functions as the oxygen-evolving anode. A LiCl – Li_2O molten salt held at 650°C serves as the electrolyte. As a potential is applied between the anode and cathode, electrons reduce the metal ion of the metal oxide to yield the base metal at the cathode. Oxide ions are released to the molten salt and transported to the anode where they are oxidised

to produce oxygen gas that is released from the cell. The half-reactions describing the process are as follows:

Cathode process: M_xO_y (s) + 2y e^- = x M (s) + y O^{2-}

Anode process: O^{2-} = ½ O_2 (g) + 2e^-

where M is the metal ion to be reduced. Actinide oxides and the bulk of the lanthanide oxides, except those that form extremely stable oxides such as Y_2O_3, are reduced to the base metal. Alkali and alkaline earth oxides react with lithium chloride to form chloride species that are soluble in the electrolyte salt. Noble metal oxides are converted to the base metal and remain in the basket with the actinide – lanthanide mixture. Iodine partitions adhered to the salt phase to form an alkali metal iodide. Oxidation products on the cladding material are converted to their metallic form by this process.

- Electrorefining: The metallic product from the electrolytic reduction process is transferred to the electrorefining process for uranium recovery. The metallic product, contained in a basket, serves as the anode in the electrorefining cell. A steel mandrel functions as the cathode. The electrolyte used in the cell is a LiCl-KCl eutectic salt containing approximately 6wt% UCl_3 at 500°C. As a potential is applied between the anode and cathode of the cell, uranium is anodically dissolved at the anode to produce uranium ions that are soluble in the electrolyte. The uranium ions are transported through the molten salt to the cathode where they are reduced to produce metallic uranium. The transuranic elements present in the feed material are oxidised and form transuranic chlorides that are soluble in the electrolyte. Lanthanides present in the feed behave similarly, also forming soluble chlorides. Noble metal fission products remain in the basket along with the cladding. Residual actinide and fission product metals contained in the cladding are electrochemically removed from the cladding during this process.
- Uranium processing: The dendritic uranium product from the electrorefiner may retain up to 15 wt% electrolyte salt, which contains transuranic and lanthanide chlorides which must be removed prior to uranium recycle. A distillation process, conducted at approximately 800°C, is used to recover the salt from the dendritic uranium. After salt removal, the uranium is consolidated to an ingot by heating the dendrites to 1 200°C. The consolidated uranium product can be used for advanced FR fuel fabrication or stored for future use.
- U/TRU recovery: The salt recovered in the uranium processing and metal waste processing (described below) operations is treated by an electrolysis process to recover the transuranic elements. In the electrolysis process, the uranium and transuranic chlorides present in the electrolyte salt are deposited at a solid cathode and chlorine gas is evolved at an inert anode (e.g. graphite). Process temperature is 500°C. Approximately 98-99 wt% of the actinides are electrowon from the salt phase during this process. Lanthanide contamination of the actinide product is calculated to be less than 10 ppm. The remaining actinide chlorides are recovered from the salt in the U/TRU drawdown process.
- U/TRU processing: Processing the U/TRU metallic product recovered in the electrolysis process consists of removing residual salt adhering to the metallic product by either low temperature distillation (T< 800°C) or phase separation of the liquid metal and molten salt. Ingots produced in this process are used in advanced FR fuel fabrication.
- U/TRU drawdown: The molten salt from the U/TRU recovery process and the U/TRU processing step is treated by another electrolysis process to recover the residual actinides. The electrolysis process results in the electrodeposition of the actinides, present in the molten salt as actinide chlorides, along with a small fraction of the lanthanides at a solid cathode. Chlorine gas is evolved at an inert anode. The actinide product, which is contaminated with lanthanides, is recycled to the uranium

electrorefining system. The LiCl-KCl eutectic salt with the bulk of the lanthanide chloride fission products is transferred to lanthanide waste form production.

- Lanthanide waste form production: Electrolysis is used to recover the lanthanide fission products from the LiCl-KCl eutectic salt discharged from the U/TRU drawdown process. The process yields a solid metallic lanthanide product at the cathode and chlorine gas at the anode. The LiCl-KCl salt discharged from this process is recycled to the electrorefiner. The recovered lanthanide metals are converted to oxides and subsequently combined with glass frit to form a lanthanide borosilicate glass, which is discharged as a high-level waste.
- Metal waste processing: Noble metal fission products and cladding recovered from the baskets used in the electrorefiner are treated by distillation to recover residual salt adhering to the materials. The salt is recycled to the U/TRU recovery process for actinide recovery. The noble metals are combined with cladding and hardware and melted to form an ingot. The ingot is discharged as a high-level waste. The remainder of the cladding material can be compacted and discharged along with the waste ingot.
- Cs / Sr waste form production: Cesium and strontium are recovered from the molten salt used in the electrolytic reduction process by zeolite ion exchange. The molten salt is contacted with zeolite to occlude the cesium and strontium chlorides. Iodine present in the molten salt as an alkali iodide is also contained in the zeolite-based waste form. The zeolite containing the cesium, strontium and iodine is mixed with glass frit and heated to produce a ceramic waste form. This waste form is held in decay storage prior to disposal. The bulk of the LiCl-Li_2O molten salt remains in the electrolytic reduction cell and is reused.

The technical maturity of the unit operations identified in the flowsheet varies from bench- to engineering-scale demonstrations. For example, electrorefining, uranium processing and metal waste processing have been demonstrated with spent nuclear fuel at the engineering-scale. Other processes such as electrolytic reduction have been demonstrated at the engineering-scale with simulant fuel and the bench-scale with irradiated LWR fuel. Yet other processes such as transuranic element recovery are being demonstrated, using Pu and Np, at the bench-scale.

Material balance

A theoretical material balance developed for the conceptual spent LWR fuel treatment process is given in Table 14. Feed material for the process was one tonne of five-year-cooled LWR fuel with a burn-up of 45 GWd/MTIHM. Actinide recovery factors were assumed to be 99.9% for U, Np, Pu, and Am, and 99.5% for Cm. A brief description of the characteristics of each of the products follows.

- Uranium product: The uranium product is used to fabricate advanced FR fuel or placed in storage for future use (e.g. re-enrichment). Transuranic element contamination of the uranium product is calculated to be less than 10 ppm.
- U/TRU product: The U/TRU product is used to fabricate advanced FR fuel. The composition of the U/TRU product is 30 wt% U – 70 wt% TRU to allow for blending with uranium to produce the desired FR fuel composition. Lanthanide contamination in the U/TRU product is calculated to be less than 10 ppm.
- Lanthanide glass: The lanthanide fission products are encapsulated in borosilicate glass and discharged as high-level waste. The calculations assume a 50 wt% loading of the lanthanides as oxides in the glass. Transuranic losses from the treatment process are encapsulated in the borosilicate glass.
- Metallic waste: Two types of metallic waste are produced in this flowsheet. One type comprises the noble metal fission products contaminated with uranium, which are alloyed with an equivalent amount of zircalloy cladding and steel hardware to form a

metallic waste form with a base composition of 85 wt% stainless steel – 15 wt% zirconium. This alloyed material is discharged as high-level waste. The other type consists of the remainder of the zircalloy cladding, which is compacted and discharged along with the metallic waste form.

- Cs / Sr waste: A 5 wt% loading was assumed for Cs in the zeolite material. Strontium and barium are also strongly occluded in the zeolite but were not considered to add to the amount of zeolite required for the waste form. Approximately 20 wt% LiCl was assumed to be contained in the zeolite. The zeolite with fission products and salt is mixed with glass frit, which was assumed to be 20 wt% of the zeolite, to make the final waste form. The ceramic waste form is held in decay storage prior to disposal.

Table 14: Theoretical material balance for spent LWR fuel

		LWR Spent fuel 45 GWd/MTIHM	Uranium product	U/TRU product	Lanthanide glass	Metallic waste	Cs/Sr waste	Gases
Actinides								
	U	940.80	934.74	5.12		0.94		
	Np	0.57		0.57	<0.01			
	Pu	11.19		11.18	0.01			
	Am	0.51		0.51	<0.01			
	Cm	0.03		0.03	<0.01			
Active metals								
	Cs	3.69					3.69	
	Sr	0.67					0.67	
	Ba	0.42					0.42	
Lanthanides								
	Ce	3.21			3.21			
	Eu	0.19			0.19			
	Gd	0.15			0.15			
	La	1.67			1.67			
	Nd	5.57			5.57			
	Pr	1.54			1.54			
	Pm	0.06			0.06			
	Sm	1.06			1.06			
	Y	0.64			0.64			

Table 14: Theoretical material balance for spent LWR fuel (continued)

		LWR Spent fuel 45 GWd/MTIHM	Uranium product	U/TRU product	Lanthanide glass	Metallic waste	Cs/Sr waste	Gases
Noble metals								
	Tc	1.07				1.07		
	Ag	0.09				0.09		
	Pd	1.67				1.67		
	Rh	0.60				0.60		
	Ru	2.96				2.96		
	Mo	4.60				4.60		
	Zr	2.93				2.93		
Gases								
	I	0.26					0.26	
	Xe	7.12						7.12
	Kr	0.25						0.25
Cladding		319.30				319.30		
Hardware		41.78				41.78		
Salt							14.76	
Glass frit					16.50		14.76	
Zeolite							73.80	
Total mass		1354.62	934.74	17.41	30.61	375.95	108.36	7.37
Balance		0.00						

Figure 23: Flowsheet of LWR spent fuel pyrochemical processing

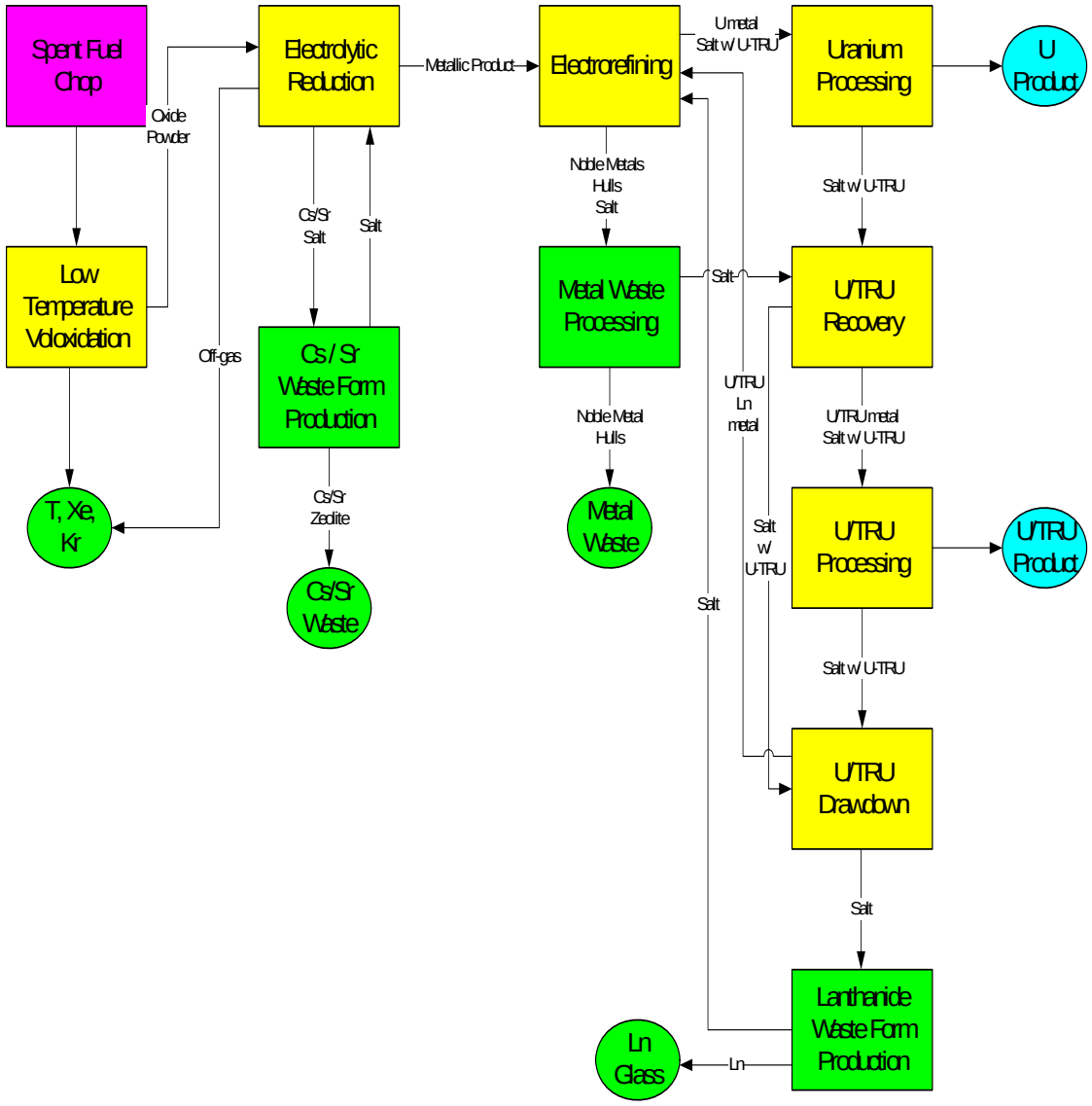

Figure 24: Flowsheet of FR spent fuel pyrochemical processing

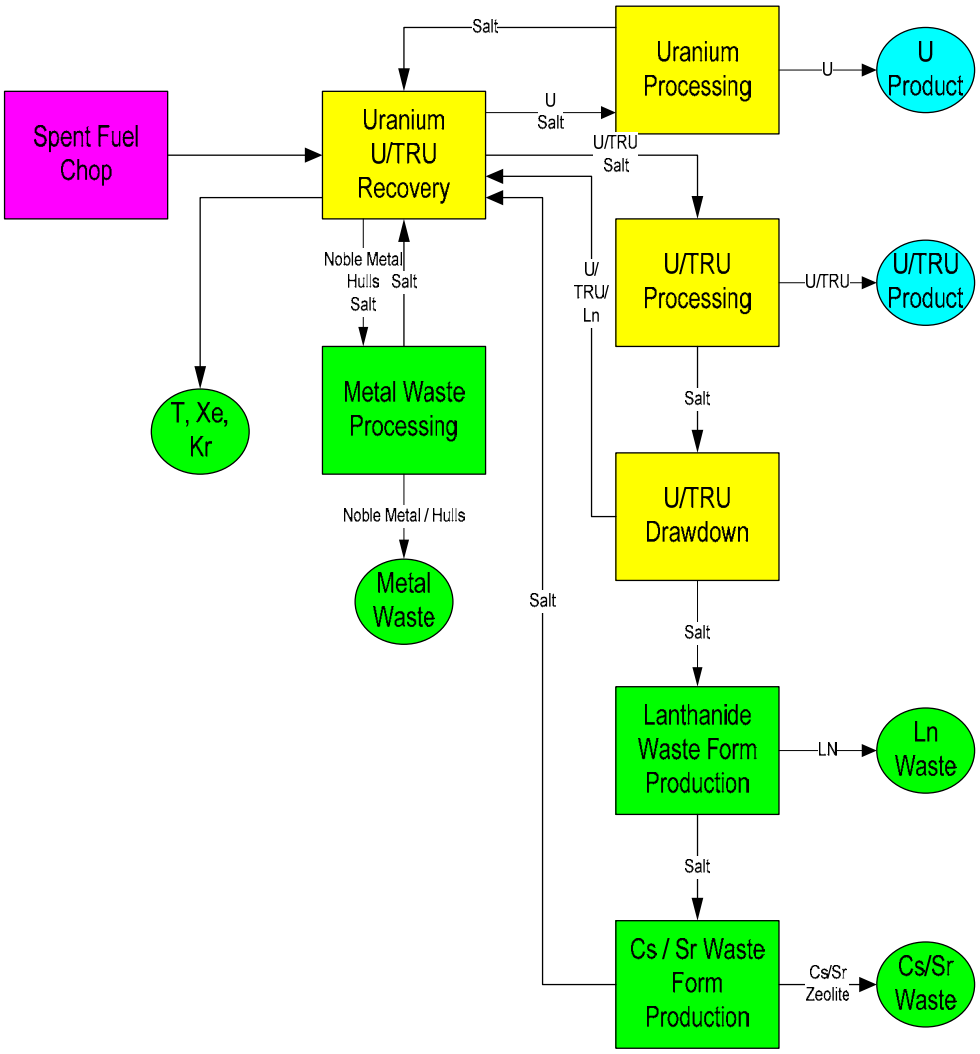

2.4.2. Metallic FR fuel

The conceptual flowsheet for the treatment of spent metallic fast reactor fuel is shown in Figure 24. The centerpiece of the flowsheet is the uranium electrorefining and U/TRU recovery process for separation of the actinides and fission products. Products from the treatment process include uranium and a uranium - transuranic alloy for recycle to advanced FR fuel fabrication, a ceramic waste material destined for decay storage (i.e. Cs/Sr product) and two high-level waste forms destined for geologic disposal, lanthanide borosilicate glass and a metal alloy, which contains Tc and other noble metals. A description of each of the spent FR fuel treatment processes and the products of those processes follows.

Process descriptions

- Fuel chopping: After removal of assembly hardware, FR fuel pins are chopped by conventional methods to produce fuel segments approximately one inch in length.

The fuel segments and metallic fines produced in the chopping process are collected and transferred to a basket, which serves as the anode in the electrorefining process. Fuel assembly hardware is transferred to the metal waste process. Noble gases released during the chopping process are collected in the off-gas system by distillation techniques and held in decay storage.

- Electrorefining: The metallic FR fuel and cladding from the chopping process is transferred to the electrorefining process for uranium recovery. The metallic fuel, contained in a basket, serves as the anode in the electrorefining cell. A steel mandrel functions as the cathode. The electrolyte used in the cell is a LiCl-KCl eutectic salt containing approximately 6 wt% UCl_3 at 500°C. As a potential is applied between the anode and cathode of the cell, uranium is anodically dissolved to produce uranium ions that are soluble in the electrolyte. The uranium ions are transported through the molten salt to the cathode where they are reduced to produce metallic uranium. The transuranic elements present in the feed are oxidised to form transuranic chlorides that are soluble in the electrolyte. Lanthanides, alkali metals including bond sodium and alkaline earth metals are also oxidised to form soluble chlorides that remain in the electrolyte salt. Noble metal fission products and cladding remain in the anode basket. Residual actinide and fission products embedded in the cladding are electrochemically removed from the cladding during this process. Noble gases remaining in the fuel matrix are released during the electrorefining process, collected in the off-gas system by distillation techniques and held in decay storage. Tritium released during the electrorefining process is captured in the off-gas system, converted to water and stored or sent to grout.
- Uranium processing: The dendritic uranium product from the electrorefiner may retain up to 15 wt% electrolyte salt, which includes the transuranic and lanthanide chlorides that must be removed prior to uranium recycle. A distillation process, conducted at approximately 800°C, is used to recover the salt from the dendritic uranium. After salt removal, the uranium is consolidated to an ingot by heating the dendrites to 1 200°C. The consolidated uranium product is used for advanced FR fuel fabrication. The salt is recycled to the electrorefiner.
- U/TRU recovery: Simultaneous with and in the same vessel as the recovery of uranium by electrorefining, an uranium – transuranic product is recovered from the electrolyte salt by electrolytic methods. The transuranic and uranium chlorides present in the electrolyte salt are deposited at a cathode using either an inert anode (e.g. graphite), which results in the chlorine gas production, or sacrificial anode. Process temperature is 500°C. Lanthanide contamination of the actinide product is calculated to be as low as 10 ppm.
- U/TRU processing: Processing the U/TRU metallic product recovered by electrolytic methods consists of removing residual salt adhering to the metallic product by either low-temperature distillation (T<800°C) or phase separation of the liquid metal and molten salt. Ingots of the U/TRU product are used in advanced FR fuel fabrication. The salt is treated in the U/TRU drawdown process.
- U/TRU drawdown: The molten salt collected from the U/TRU processing step is subjected to an electrolysis step to recover the actinides. The drawdown process (T=500°C) consists of electrodeposition of the actinides, present in the molten salt as actinide chlorides, along with a small fraction of the lanthanides at a solid cathode. Chlorine gas is evolved at an inert anode. The actinide product, which is contaminated with lanthanides, is recycled to the uranium electrorefining system. The LiCl-KCl eutectic salt that contains the fission products is transferred to lanthanide waste form production.
- Lanthanide waste form production: Electrolysis is used to recover the lanthanide fission products from the LiCl-KCl eutectic salt discharged from the U/TRU

drawdown process. The electrolysis process yields a solid metallic lanthanide product at the cathode and chlorine gas at the anode. The lanthanide metals are subsequently converted to oxides and combined with glass frit to form a lanthanide borosilicate glass, which is discharged as a high-level waste. The LiCl-KCl salt, which contains Cs and Sr, is transferred to Cs/Sr waste form production.

- Metal waste processing: Noble metal fission products and cladding recovered from the baskets in the electrorefiner are subjected to salt distillation process to recover residual salt adhering to the materials. The salt is recycled to the electrorefining process. The noble metals are combined with an equivalent amount of cladding (and hardware) and melted to form an ingot. The ingot is discharged as a high-level waste. The remainder of the cladding material can be compacted and discharged along with the waste ingot.
- Cs / Sr waste form production: Cesium and strontium are recovered from the molten salt after the lanthanide waste production process. The molten salt is contacted with a zeolite to occlude the cesium and strontium chlorides. Iodine present in the molten salt as an alkali iodide is also contained in the zeolite-based waste form. The zeolite containing the cesium, strontium and iodine is mixed with glass frit and heated to yield a ceramic waste form, which is held in decay storage prior to disposal. The bulk of the salt, including any residual Cs and Sr, is recycled to the electrorefining process.

As discussed in the section for LWR fuel treatment, technical maturity of the unit operations identified in the flowsheet varies from bench- to engineering-scale demonstrations. For example, electrorefining, uranium processing and metal waste processing have been demonstrated with spent nuclear fuel at the engineering-scale. Transuranic element recovery via electrolysis has been demonstrated, using Pu, at the bench-scale while several engineering-scale experiments have been completed for Pu recovery using a liquid cadmium cathode. Other operations such as U/TRU processing have not been demonstrated for this application but sufficient data exist to suggest process viability. Process validation tests as well as an integrated demonstration of the flowsheet are planned.

Material balance

A theoretical material balance developed for the conceptual spent FR fuel treatment process is shown in Table 15. Feed material for the process was one tonne of five-year-cooled metallic FR fuel with a burn-up of 93 GWd/MTIHM. Actinide recovery factors were assumed to be 99.9% for U, Np, Pu, and Am, and 99.5% for Cm. A brief description of the characteristics of each of the products is provided.

Table 15: Theoretical material balance for spent metallic FR fuel

		LWR Spent fuel 93 GWd/MTIHM	Uranium product	U/TRU product	Lanthanide glass	Metallic waste	Cs/Sr waste	Gases
Actinides								
	U	703.60	337.90	365.00		0.70		
	Np	2.41		2.41	<0.01			
	Pu	179.00		178.82	0.18			
	Am	11.90		11.89	0.01			
	Cm	3.34		3.34	<0.01			
Active metals								
	Cs	10.56					10.56	
	Sr	1.26					1.26	
	Ba	4.44					4.44	
Lanthanides								
	Ce	5.98			5.98			
	Eu	0.33			0.33			
	Gd	0.35			0.35			
	La	3.32			3.32			
	Nd	10.08			10.08			
	Pr	3.13			3.13			
	Pm	0.17			0.17			
	Sm	3.16			3.16			
	Y	0.71			0.71			
Noble metals								
	Tc	2.29				2.29		
	Ag	0.69				0.69		
	Pd	7.09				7.09		
	Rh	2.57				2.57		
	Ru	8.31				8.31		
	Mo	8.89				8.89		
	Zr	7.42				7.42		
Gases								
	I	1.02					1.02	
	Xe	12.94						12.94
	Kr	0.68						0.68
	Cladding	4739.00				4739.00		
	Zr	110.94				110.94		
	Salt						42.24	
	Glass frit				31.76		42.24	
	Zeolite						211.20	
Total mass		5845.58	337.90	561.45	59.19	4887.90	312.96	13.62
Balance		0.00						

- Uranium product: The uranium product is used to fabricate advanced FR fuel. Transuranic element contamination of the uranium product is of no consequence because the uranium is recycled to FR fuel fabrication.
- U/TRU product: The U/TRU product is used to fabricate advanced FR fuel. The U-TRU ratio in the product is 65 wt% U-35 wt% TRU to allow for blending with additional U during the fuel fabrication process to meet fuel specifications. Lanthanide contamination in the U/TRU product is calculated to be as low as 10 ppm.
- Lanthanide glass: The lanthanide fission products are encapsulated in borosilicate glass and discharged as high-level waste. The calculations assume a 50 wt% loading of the lanthanides as oxides in the glass. Transuranic losses from the treatment process are encapsulated in the borosilicate glass.
- Metallic waste: The metallic waste consists of two materials. In one material, the noble metal fission products contaminated with uranium are alloyed with an equivalent amount of cladding and hardware to form a metallic waste form with a base composition of 85 wt% stainless steel-15 wt% zirconium. This alloyed material is discharged as high-level waste. The remainder of the steel cladding (and hardware) is compacted and discharged along with the metallic waste form.
- Cs / Sr waste: A 5 wt% loading was assumed for Cs in the zeolite material. Strontium and barium are also strongly occluded in the zeolite but were not considered to significantly add to the amount of zeolite required for the waste form. Approximately 20 wt% LiCl salt was assumed to be contained in the zeolite. The zeolite with fission products and salt is mixed with glass frit, which was assumed to be 20 wt% of the zeolite, to make the final waste form. The ceramic waste form is held in decay storage prior to disposal.

References

[1] C.E. Till, Y.I. Chang and W.H. Hannum (1997), "The Integral Fast Reactor – An Overview", *Progress in Nuclear Energy*, 31, 1-2, 3.

[2] National Research Council (2000), "*Electrometallurgical Techniques for DOE spent Fuel Treatment: Final Report*", National Academy Press, Washington, DC.

[3] C.E. Stevenson (1987), "The EBR II Fuel Cycle Story", *American Nuclear Society*, LaGrange Park, IL USA.

[4] R.K. Steunenberg, R.D. Pierce and L. Burris (1969), "Pyrometallurgical and Pyrochemical Fuel Processing", *Progress in Nuclear Energy Series III*, Process Chemistry, 461.

[5] K. Gourishankar, L. Redey and M.Williamson (2002), "*Electrochemical Reduction of Metal Oxides in Molten Salts*", Light Metals 2002, TMS, 1075.

2.5. PyroGreen (reduce radiotoxicity to the level of low and intermediate level waste) (LILW)

2.5.1. Background

As of 2009, thirty one (31) countries have operated the world's 439 nuclear power plants equivalent to 372 GWe and 33 new nuclear power plants are under construction [1]. The share of nuclear energy in electricity generation is 23% in OECD countries and 16% in the world [2]. However, the past 50 years' operation of nuclear power plants has produced enormous amounts of spent nuclear fuels (SNF's). Because of their high radioactivity requiring unprecedentedly-long management periods, and the strong opposition of the general public, SNFs are becoming one of the most critical issues that must be overcome for the sustainable development of effective nuclear energy systems.

Some countries have unfavourable geological conditions for a deep geological repository. These countries used to meet difficulties regarding environmentally and publicly acceptable solutions for SNFs. Even for countries with geologically favourable sites, obtaining the societal support is hard because of the large uncertainty involved in the extraordinarily long time required for institutional controls. The Korean peninsula is geologically a very old terrain with an aggressive climate. Public opposition to the central SNF interim storage has been vigorous in the Republic of Korea whereas the permanent storage site for low-and intermediate-level waste (LILW) has been well accepted.

It is expected that all SNF storage pools in existing nuclear power plants in the Republic of Korea will be exhausted by 2016. The Korean government has decided to increase nuclear electricity from 36% today to 59% by 2030, in order to cope with energy insecurity and climate change. With the rapidly increasing demand for nuclear power, uranium price is expected to increase. Long outlooks for nuclear power suggest that the recycling of SNF's can be economically viable even by wet-separation and MOX fuel fabrication.

However, commercial reprocessing of SNF's by the wet-separation process has been stopped in the USA due to its capability to produce high purity plutonium. As a more proliferation-resistant alternative, modified wet-separation processes are being developed worldwide. While these advanced wet-separation processes have the potential for eliminating pure plutonium stream, their final wastes are high-level wastes with a total volume that is not significantly smaller than that of SNF's. For these reasons advanced wet-separation processes are not expected to solve SNF problems of countries with high population density in poor geological conditions.

The eutectic chloride-salt based pyroprocess, originally developed by Argonne National Laboratories of the USA has advantages in proliferation resistance, criticality safety, and compactness. KAERI has further improved the pyroprocess by employing voloxidation, electrolytic reduction and zone-freezing technology. KAERI plans to construct an engineering demonstration facility for the improved pyroprocess using surrogate materials by 2016. While the improved pyroprocess has potential advantages over wet-separation processes in the reduction of the waste volume, a significant amount of high-level waste is still expected. Therefore, the pyroprocess may not be able to convince the public to accept uncertainty with a long control period.

Since 1996, Seoul National University (SNU) has explored the concept of sustainable nuclear power based on the Proliferation-resistant, Environment-friendly, Accident-tolerant, Continual and Economical Reactor (PEACER). The environment-friendliness of the PEACER concept has been the driving force for the development of an advanced pyroprocess technology for the elimination of all SNFs from pressurised light-water reactor (PWR) and pressurised heavy water reactor (PHWR) to leave behind only low-and intermediate-level waste (LILW).

The flowsheet for the advanced Pyroprocess, designated as PyroGreen, has been evolved from KAERI's improved pyroprocess with special consideration to proliferation resistance, economy, and safety [3] and [4]. To ensure its proliferation resistance, PyroGreen is proposed to be built and operated by a multi-national consortium with due compliance with IAEA and related international protocols for safeguard and security assurances. Materials balances have been established by combining pyrochemical processes that have been developed and experimentally demonstrated either at KAERI or elsewhere. The multi-stage counter-current salt purification process employed in PyroGreen has been evaluated based on available experimental data on unit process by using a computational demonstration at the Nuclear Transmutation Research Center of Korea (NUTRECK) of SNU. The laboratory scale demonstration of PyroGreen has been postulated for 2020 as its high-quality salt purification processes require significant R&D efforts.

2.5.2. Objective

This chapter explains the flowsheet for PyroGreen that has been designed to satisfy conditions for converting all SNFs into low-and intermediate-level waste in a single stratum with fast reactor transmutation technology. The final wastes, stabilised in ceramic waste forms, are assumed to be disposed of in a geological repository with a depth and design that are adequate to eliminate the human intrusion event from risk-significant long-term scenarios. Because transuranic (TRU) elements have long half-life and high chemical reactivity, maximising the recovery of TRU elements from waste stream within the economical competitiveness of nuclear power option is the principal objective of the PyroGreen flowsheet [5].

Decontamination factor (DF) is defined for an isotope as the ratio of the total amount of the isotope in the input stream to that in the final waste stream, as follows [6]:

$$\text{DF for TRU elements} = \frac{\text{the amount of initial TRU in input stream}}{\text{the amount of final TRU in waste stream}}$$

The PyroGreen flowsheet is shown in Figure 26. It is assumed that initial SNFs are 10 MTHM (Metric Tonnes of Heavy Metal) of oxide fuel with the enrichment of initial 4.5 w/o, the burn-up of 45 000 MWD/MTU, and 5-year cooling. The previous study on PEACER showed that DF for TRU should reach up to 37 000 in order to meet Korean regulatory requirements for low-and intermediate-level waste [6]. Therefore, the PyroGreen flowsheet has been constructed to meet the target DF for TRU.

2.5.3. Methodology

The PyroGreen flowsheet utilises the KAERI's pyroprocessing flowsheet submitted to OECD/NEA in March 2007 as its backbone [7]. Several additional processes introduced by SNU serve mainly to increase DF for TRU. The proposed PyroGreen flowsheet adds three key processes to KAERI's flowsheet, as shown in Figure 25. The three new processes cover Zircaloy hull cleaning, salt waste purification and ceramic waste fabrication as well as the fabrication of Tc and I transmutation targets.

Figure 25: PyroGreen process consisting of existing KAERI's pyroprocess (highlighted) and three new processes (6, 7 and 8b)

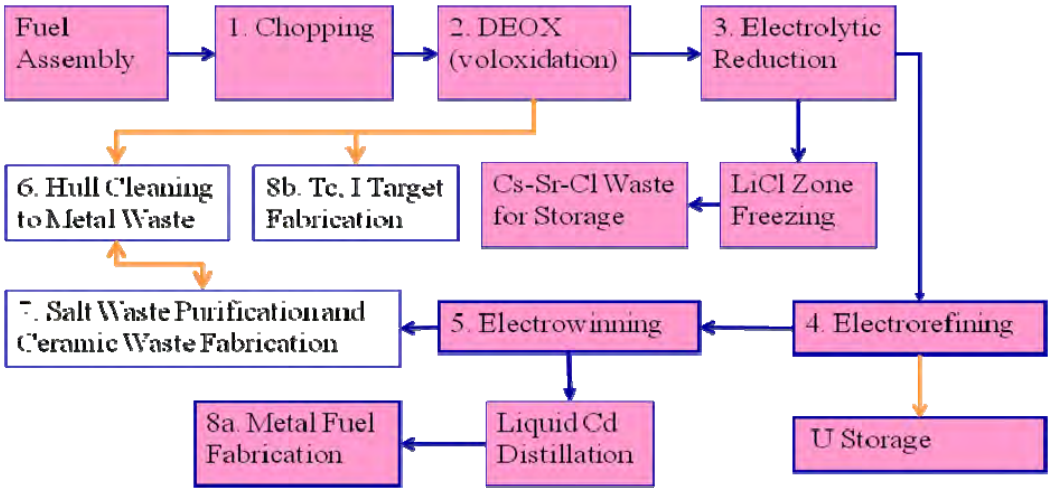

2.5.4. Description and mass balance of unit process in SNU's PyroGreen

SNU's PyroGreen flowsheet is composed of eight (8) important processes: chopping, DEOX, electrolytic reduction, electrorefining, electrowinning, salt purification, hull electrorefining, and fuel fabrication. The three additional processes in PyroGreen introduced at final steps in order to significantly reduce TRU elements lost into the final waste streams are hull electrorefining, salt purification, and Tc/I target fabrication. The salt purification process of PyroGreen involves eutectic LiCl-KCl salts and ternary LiCl-KCl-LiF. Salt purification processes introduced in PyroGreen utilise bismuth liquid metal as the medium for reductive extraction. Mass balance of processes was calculated by computational results and experimental data in KAERI.

Chopping

- Function and process description: SNF assembly is disintegrated to release fuel rods. Individual fuel rod is mechanically cut into short pieces as a favourable form in the rest of the processes [8].
- Mass balance: Although volatile fission products are produced during the chopping, it is assumed that steady-state operation allows for capturing all gaseous effluents.

DEOX

- Function and process description: DEOX is a combination of the words declad and oxidise, which was developed by collaborative research by KAERI and Idaho National Laboratory (INL) as a part of the International Nuclear Energy Research Initiative (INERI) project. DEOX is the step preceding electrolytic reduction. To enhance the efficiency of the electrochemical reaction during electrolytic reduction, the DEOX process oxidises spent oxide fuels into U_3O_8 and separates SNFs from the cladding [9]. DEOX can be described in terms of decladding and voloxidation. Decladding in the DEOX is carried out by using voloxidation, which involves volatilisation of volatile species in spent fuels and oxidation of uranium dioxide into U_3O_8 [10]. In the volatilisation process, most of Tc and some of the other noble metal (NM) as well as volatile species such as iodine was extracted as volatile fission products. Oxidation occurs in air at 1 200^{0}C [11]. U_3O_8 evolves in pulverised particles which improves reaction rate and conversion efficiency in the subsequent electrolytic reduction [8].

Figure 26: Flowsheet and mass balance of 10 MTHM of oxide fuel with 4.5 wt% ^{235}U, 45 000 MWD/MTU, 5-year cooling

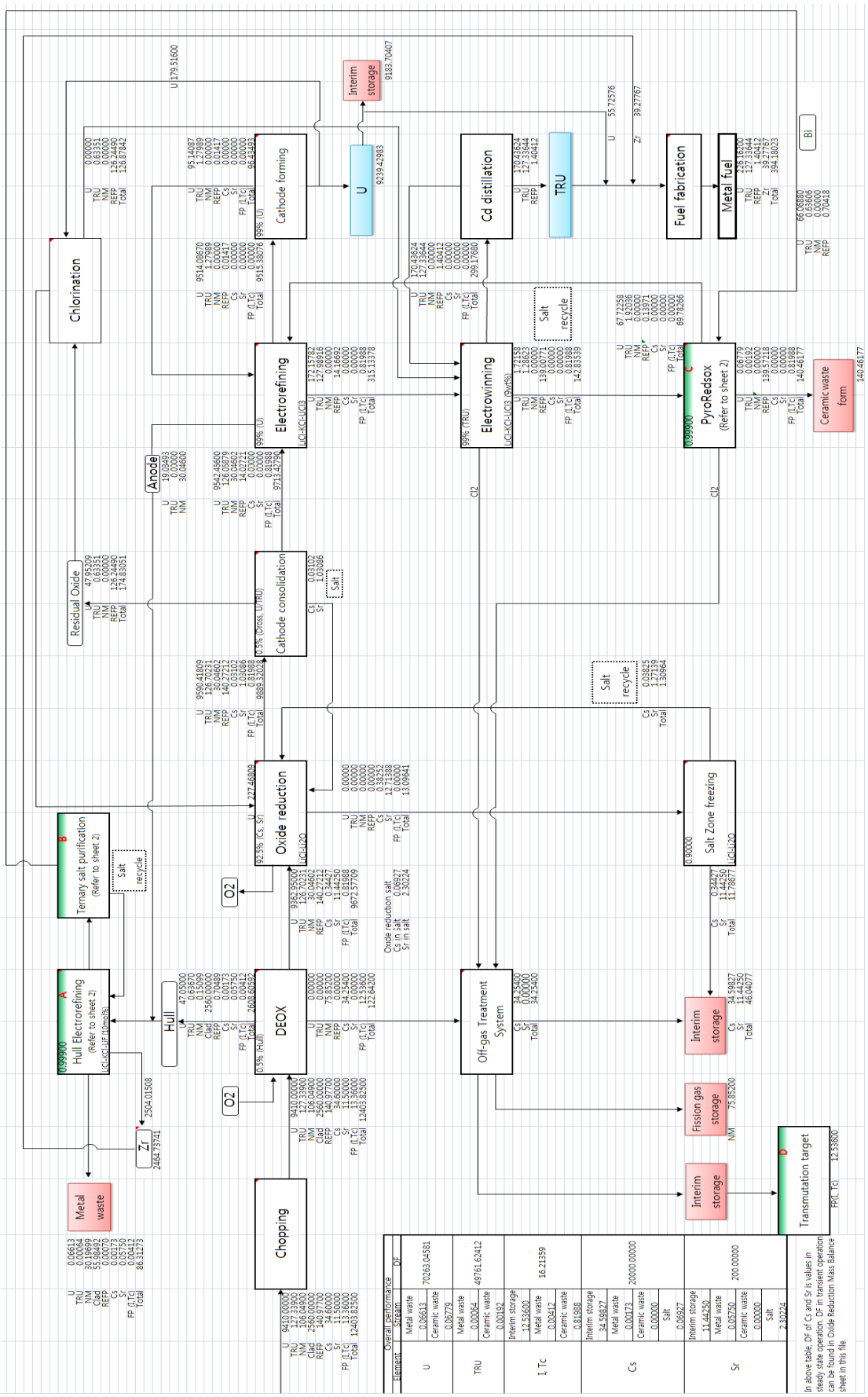

Figure 26: Flowsheet and mass balance of 10 MTHM of oxide fuel with 4.5 wt% ^{235}U, 45 000 MWD/MTU, 5-year cooling (continued)

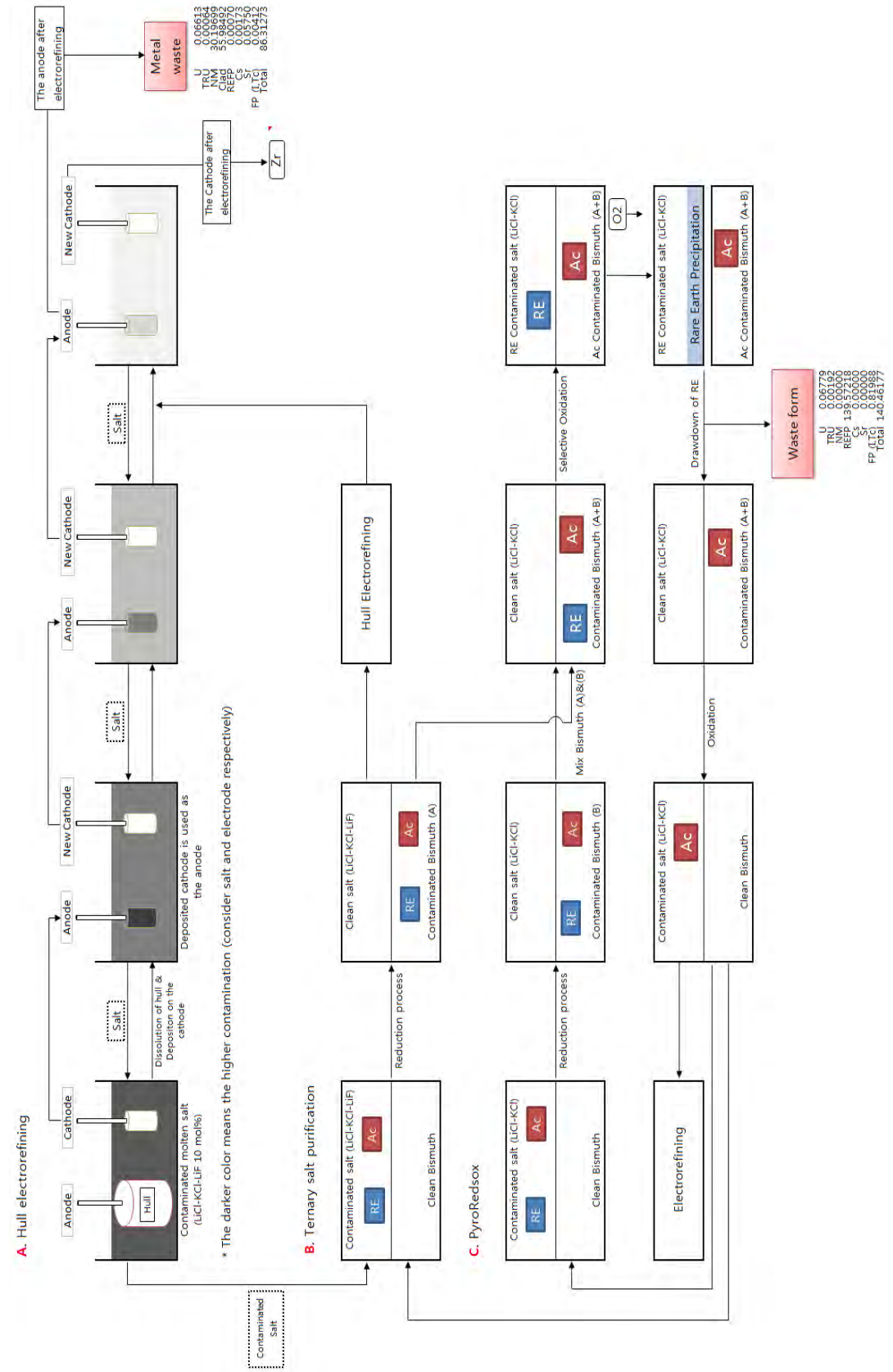

The volume increase of SNF during the oxidation reactions induces tensile stress to cladding rupture, leading to the separation between fuel and cladding. Off-gas treatment system (OTS) traps volatile fission products generated during the DEOX. The OTS is included in the DEOX furnace which composed of vertically separated 4 zones in KAERI's test runs. The bottom zone contains SNF and 3 other zones in the upper part trap fission products using a lot of filters. Each zone is operated at different temperatures and this temperature difference can separate fission products having different boiling points [12], [13]. Figure 27 (a) and (b), respectively, show KAERI's second generation DEOX furnace and the off-gas trapping system.

After the DEOX process, small amounts of fuels still remain in the cladding hulls rendering them to be classified as high-level waste (HLW). In PyroGreen the hull is electrorefined to sufficiently recover TRU from the waste stream. Hence, the cladding is transferred to hull electrorefining for the final cleaning treatment in ternary salt.

Figure 27: Apparatus for DEOX process developed by KAERI [12]

(a) Second generation DEOX Furnace

(b) Off-gas trapping system

- Mass balance: 0.5% of SNF remains in the cladding after the DEOX process. In the OTS, I, Tc, and noble metal are trapped. The removal efficiency of each fission product is shown in Table 16 [7], [14].

Table 16: Removal yield of OTS

Temperature	Removal yield (wt%)						
	Mo	Ru	Rh	Te	Cs	I	Tc
1 200^{0}C	80	99	80	90	99	100	99

71.53% of noble metal, 99% of Cs, and 99% of Tc in initial SNFs of the DEOX are filtered in the OTS. Cs is transferred to the interim storage and Tc and I are fabricated into transmutation target in the nuclear transmutation system to be turned into stable nuclides.

Electrolytic reduction

- Function and process description: For the electrorefining process, pulverised oxide fuel form is reduced into metal form. The oxide fuel is reduced in an electrolytic cell containing LiCl-Li2O (3 wt%) molten salt. The reaction formula is as follows [8]: the general principle of electrolytic reduction is described in Figure 28.

Cathode reaction

$$Li^{+} + e^{-} \rightarrow Li$$

$$M_xO_y + 2yLi \rightarrow xM + yLi_2O$$

where oxide (M_xO_y) includes actinide (Ac), noble metal (NM), and rare earth (RE).

Anode reaction

$$O^{2-} \rightarrow O_2 \uparrow + 2e^{-}$$

Figure 28: Schematic of electrolytic reduction process [8]

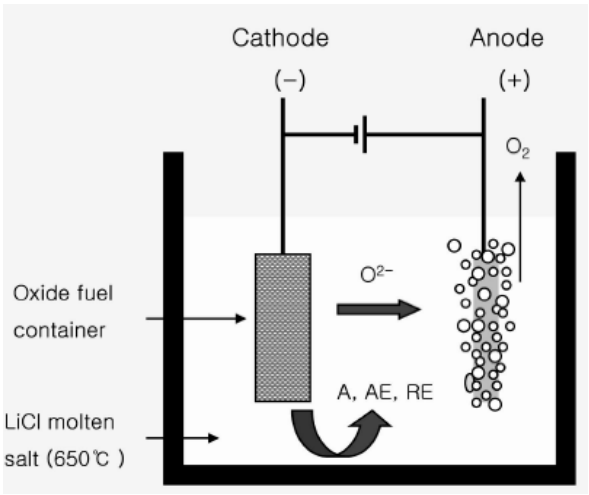

- Mass balance: Through the electrolytic reduction, 99.5% of oxides is reduced to metals and the remaining 0.5%, unreduced oxides, is transferred to the chlorination process for completed reduction after the cathode consolidation. About 92.5% of Cs and Sr introduced to the electrolytic reduction remain in the LiCl-Li_2O molten salt [7]. In the purification process, salt zone-freezing, of LiCl-Li_2O molten salt, 90% of Cs and Sr are removed. Then 10% of Cs and Sr are recycled with the molten salt to the oxide reduction process. In the equilibrium state, 92.5% of Cs and Sr are removed by the zone-refining and the remaining 7.5% is carried to the cathode consolidation. The target DF for Cs and Sr is reached within three stages of zone-refining. The purification method of LiCl-Li_2O molten salt is explained in Section 4.7.

Electrorefining

- Function and process description: Electrorefining is an electrochemical process to dissolve impure metallic uranium into molten salt and then selectively reduce purified metallic uranium using different electrode potential as shown in Figure 29. The uranium is dissolved from the anode basket containing small pieces of metallic fuel form to LiCl-KCl molten salt. Dissolved uranium is electro-transported, reduced and deposited on the cathode surface [15]. In order to deposit pure uranium on the cathode

surface, sufficient uranium ions should be initially present in the molten salt before the cell operation. Therefore, the electrorefiner uses LiCl-KCl-UCl_3 (~9 wt%) molten salt as a means to supply sufficient uranium ions [16]. Undissolved uranium and NM in the anode basket after electrorefining is transferred to hull electrorefining process of PyroGreen, where actinides with some rare earth elements are recovered and recycled.

Figure 29: Schematic of electrorefining process [8]

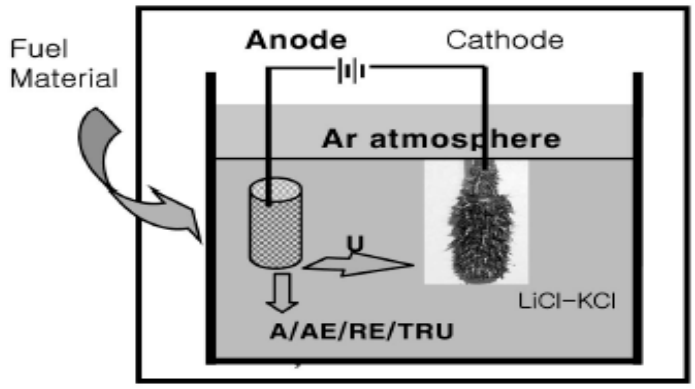

- Mass balance: In the electrorefining, about 99% of uranium is recovered with 1% of TRU and 0.1% of rare earth elements (RE). Deposited uranium on the cathode surface forms a dendrite structure which includes metal chloride and the molten salt at 20 ~ 40 wt% [8]. In order to recover pure uranium metal from the dendrite, a distillation method using the difference of vapour pressure is applied. Figure 30 shows the vacuum evaporation apparatus used in the distillation method. The experimental results showed that more than 99% of salt from the dendrite could be removed [17]. Removed molten salt is recycled to electrorefining. A portion of recovered uranium is transferred to the chlorination process to produce UCl_3. This UCl_3 reacts with the unconverted oxides in electrolytic reduction [7].

$$RE2O_3 + 2UCl3 \rightarrow 2RECl_3 + UO + UO_2$$

$$TRUO_2 + UCl_3 \rightarrow TRUCl_3 + UO_2$$

Product UO_2 from the above reactions is fed to the electrolytic reduction while RE and TRU are transferred to the electrowinning process.

Electrowinning

- Function and process description: Electrowinning is an electrochemical process to reduce dissolved uranium and TRU into liquid metal solvent. In contrast to electrorefining, electrowinning uses a liquid cadmium cathode which reduces the equilibrium potential difference among actinide elements. This diminished potential difference by the presence of Cd forces the simultaneous recovery of uranium and TRU [18], [19]. Hence, liquid Cd cathode plays as an intrinsic barrier to proliferation.
- Mass balance: Electrowinning recovers 99% of uranium and TRU with 1% of RE. Because uranium is in the liquid cadmium cathode, the metal mixture of uranium, TRU and RE can be recovered using the distillation of cadmium. According to experimental results, more than 99% of cadmium can be removed in a single stage [8].

Figure 30: Vacuum evaporation apparatus [17]

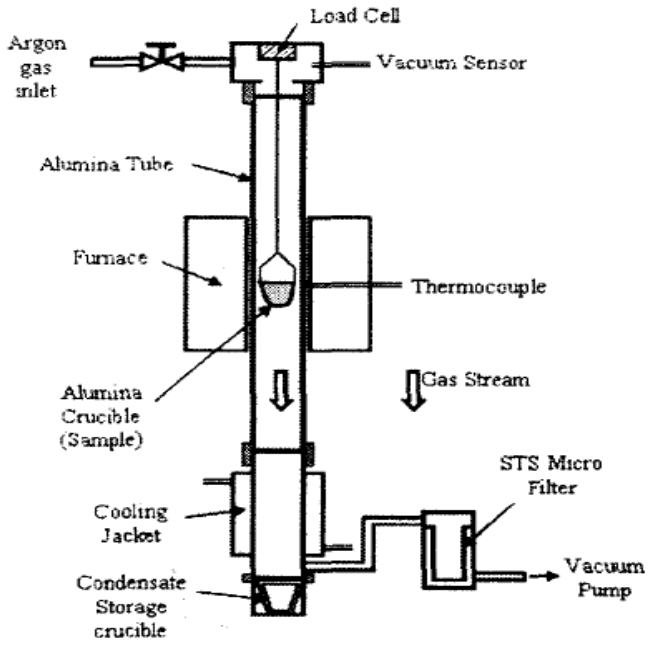

Hull electrorefining

- Function and process description: Cladding hull containing small amounts of U and TRU from DEOX as well as uranium and NM remained in the anode of electrorefiner is introduced to the hull electrorefining. The cladding of PWR made of Zircaloy-4 has the following composition: Zr 97.911%, Sn 1.6%, Fe 0.225%, Cr 0.125%, Ni 0.002% [20]. Zircaloy-4 hull with fuel residue at the inner surface falls in to the high-level waste category if directly disposed of. The multi-stage hull electrorefining is employed to recover zirconium, U and TRU from the waste stream and the recovered actinides are recycled back to the main process stream. According to literature results, the multi-stage Zircaloy hull electrorefining can yield a very high decontamination factor to clear produced Zr from radioactive material [21], [22].

Hull electrorefining uses LiCl-KCl-LiF (10 wt%) molten salt. Using only chloride molten salt produces sub-halide, which decreases the dissolution speed of zirconium into the molten salt. On the other hand, fluoride molten salt generates solidified fluorides on the deposition. In order to remove these solidified fluorides, a complicated chemical treatment is required and this treatment increases waste volume. Therefore, to overcome these difficulties, the ternary mixture of chloride and fluoride molten salt is used in hull electrorefining [21].

A counter-current multi-stage electrorefining process has been employed. Zircaloy hull in the anode basket is dissolved into the molten salt and deposited on the solid cathode. The used cathode in the previous step is employed as an anode in the next step with the new cathode [21]. With this change, molten salt also flows from the final electrorefiner to the first electrorefiner, accompanying the increases in the contamination level in the salt. This method is derived from the multi-stage counter-current reductive extraction developed by the Argonne National Laboratory (ANL) [23]. Most contaminated molten salt and the anode basket meet in the first step while the cleanest molten salt and the anode are in the last step. Details of this multi-stage counter-current electrorefining process are shown in Figure 31, where the higher contamination level is indicated by the darker colour of the salt. In order to reach the radiation clearance level for Zr, 4 electrorefining stages are required.

Figure 31: Schematic of multi-stage counter-current hull electrorefining

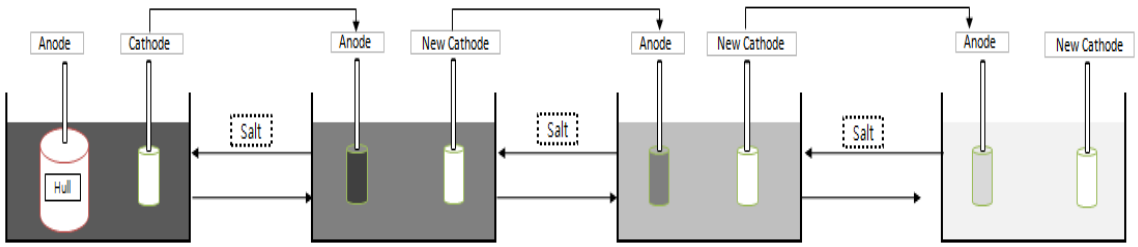

In each step, undissolved materials remain in the anode basket. These materials are combined with the anode of the next electrorefiner. In the final step, sufficiently pure zirconium is produced on the cathode surface. The undissolved materials in the anode basket of the final step are processed as a final ceramic waste form.

- Mass balance: It is assumed that 99.9% of zirconium is recovered out of zircaloy that has 97.911% of Zr. Hence 97.81% of initial zircaloy is finally recovered as pure zirconium and cleared from radioactive material. Figure 32 shows that the finally produced Zr from 4 stage electrorefining can reach the clearance level.

Figure 32: The results of hull electrorefining tests [21]

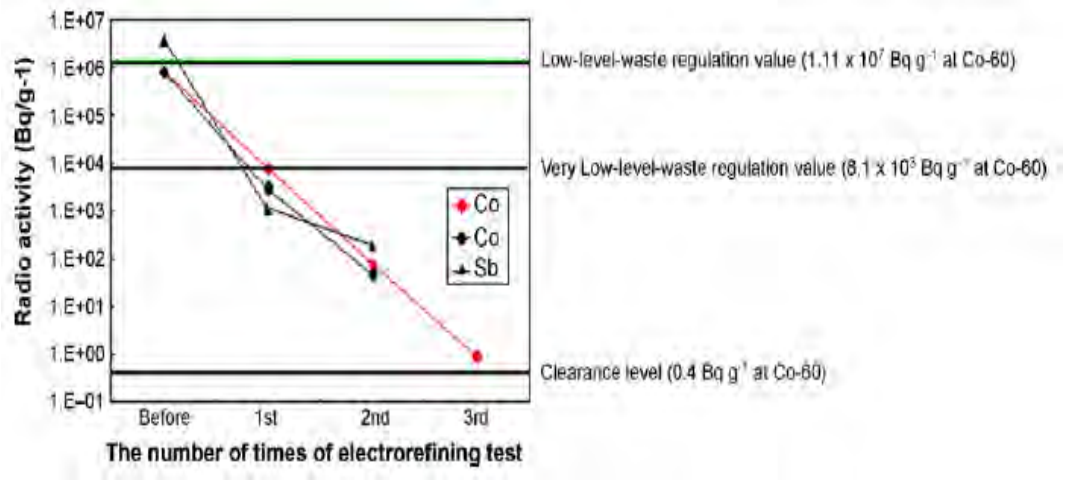

Salt purification

- Zone freezing: About 92.5% of Cs and Sr in the electrolytic reduction remain in the LiCl-Li2O molten salt. Continuous accumulation of Cs and Sr in molten salt causes the uncontrolled melting point of the salt and this molten salt should be regularly replaced with clean salt [24]. To avoid the frequent replacement of the salt and reduce total salt waste volume, zone-freezing has been developed by KAERI. The zone-refining process separates a significant fraction of Cs and Sr from the molten salt. Figure 33 shows the zone-freezing apparatus. According to literature results, 90% of Cs and Sr can be recovered from the molten salt to interim storage and the remaining 10% remain in the salt [25]. The separated Cs and Sr is stored in interim storage with trapped Cs in the OTS in the DEOX for about 200 years before the final disposal as LILW. The feasibility of utilising Cs for an industrial radiation source and Sr for long-life batteries is currently investigated.

Figure 33: Zone freezing apparatus [25]

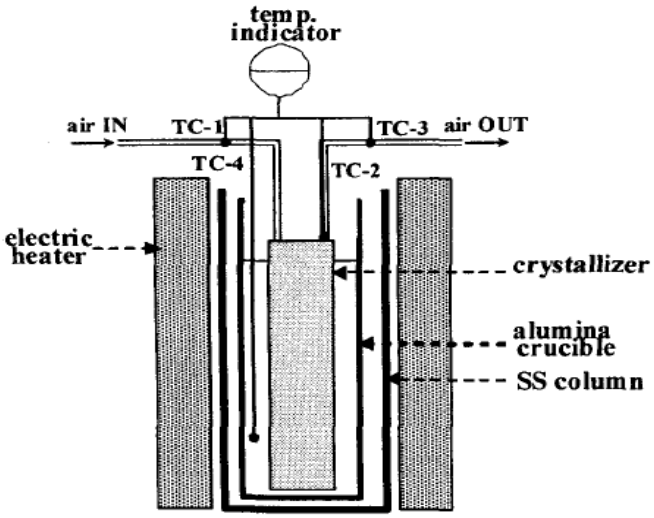

- Ternary salt purification: Ternary salt purification is a process to purify contaminated LiCl-KCl-LiF molten salt generated from hull electrorefining. Cleaned molten salt is recycled for the subsequent hull electrorefining. Actinides and RE in contaminated LiCl-KCl-LiF molten salt are reduced into clean bismuth liquid metal cathode. The ternary salt purification process is shown in Figure 34.

Figure 34: Ternary salt purification

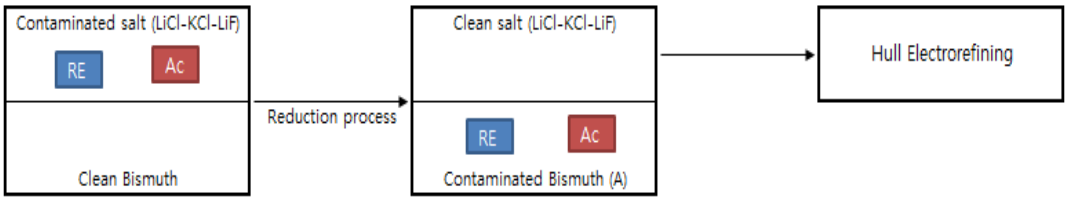

- PyroRedsox: In PyroGreen a new process named PyroRedsox is introduced by combining reductive extraction and selective oxidation. Reductive extraction separates different elements by using the different distribution tendencies of each element between the contacted two solvents [18]. In this process, the contacted two solvents are bismuth liquid metal and LiCl-KCl molten salt.

The purification targets of PyroRedsox include the contaminated bismuth from the ternary salt purification and the contaminated molten salts from electrorefining and electrowinning. PyroRedsox uses bismuth instead of cadmium as liquid metal solvent in order to obtain high separation efficiency between rare earth elements (RE) and actinides [26].

The detailed unit process is described in Figure 35. Molten salt from electrorefining and electrowinning is contacted with bismuth liquid metal. RE and actinides are reduced to metals in liquid bismuth. The contaminated bismuth from the ternary salt purification process is added to this contaminated bismuth. RE in bismuth is selectively oxidised to molten salt while actinides are retained. Molten salt containing selectively-oxidised RE can be subjected to oxygen gas flow to precipitate RE in the form of precipitated solid oxides.

Because of the difficulty of complete separation between actinides and RE, actinides retained in the bismuth are oxidised to the molten salt and this molten salt is recycled back to the electrorefining process. About 99.9% of uranium and TRU and 0.1% of RE are recovered into the molten salt. Cleaned bismuth is then transferred to ternary salt purification and PyroRedsox. As a final waste stream, precipitated RE is stabilised in the ceramic waste form that includes a small amount of actinides.

Figure 35: PyroRedsox flowsheet

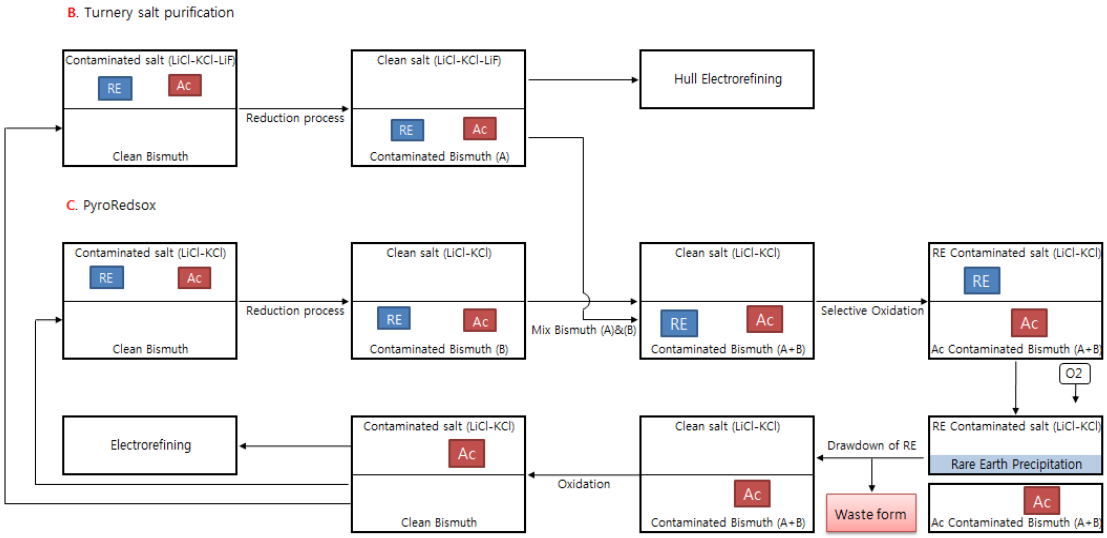

Fuel fabrication

- Function and process description: In the same approach as KAERI's Pyroprocess, recovered uranium and TRU are used for the fabrication of metallic fuel in the fast reactor which can transmute and eliminate long-living radioactive isotopes. The metallic fuel composition of the lead-bismuth-cooled PEACER (Proliferation-resistant, Environment-friendly, Accident-tolerant, Continual and Economical Reactor) has been employed in PyroGreen flowsheet.
- Mass balance: Fuel composition of PEACER is 57.6% of uranium, 32.4% of TRU and 10% of zirconium [27]. In the fuel fabrication, the recovered zirconium of the hull electrorefining and the uranium extracted by the electrorefining are used.

Tc and I target fabrication

- Tc and I target description: The transmutation reactor, PEACER, has its reactor core design with peripheral target regions for stabilising Tc and I in the epi-thermal neutron spectrum. The epi-thermal spectrum is established by the introduction of the calcium hydride block contained in a monolithic target assembly. The Tc target consists of Tc-Cr alloy rods in the form of Tc_6Zr [28]. The iodine target consists of calcium iodide powders in the form CaI_2 contained in a stainless steel tube.
- Tc and I target fabrication: Tc-Zr alloy rods can be fabricated by powder mixing and vacuum arc-melting followed by casting. Calcium iodide powder can be produced by the existing commercial process.

2.5.5. Conclusion

SNU's PyroGreen flowsheet is composed of 8 unit processes in order to meet the LILW requirements on DF for important radioactive elements. KAERI's improved Pyroprocess has been used as the backbone of PyroGreen. Overall DF of important nuclides is presented in Table 17. Overall DF for TRU and U reaches about 50 000 and 70 000, respectively. Purified Zr from the cladding hull can be cleared from radioactive material control. Therefore the volume of final low-and intermediate-level waste can be significantly reduced from that of initial spent nuclear fuels.

Table 17: Overall DF[11] in PyroGreen flowsheet

Overall performance			
Element	Stream (Kg)		DF
U	Metal waste	0.06613	70 263
	Ceramic waste	0.06779	
TRU	Metal waste	0.00064	49 761
	Ceramic waste	0.00192	
I and Tc	Interim storage	12.53600	16
	Metal waste	0.00412	
	Ceramic waste	0.81988	
Cs	Interim storage	34.59827	20 000
	Metal waste	0.00173	
	Ceramic waste	0.00000	
	Saturated in salt	0.06927	
Sr	Interim storage	11.44250	200
	Metal waste	0.05750	
	Ceramic waste	0.0000	
	Saturated in salt	2.30224	

11 In Table 2, DF of Cs and Sr are values in steady-state operation. DF of initial transient operation is found in the last table of this document.

References

[1] International Atomic Energy Agency (2007), *Nuclear Technology Review* 2007, Vienna.

[2] OECD/NEA (2008), Nuclear Energy Outlook 2008 - Executive Summary, Paris.

[3] M. S. Yang, K. C. Song, S. W. Park (2007), DUPIC and other advanced fuel cycle options in Korea, *Journal of Nuclear Materials*.

[4] Ministry of Education (2008), Science, and Technology of the Republic of Korea, Atomic Energy White Paper 2008, p. 60.

[5] W. S. Park, H. S. Shin, and T. Y. Song (1996), Transmutation Capability Evaluation for the Transmutation Systems, KAERI/TR-632/96, p. 1.

[6] S. I. Kim, K. J. Lee (2007), Requirement of decontamination factor for near-surface disposal of PEACER wastes, *Progress in Nuclear Energy*, vol. 49, pp. 14-19.

[7] E. H. Kim (2007), Flowsheet Study for A Pyroprocess of An Oxide to A Metal, KAERI.

[8] J. H. Yoo, C. S. Seo, E. H. Kim, H. S. Lee (2008), A Conceptual Study of Pyroprocessing for Recovering Actinides from Spent Oxide Fuels, *Nuclear Engineering and Technology*, Vol. 40, No. 7.

[9] K. J. Lee, Y. J. Shin (1989), *Nuclear Chemical Engineering*, Korea Nuclear Society.

[10] B. H. Park, C. S. Seo (2008), A semi-empirical model for the air oxidation kinetics of UO_2, *Korean J. Chem. Eng.* 25(1), 59-63.

[11] Ministry of Knowledge and Economy of the Republic of Korea (2006), NUTRECK final report for the first stage.

[12] D. L. Wahlquist, K. J. Bateman, B. R. Westphal (2008), Second Generation Experimental Equipment Design to Support Voloxidation Testing at INL, ICONE 16, Florida, USA, 11-15 May 2008.

[13] B. R. Westphal, J. J. Park, J. M. Shin *et al.* (2008), Selective Trapping of Volatile Fission Products with an Off-Gas Treatment System, Separation Science and Technology, 43: 2695-2708.

[14] Korea Atomic Energy Research Institute (2007), Development of Voloxidation Process for Treatment of LWR Spent Fuel, KAERI/RR-2840/2006.

[15] S. X. Li (2002), Anodic Process of Electrorefining Spent Nuclear Fuel in Molten LiCl-KCl-UCl3/Cd System, the 201st Meeting of Electrochemical Society/ *13th International Symposium on Molten Salts,* PA, USA, 12-27 May 2002.

[16] H. S. Kang, M. S. Woo, H. S. Lee (2008), Production of LiCl-KCl-UCl_3 using Cd and Cl_2 reaction, Korean Radioactive Waste Society Spring.

[17] D. W. Jo, S. B. Park, C. H. Cho (2008), Study on the Salt Distillation Process of U Deposition, Korean Radioactive Waste Society Spring.

[18] J. D. Bae (2006), A Computational Analysis of Pyrochemical Processing for Nuclear Transmutation, Master Thesis of Seoul National University, p. 6.

[19] T. Nishimura *et al.* (1998), Development of An Environmentally Benign Reprocessing Technology-Pyrometallurgical Reprocessing technology, *Progress in Nuclear Energy*, Vo. 32, No. 34, pp. 381-387.

[20] W. D. Bond, J. C. Mailen, G. E. Michaels (1992), Evaluation of Methods for Decladding LWR Fuel for a Pyroprocessing-Based Reprocessing Plant, ORNL/TM-12104.

[21] T. Goto, T. Nohira, R. Hagiwara *et al.* (2008), Selected topics of molten fluorides in the field of nuclear engineering, *Journal of Fluorine Chemistry*.

[22] R. Fujita, H. Nakamura, K. Mizuguchi *et al.* Development of a Pyrochemical Process in Molten Salts for Treating Radioactive Waste from Nuclear Fuel Cycle Facilities.

[23] T. Kobayashi (2006), An Assessment of the Multi-stage Counter Current Extraction of TRUs from Spent Molten Salt into Liquid Metal, *Journal of Nuclear Science and Techonology,* Vol. 43, No. 7, pp. 819-823.

[24] K. H. Oh, J. H. Lee, H. S. Lee (2008), Separation of CsCl and $SrCl_2$ in LiCl-CsCl-$SrCl_2$ Mixture Using Crystallization Methodology, Korean Radioactive Waste Society Fall, pp. 221-222.

[25] S. G. Byeon, Y. J. Cho, H. S. Lee (2008), Separation of Group 1 and 2 in Periodic Table Elements Using Melting Crystallization Methodology, *Korean Radioactive Waste Society Fall,* pp. 166-167.

[26] K. Kinoshita, T. Inoue, S. P. Fusselman *et al.* (1999), Separation of Uranium and Transuranic Elements from Rare Earth Elements by Means of Multistage Extraction in LiCl-KCl/Bi System, *Journal of Nuclear Science and Technology*, Vol. 36, No. 2, pp. 189-197.

[27] J. Y. Lim and M. H. Kim (2007), New LFR design concept for effective TRU transmutation, *Progress in Nuclear Energy*, Volume 49, Issue 3, 230-24.

Chapter 3: Fluoride volatility process

3.1. Fluoride volatility process

3.1.1. Introduction

The insensitiveness of the fluoride volatility process to radiation gives an opportunity to reprocess SNF with any short cooling period, which is especially important for the fast breeders NFC [1], [2]. The most notable feature of the process is the exceptional selectivity in separating uranium and plutonium from fission products. Hexafluorides of uranium and plutonium (as well Np, Mo, W and some others) have unique physical and chemical properties – low melting temperatures (under pressure) and boiling (sublimation) from solid state. Main physical-chemical properties for fluorides of some actinides and fission products are given in Table 18. The saturated vapour pressures of uranium and plutonium hexafluorides are equal to that of the atmosphere at 56.4 and 62.3^{0}C respectively, while fluorides of fission products belonging to groups 1-4 of the periodic system are non-volatile at these temperatures and those belonging to groups 6 and 7 are low-volatile. Uranium and plutonium hexafluorides separated from fission products can be easily transformed to either metal or dioxide. The radioactive waste consisting of the fluorides of fission products are produced straightly in the very compact form.

3.1.2. Current status

The development of the fluoride volatility process (FVP) was initiated in Russia in the early 1950s by the RRC-Kurchatov Institute and VNIIkHT (Moscow). Both institutes possessed powerful equipment for the production of elemental fluorine and developed the processes for the production of uranium hexafluoride, initially for the purposes of uranium isotopic enrichment. Later RIAR (Dimitrovgrad) was involved in the R&D and the experimental installation FREGAT for the fluoride volatility reprocessing of SNF from fast BOR-60 reactor had been designed and constructed in the hot cells at RIAR in the early 1960s.

Though the physical and chemical principles of the process are simple, there are technical problems connected with the properties of fluorine, such as its exceptional chemical reactivity and the high thermal output of the fluorination reactions. In spite of the fact that the industrial production of uranium hexafluoride was mastered long ago, to optimise the process of spent fuel fluorination extensive R&D was required to achieve efficient heat removal at sufficiently small (criticality safe) sizes, and adequate filtration of the gaseous flow at the outlet of the apparatus.

The problem of control over U_3O_8 fluorination in the fluidised bed was studied at the Kurchatov Institute [3]. The throughput reached by the experimental fluorinator with a diameter of 100 mm comprised 790 kg of uranium/hr per square meter of the fluorination zone cross-section. The process conditions under which the fluidised bed does not take were calculated and experimentally confirmed. Elutriation of U_3O_8 fines from the fluid bed was compensated by using a high-efficiency filter bed formed of the same material as the fluid bed and returning the filter bed down in the reaction zone. A fluorinator with a criticality-safe cross-section of 0.1 x 0.4 m is able to process 100 tonnes/year of irradiated fuel in an experimental plant.

In the fluorination of a uranium-plutonium mixture, uranium hexafluoride is formed much more readily than plutonium hexafluoride; this makes it possible to separate the majority of uranium from plutonium during the fluorination step. The equilibrium constant for the reaction $PuF_4 + F_2 = PuF_6$ at 500°C is only 0.01 [4], which gives a low rate of PuF_6 formation even with a large flow of fluorine. Atomic fluorine produced in high frequency discharge can be used to increase the concentration of plutonium hexafluoride in the gas stream [5]. In this case heating is not required. In experiments, the average rate of UF_6 formation from UF_4 used as an imitator of PuF_6 was 20-57 kg U per m^2 per hour, i.e. 2.5-4 times higher than that attained for the formation of PuF_6 with molecular fluorine. Corrosion of structural materials is not a problem in fluorination at 500°C. In any case, it is reasonable to fluorinate not only plutonium but also uranium in a cold fluidised bed using atomic fluorine. This makes it possible to avoid some engineering problems concerned with heating the apparatus to 500°C as well as increasing the degree of purification of both U and Pu from fission products at the fluorination stage.

Another method of fluorination of irradiated fuel, used in a flame-type cold-wall apparatus, was also developed in Russia. At a flame temperature of 1 300 K, uranium and plutonium are fluorinated at a high rate. In bench-scale experiments on the fluorination of spent fuel, yields of uranium and plutonium above 99% and 89-91% respectively were obtained [6]. This apparatus would be useful, for example, in the head end for the fluorination of the bulk of the fuel, followed by fluorination of the plutonium-bearing residue by atomic fluorine in a separate facility. Purification of uranium hexafluoride from volatile fluorides, including fission products fluorides, has been successfully demonstrated on an industrial scale. Small bath of UF_6 (hundreds kilograms) can be conveniently purified by a sorption method using NaF, while distillation of liquid UF_6 does best of all for large-scale production [7-9].

The decisive advantage of the fluoride volatility process - possibility of producing nonvolatile fission products in a compact form - has been experimentally demonstrated in the FREGAT installation by the reprocessing of just over 4 kg of irradiated uranium dioxide with an average burn-up of about 10%, from an initial enrichment of 90% of ^{235}U, cooling of 6 months. About 85% of the total radioactivity was concentrated in the residues, which did not exceed 15% of the fuel mass [9]. Thus, the volume of the solid media containing the fission products extracted from a unit mass of irradiated fuel at a fluoride facility would be tens of times smaller than at a solvent extraction plant. This is explained by the absence of buffer tanks for dissolved fuel and for the raffinate and concentrate. In an accident the solid materials produced in the fluoride process could not escape far from the container (with the exception of aerosols), while the liquids produced in the solvent extraction could be carried for large distances.

3.1.3. Summary

- FVP is studied quite well on the fundamental chemical level (thermodynamics, and kinetics fluorination reactions for the chemical elements and their compounds from SNF).
- As a first approximation it is possible to consider, that all SNF components are fluorinated by elementary fluorine up to the end, i.e. quantitatively, except for plutonium which is easily fluorinated to PuF_4 and it is difficult - to PuF_6.
- In the FVP process it is expedient to allocate plutonium with atomic fluorine in the form of PuF_6. Apparently, plutonium will be difficult for clearing highly radioactive impurity, which in this case is the positive factor as it meets the requirements of non-prolifiration.
- As a result of high-temperature SNF fluorination the mix of the higher fluorides of fuel components is formed. Volatile fluorides neptunium and some fission products (NpF_6, MoF_6, IF_7, TeF_6, SeF_6, SbF_5, NbF_5, RuF_5) arrive together with UF_6 on a step of

distillation and after branch from UF_6 are fixed together or selectively on firm sorbents.

- The FVP process is represented as the most simple method, allowing to allocate technetium and iodine from a waste stream.
- Americium and curium as well as ^{93}Zr, ^{135}Cs, ^{137}Cs, ^{90}Sr and rare earths are formed as non-volatile fluorides which get to "candle end".
- A small degree of the behaviour of non-volatile americium and curium in FVP processes is studied.

Table 18: Physical- chemical properties for fluorides of some actinides and fission products

Fluoride	Molecular mass	Temperature, °C		Density, kg/m^3	$-\Delta H_{298}$, kcal/mole	$-\Delta G_{298}$, kcal/mole	Heat of evaporation, kcal/mole
		$T_{melting}$	$T_{boiling}$				
UF_6	352.07	64.05*	56.4	5060	510.77**	428.5**	11.87
UF_5	333.07	348***	-	5510 (α)	490.0	465.0	-
				6450 (β)	491.0	466.0	-
UF_4	314.07	1036	1723	6950	453.7	428.5	51.2
PuF_6	353	50.6	62.3	-	407.4**	-	11.6
PuF_4	315.07	1037	1427	7000	414.4	402.5	47
NpF_6	351	54.8	55.2	-	472 (cr)	443 (кр)	-
MoF_6	210	17.6	33.9	-	372.3	350.8 (g)	6.6
NbF_5	188	80	235	-	433.5 (cr)	406.2 (cr)	16.0
RuF_5	196	101	280	-	213.4 (кр)	-	15.2
SbF_5	216.7	6	143	-	305 (l)	-	-

* in ternary point
** for gaseous UF_6 & PuF_6
*** in UF_6 atmosphere

References

[1] Conceptual Design Study of a Fluoride Volatility Plant for Reprocessing LMFBR Fuels. USAEC Report ANL-7583, July 1969.

[2] U.D. Veriyatin, N.P. Galkin, V.A. Zuev *et al.* (1971), The main problems of the reprocessing of fast-breeder fuel rods. *Atomnaya Energiya*, v. 31, issue 4, October 1971, p. 375 (in Russian).

[3] O. Lebedev, M.V. Muraschov, V.N. Prusakov (1973), The stability investigation of U_3O_8 fluid-bed fluorination. Preprint IAE-2328 (in Russian).

[4] L.E. Trevorrow, W.A. Shinn and R.K. Steunenberg (1961), The Thermal Decomposition of Plutonium Hexafluoride. J. Phys. Chem., v. 65, 398-403.

[5] Lebedev, M.V. Muraschov, V.N. Prusakov (1978), The investigation of atomic fluorine flow production in HF-discharge. Kchimiya Visokikch Energii.v.12, No 6, p.533 (in Russian).

[6] M.A. Demiyanovich, V.N.Prusakov, O.V.Skiba (1982), The fluorination of irradiated MOX-fuel in a flame-type reactor, Preprint NIIAR-50(565), Dimitrovgrad, (in Russian).

[7] R.P.Milford (1958), Engineering Design of Oak Ridge Fluorine Volatility Pilot Plant. Ind. Eng. Chem, 50: 187-191.

[8] V.N.Prusakov, V.K.Ezshov, O.G.Lebedev, V.K.Popov (1966), Some Aspects of Reprocessing of Irradiated Nuclear Fuel by Fluoride Volatility Method. Report to the 36th Congress on Applied Chemistry, Brussel.

[9] I.K.Kikoin, V.A.Tsikanov, M.A.Demiyanovich *et al.* (1976), The experimental recovery of BOR-60 irradiated fuel by fluoride-volatility method. Preprint NIIAR P-18(284), Dimitrovgrad, (in Russian).

3.2. Uranium and protactinium removal from fuel salt compositions by fluorine bubbling

One of the most suitable options envisages uranium distillation in the form of UF_6 by means of fluorine bubbling through the molten salt. The process was used for recycling fuel from ARE and MSRE test molten salt reactors [1]. When fluorine bubbles through the molten salt, the reaction of UF_6 formation takes place on the gas-liquid phase interface. The rate $UF_4 + F_2 \leftrightarrow UF_6$ reaction at 500—600°C is very high, which would lead one to expect the mass transfer of uranium compounds in the liquid phase to be the limiting stage of the process. Kinetics of uranium bringing out in the process of fluorine interaction with LiF—BeF_2—UF_4 melt was studied in the RRC - Kurchatov Institute both under static and dynamic conditions [2],[3].

3.2.1. Static conditions of uranium removal

Under static conditions with fixed phase interface area, provided the melt's mechanical mixing up by gas bubbles is ruled out, the slowest (limiting) stage of the process can be studied without any interference, i.e. in its pure form. Fluorination of 50LiF-48BeF_2-2UF_4 (in % mole) melt was carried out in a cylindrical nickel vessel fitted with a sampling device. Uranium content in the samples was determined by activation technique. The kinetics of UF_6 removal from the molten salt system was studied in the temperature range of 450—600°C. In Figure 36, the logarithm of uranium relative concentration in the melt is plotted against the time of fluorination. It can be seen that the fluorination process kinetics can be described by an equation of the first order. Mass-delivery coefficients calculated based on experimental data are presented in Table 19.

Figure 36: Logarithm of uranium relative concentration in the salt melt versus fluorination time (minutes)

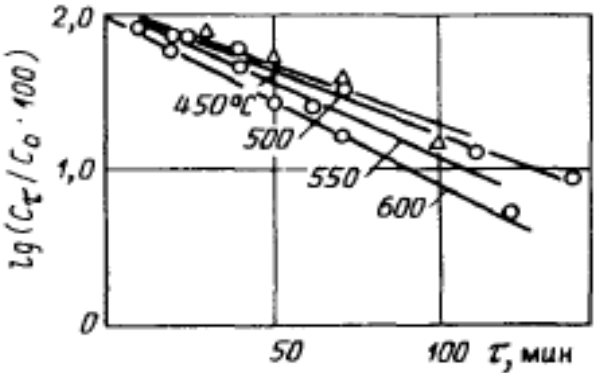

The experimental data allow us to estimate essential proportions of a molten salt mirror in the process equipment to be used for the processing of fuel salt composition, provided fluorination is performed under static conditions. Having assumed the melt's volume to be about 50 m^3, we will get the melt-fluorine interface area to be about 30 m^2 for ten-days' reprocessing cycle. The value corresponds to a rather large size of the processing facility. That is why it seems to be expedient to design fluorinators, using one or another way of increasing the fluorine-melt contact area, such as, for instance, bubbling, the melt's dispersion in fluorine atmosphere and application of film apparatus.

Table 19: The mass-delivery coefficient and diffusion layer as a function of the salt fluorination temperature

Temperature, °C	Viscosity η, 10^{-3} H s·m^{-2}	Diffusion factor D, 10^{-9} m^2 s^{-1}	Mass-delivery coefficient β, 10^{-5} m·s^{-1}	Diffusion layer δ, 10^{-4} m
450	7.1	0.34	0.44	0.8
500	4.1	0.62	0.53	1.1
550	2.7	1.03	0.62	1.6
600	1.8	1.6	0.85	1.9

3.2.2. Dynamic conditions of uranium removal

The kinetics of uranium removal from LiF-BeF_2 melt was studied in experiments on the fluorination of uranium salts containing UF_4 and UO_2F_2, dissolved in the melt, under dynamic conditions–by fluorine bubbling through the liquid. UO_2F_2 was chosen as an object of the investigation because of its presence in uranium tetrafluoride and also for the reason of its eventual formation as a result of the fuel salt oxidation if air, water vapour or some other oxide impurities get into the salt.

A salt mixture of 50LiF-49.5BeF_2-0.5UF_4 or UO_2F_2 (in % mole) was charged into the reaction vessel. Uranium concentration in the samples was measured by activation technique. The kinetics of uranium tetrafluoride fluorination in LiF-BeF_2 –UF_4 melt was studied in the temperature range of 520-600^{0}C. In Figure 37 the kinetic curves are presented – uranium relative concentration in the melt is plotted as a function of time. Within the indicated temperature range 50% uranium recovery was attained for 2-4 minutes, 99% recovery was attained for 20 minutes at 600^{0}C.

Remember that, under static conditions within 450-600^{0}C temperature range, 50% recovery of uranium from fluoride melt of the same composition was attained during 25-50 minutes. Thus, the rate of uranium removal from the fluoride melt by fluorine bubbling is by about an order of magnitude higher than the removal rate under static conditions. The result is in good agreement with the estimated increase in the mass-exchange interface area in the process of bubbling.

The kinetic curves of UO_2F_2 fluorination in the salt melt are shown in Figure 38, 50% uranium recovery in the temperature range of 520-640^{0}C was attained for 4-6 minutes, 99% recovery was attained for 34 minutes at 600^{0}C. As long as the alteration of the total fluorine pressure in the system did not exceed 5%, and owing to the kinetic curves' (Figure 38) affinity, it had become possible to determine the activation energy of the process of UO_2F_2 fluorination in LiF-BeF_2 –UO_2F_2 melt. The activation energy value proved to be 25.2±2.0 kJ/mole. The low value of activation energy gives additional evidence in favour of the assumption of diffusion's limiting role in the fluorination process. The

decrease in the rate is conditioned by the difference in the uranium compounds' mobility in the melt.

It follows from the experimental data that UO_2F_2 presence (in significant amounts) in LiF-BeF_2 –UF_4 melt may turn out to be the reason for the reduction of the rate of uranium removal from the melt. The studies' results have shown, that the bubbling type apparatus can be used for efficient reprocessing of the molten salt fuels, and the kinetic data gained can be used in calculating and designing high-efficiency fluorinators.

Figure 37: Kinetic curves of uranium relative concentration alteration in LiF-BeF_2 melt (minutes)

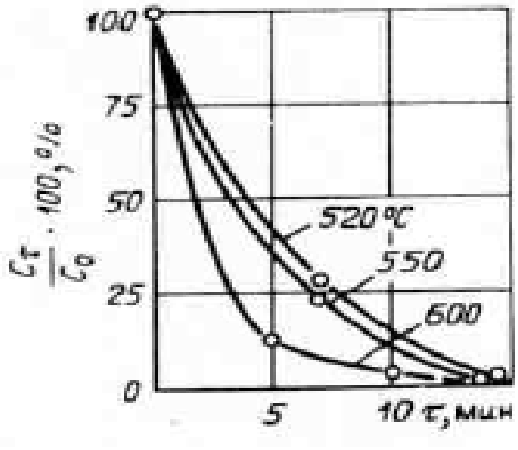

Figure 38: Kinetic curves of uranium relative concentration alteration in LiF-BeF_2 –UO_2F_2 melt (minutes)

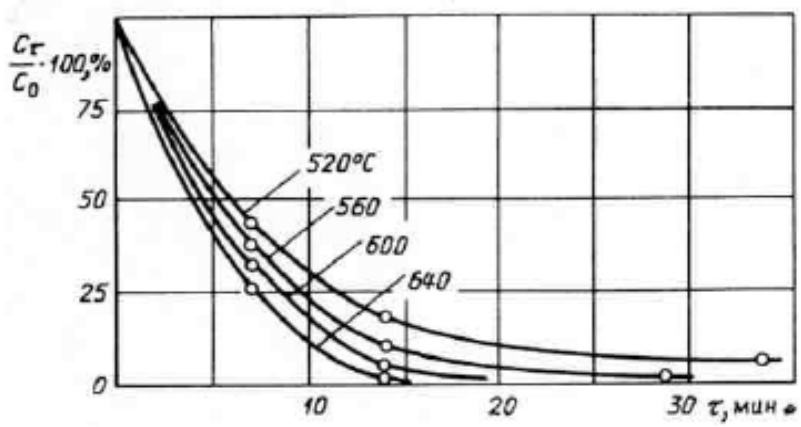

3.2.3. Protactinium removal

For LiF-BeF_2 –ThF_4- UF_4 thermal molten salt breeder reactor (MSBR) in the reactor processing unit the continuous removal of protactinium from molten salt fuel was required. In the MSBR design protactinium removal from fuel salt is envisaged to be performed using reductive extraction in liquid bismuth with lithium addition [1]. The method, however, has a number of disadvantages, such as low protactinium recovery and process rate, eventual contamination of the main reactor circuit with bismuth, etc. As a result, the issue of the development of a more efficient method of protactinium removal remains to be pressing.

In this connection a method of protactinium removal from irradiated thorium tetrafluoride dissolved in LiF-BeF_2 melt seems to be of interest [6]. In order to increase

protactinium recovery and the process rate, fluorine gas bubbling through the melt at 700-750^{0}C has been proposed. Under the conditions of fluorine bubbling protactinium tetrafluoride is oxidised to PaF_5 and removed from the salt with the flow of unreacted fluorine.

The experiments were performed in the following way. A thorium tetrafluoride dose by weight of about 1.5 g was irradiated in a test nuclear reactor. Four tests were carried out. In each of the tests about $2\cdot 10^{-6}$ g of ^{233}Pa were produced. The irradiated ThF_4 containing salt was put into a fluorinator with a 27 mm inner diameter and dissolved in $LiF\text{-}BeF_2$ molten salt mixture. At the temperature of 750^{0}C and fluorine pressure of 50 kPa the normalised rate of PaF_5 removal from the salt surface into the fluorinator's "cold" zone with the wall temperature of 400^{0}C is $\Delta m/m/\tau \approx 5\cdot 10^{-2}\,hr^{-1}$. In this case the ^{233}Pa recovery from the salt reached 98%. Thus, using fluorine bubbling, the process of protactinium removal can be intensified by an order of magnitude as compared to the static fluorination method.

The described method of protactinium removal from the fuel salt may be considered very efficient; because it allows performing protactinium removal for less than 10 hours (i.e. a very quick correction of the fuel salt can be made). Thereat, it is possible to remove protactinium with its initial content in the salt at the level of a few parts per million, which is of importance, for instance, to implementing two zone two liquid molten-salt reactor designs.

References

[1] A.M. Weinberg *et al.* (1970), A review of molten salt reactor technology, *Nucl. Appl.&Tech.,* v.8, No. 2.

[2] Novikov V.M., Ignatiev V.V., Fedulov V.I., Cherednikov V.N., Molten salt nuclear energy systems - perspectives and problems, Energoatomizdat, Moscow, 1990.

[3] Yu. P. Korchagin *et al.* (1981), The kinetic study of uranium removal from molten fluorides by gas phase fluorination technique, In Collection Book "Uranium Chemistry". – Moscow: Nauka, p.360-363 (In Russian).

[4] A.A. Klimenkov *et al.* (1987*), Atomnaya Energia,* v.62, No 2, p.119.

[5] N.P. Galki *et al.* (1961), Chemistry and Technology of Uranium Fluorides. – Moscow, Atomizdat, p.348.

[6] L. Stein (1964), Protactinium fluorides// Inorganic chemistry, v.3. No.7, p.366-380.

3.3. Flowsheet studies on non-aqueous reprocessing of LWR/FBR spent nuclear fuel

Possible flowsheets for non-aqueous reprocessing of LWR/FBR (fast breed reactor) SNF are shown in Figures 1 and 2. These options differ only in the mass flows of uranium and plutonium to be reprocessed.

The difference of the above mass flows should be reflected in the "cinder" amounts (depending directly on plutonium content) as well as the dimensions of the main equipment, in particular of the pyroelectrochemical cells. Note that the basic process steps remain the same in both cases. In general the SNF batches in both LWR/FBR blanket and FBR core could be reprocessed consecutively in the same facility.

The spent fuel assemblies are initially subjected to disassembling followed by cutting of fuel rods to lengths allowing effective oxygen access to the pellets to perform the oxide fuel voloxidation process at 700-800^{0}C. The oxide powder produced is then continuously

injected into a vertical apparatus of the tube-type through a nozzle top-down mixing with the fluorine stream heated previously to initiate the powder fluorination. The stable torch is created at a continuous fluorination process with the temperature being about 1 200^{0}C.

The uranium hexafluoride as well as the TRU (Np, Pu Am, Cm) and the fission products fluorides are produced as a result of the fluorination process. As for plutonium, due to a small excess of fluorine only a small part of plutonium forms hexafluoride with the most part produced as plutonium tetrafluoride. The torch fluorination process proceeds incompletely, leaving a "cinder" (comprising about 1-20 percent of a total mass fluorinated depending upon the plutonium content in the powder to be fluorinated), which is deposited at the lower part of the fluorinator and filters.

The uranium hexafluoride with Np and FP (fission product) volatile (including Tc) fluorides and probably trace quantities of plutonium (and MA: minor actinides) hexafluoride are collected in a cold trap (desublimator) at a temperature about -70^{0}C. The gas flow consisting of the fluorine surplus is directed to the entrapping step where it is utilised on UO_2 (300^{0}C) forming the lower uranium fluorides.

The separation of UF_6 from Np and FP volatile fluorides is carried out in a set of distillation columns. UF_6 DF at this step is no less than 10^7.

Purified UF_6 is directed to ^{235}U re-enrichment with subsequent pyrohydrolysis for common fuel fabrication or MOX-fuel fabrication. $^{232}UF_6$ stream from re-enrichment is going to the FBR fuel fabrication process.

FP volatile fluorides separated in the distillation process are fixed at sorbents (NaF etc.) and are directed to conditioning and ultimate disposal.

The "cinder" produced at the fuel fluorination step consisting of FP (including REE), Pu, and MA non-volatile fluorides is transferred to the appropriate molten salt pyroelectrochemical cell operating at 660^{0}C for plutonium and remainder (trace) uranium recovery on Cd liquid cathode. The DF of U and Pu at this stage is about 10^3.

The remaining MA-REE fraction partitioning should be carried out in a separate molten salt electrochemical cell. The separated MA, and if necessary part of the plutonium, would be transferred to the MOlten Salt Actinide Recycler Transmuter (MOSART) system for transmutation and the FP (including REE: rare earth elements) are transferred to conditioning and ultimate disposal.

Materials streams directed to the 2 400 MWt MOSART system and leaving it are given in Figure 3. At the end of the MOSART service life, radioactive materials of a reactor and processing system should be directed for treatment and disposal. As can be seen, MOSART consumes about 0.8 tonnes of TRU's per year. Streams of graphite are average in view of 20 tonnes reflector replacement every 4 years. It is supposed to accumulate this graphite during all time of the MOSART operation in reactor building. There would be little or no routine gaseous and liquid radioactive effluents, no shipment of irradiated spent fuel during the normal plant life and relatively little solid radioactive waste. In contrast with these more favourite features, the MOSART at the end of life would involve a more complex decommissioning programme and a larger solid waste disposal task. In addition, during operation, the retention of tritium and the relatively larger inventory of radionuclides may require extra efforts to avoid possibly unfavourable effects.

Table 20 shows the radionuclides content for the LWR SNF at burn-up of 50 GWd/t of the fuel with SNF cooling time of 3 years and Table 21 shows the radionuclides content for the FBR SNF at burn-up of 62.8 GWd/t of HM (Heavy Metal: U, Pu) with SNF cooling time of 1 year.

Table 20: Radionuclides content for the LWR SNF (Burn-up: 50 GWd/t of the fuel; SNF cooling time: 3 years)

#	Nuclides group	Element	Content, kg/t SNF	Mass flow, kg/TWhe
1	FP forming non-volatile fluorides (apart from REE)	Rb, Sr, Zr, Rh, Pd, Ag, Cd, Sn, Cs, Ba, Y	16.17	37.41
2	REE	La, Ce, Pr, Nd, Pm, Sm, Eu, Gd, Tb, Dy, Ho	12.44	28.79
3	Total FP forming non-volatile fluorides		28.59	66.16
4	FP forming volatile fluorides	Se Mo Ru. Sb Te Nb	8.86	20.50
5	FP Gaseous	T, Kr, Xe, I	8.28	19.16
6	Tc		0.92	2.13
7	Total FP		46.63	107.90
8	Np		0.65	1.50
9	Pu		11.30	26.15
10	MA	Am, Cm	0.58	1.34
11	Total U		822.20	1902.60
12	Including ^{232}U		7.86E-04 g/t	
	O		118.59	

Table 21: Radionuclides content for the FBR SNF (Burn-up: 62.8 GWd/t of HM; SNF cooling time: 1 year)

#	Nuclides group	Element	Content, kg/t HM	Mass flow, kg/TWhe
1	FP forming non-volatile fluorides (apart from REE)	Rb, Sr, Zr, Pd, Cd, Sn, Cs	9.52	19.04
2	REE	Ce, Nd, Sm, Eu	7.24	14.48
3	Total FP forming non-volatile fluorides		16.76	33.52
4	FP forming volatile fluorides	Se Ru. Sb Te Nb (trace qts)	1.41	2.82
5	FP Gaseous	T, Kr, Xe, I	3.19	6.38
6	Tc		1.59	3.18
7	Total FP		22.95	45.9
8	Np		0.21	0.42
9	Pu		149.21	298.42
10	MA	Am, Cm	3.66	7.32
11	Total U		846.61	1693.22
12	Including ^{232}U		1.38E-03	

Legend to Figures 1 and 2	
RW-1	T, Kr, Xe, I
RW-2	T, Kr, Xe
RW-3	Mo, Sb, Nb, Ru, Te
RW-4	Cs, Rb, Ru, Te
RW-5	Cs, Rb, Ba, Sr, Y, Rh, REE
RW-6	SFA shrouds & fuel pins cladding

References

[1] OECD/NEA (2001), Trends in the Nuclear Fuel Cycle. Economic, Environmental and Social Aspects, OECD Publications, 2, rue Andre-Pascal, 75775 Paris Cedex 16, France.

[2] V.M.Korotkevich, E.G.Kudryavtsev (2003), Some aspects of the Russian Nuclear Fuel Cycle Development, IAEA International Conference on Storage of Spent Fuel from Power Reactors, Vienna, 2-6 June 2003.

[3] Integrated US. Used Fuel Strategy (2008), Analyses Performed by the International Nuclear Recycling Alliance (INRA), 1 May 2008. US DOE Report Under Contract # DE-FC01-07NE24505.

[4] V. Novikov, O. Lebedev (1991), A Soviet View of the Pros and Cons of Reprocessing. *Proceedings of the 16th International Symposium held by the Uranium Institute*. London, 4-6 September 1991.

[5] M.A.Demiyanovich, V.N.Prusakov, O.V.Skiba (1982), The fluorination of irradiated MOX-fuel in a flame-type reactor. Preprint NIIAR-50(565), Dimitrovgrad, (in Russian).

[6] I.K. Kikoin, V.A. Tsikanov, M.A. Demiyanovich *et al.* (1976), The experimental recovery of BOR-60 irradiated fuel by fluoride-volatility method. Preprint NIIAR P-18(284), Dimitrovgrad, (in Russian).

[7] V.V. Shatalov *et al.* (2001), Fluoride gas technology of SNF reprocessing, "Atomic Energy", issue 3, pp. 212-222.

[8] A Conceptual Design Study of a Fluoride Volatility Plant for Reprocessing LMFBR Fuels. USAEC Report ANL-7583, July 1969.

[9] A.V. Bychkov, S.K. Vavilov, P.T. Porodnov *et al.* (1993), "Pyroelectrochemical Reprocessing of Irradiated Uranium-plutonium Oxide Fuel for Fast Reactors", *Proc. Int. Conf. GLOBAL'93*, Seattle, WA, 12-17 September 1993, ANS, Vol. 2, pp. 1351-1356.

[10] W. Forsberg, V. Ignatiev, C. Lebrun, E. Merlet-Lucotte, C. Renault (2007), Liquid salt applications and Molten Salt Reactors, *Revue Generale Nucleaire, Societe Francaise D'Energie Nuclearire*, N4, pp. 63-71.

Figure 39: Reprocessing of SNF from LWR by fluoride volatility & pyroelectrochemical methods (Burn-up: 50 GWd/t, cooling time: 3 years)

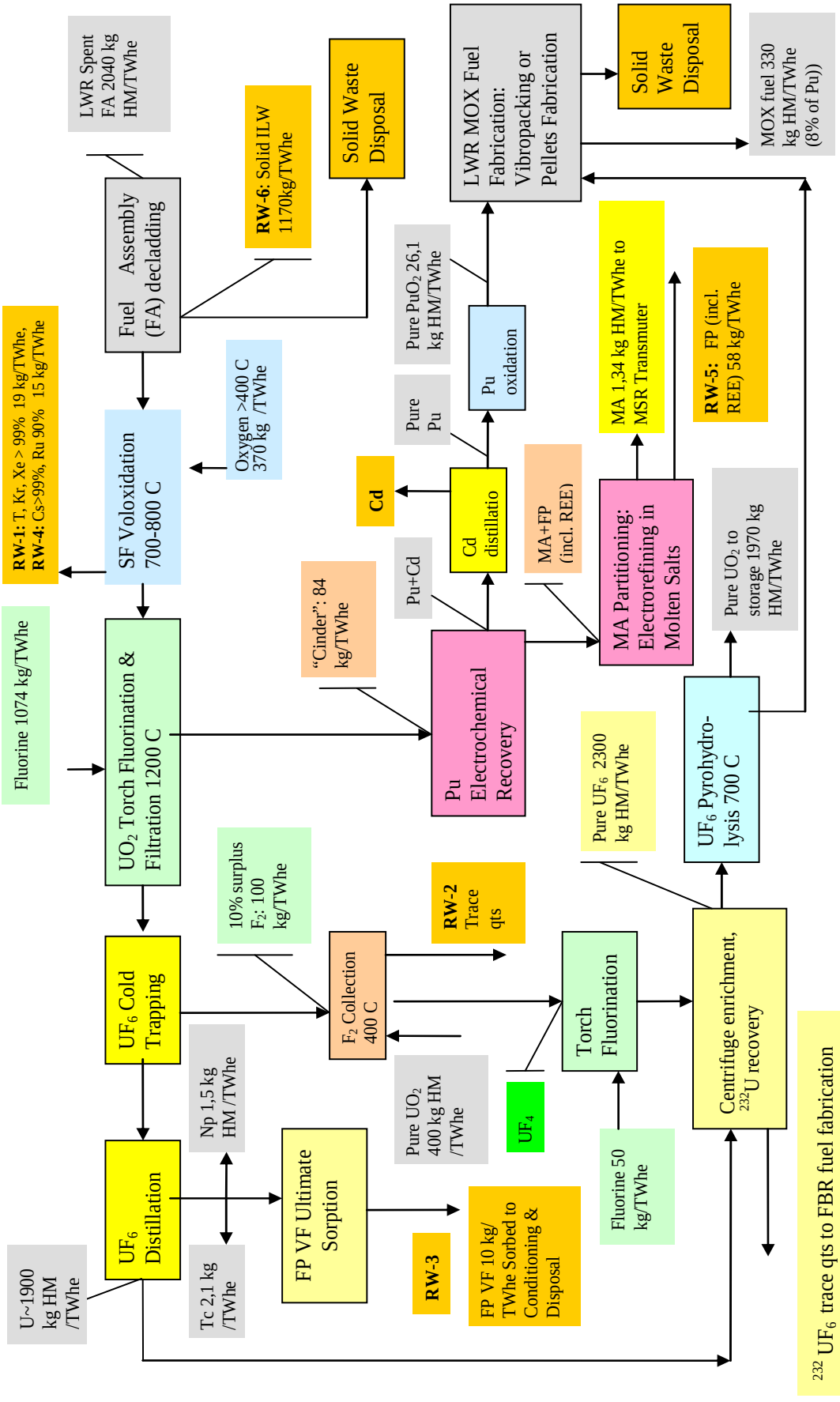

Figure 40: Reprocessing of FBR SNF by fluoride volatility & pyroelectrochemical methods (Burn-up: 62.8 GWd/t, cooling time: 1 year)

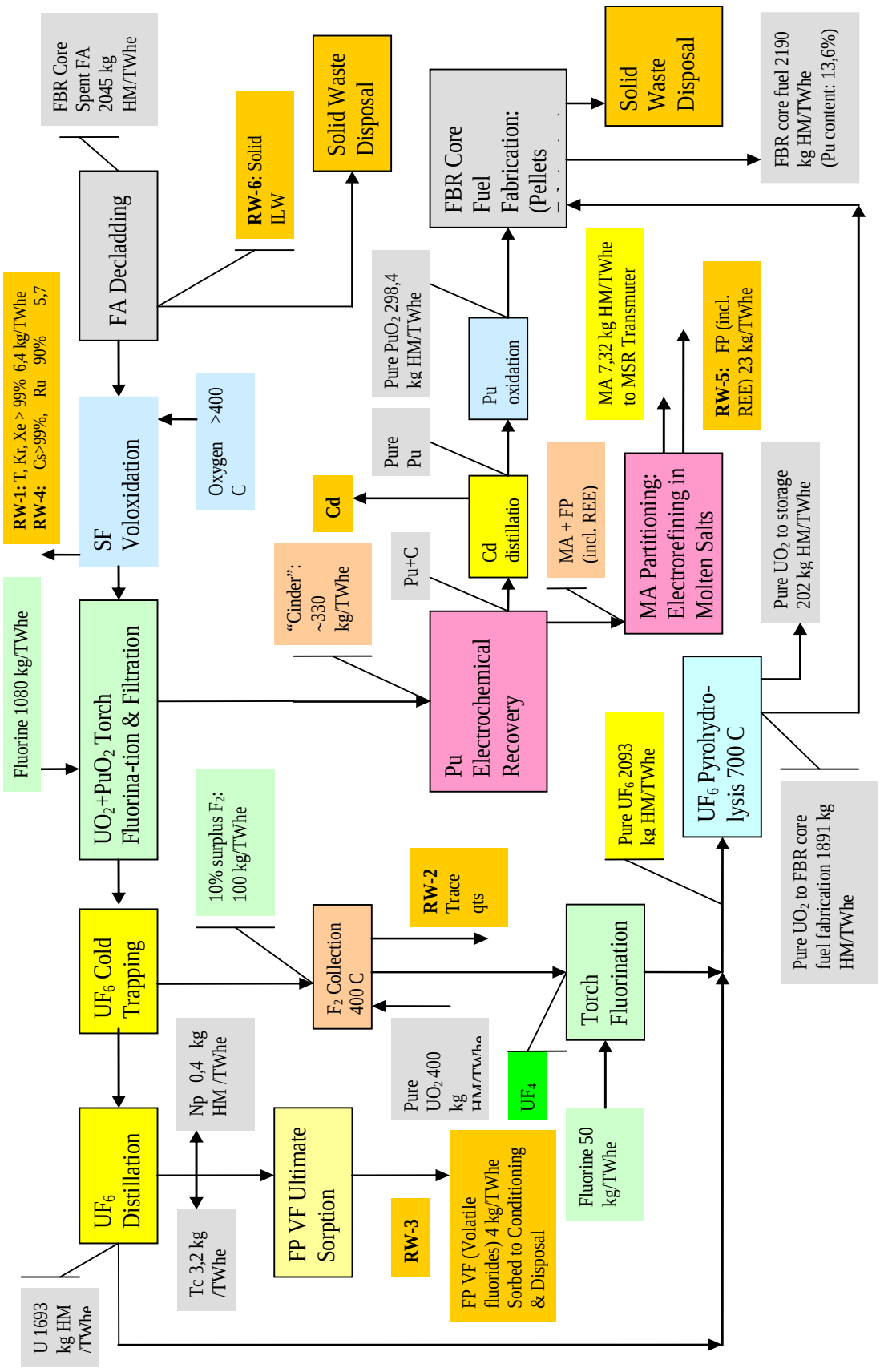

Figure 41: Materials flow diagramme for 2 400 MWt MOSART system

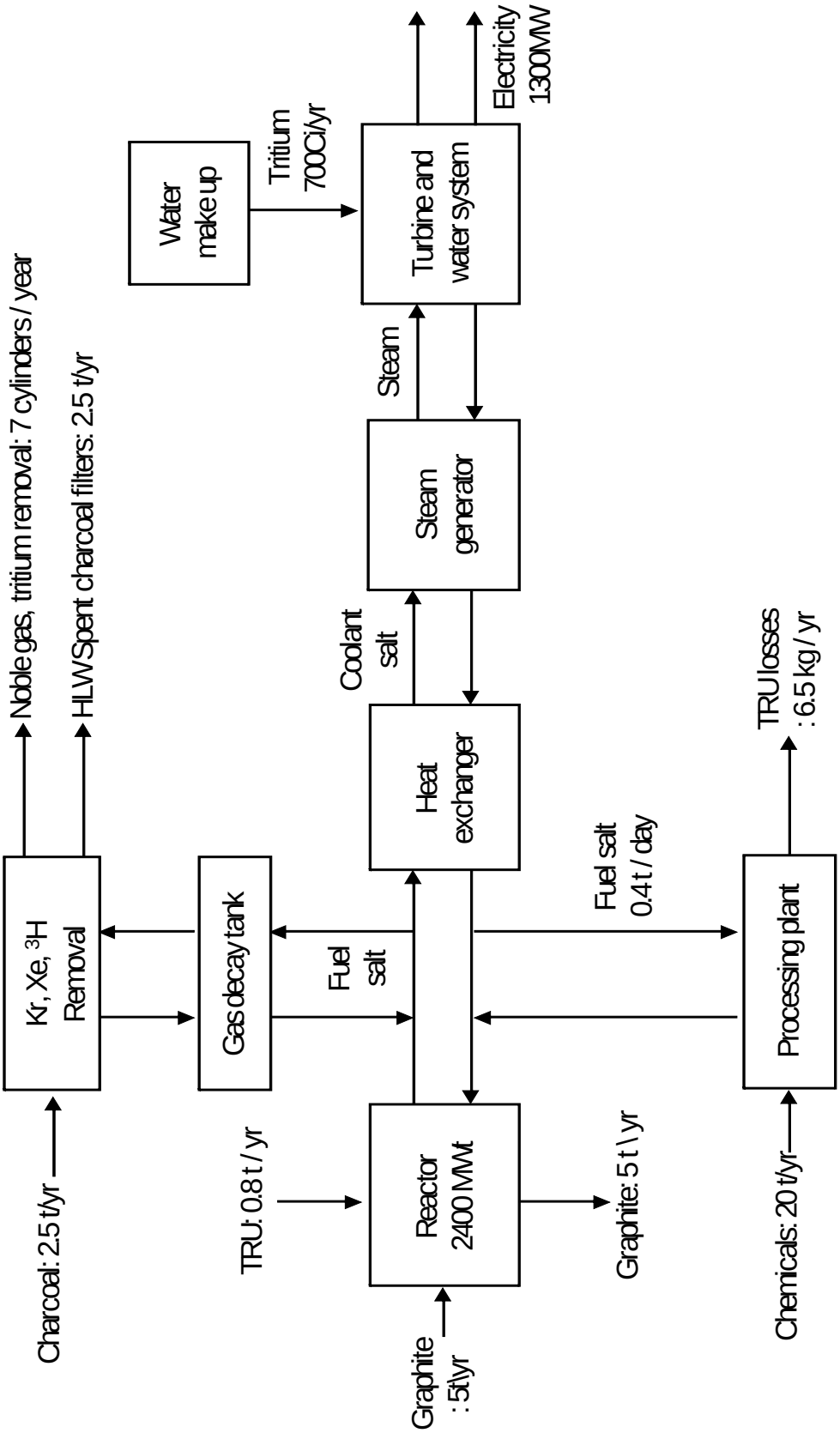

Appendix A: Flowsheet studies of RIAR (Russian Federation)

НИИАР

Flowsheet studies

Russian RIAR contribution

SSC RIAR, Dimitrovgrad-10, Ulyanovsk region, Russia, 433510,
?-mail: bav@niiar.ru , Web site: http://www.niiar.ru

Official Investment Frames for Russian Nuclear Renaissance

НИИАР

- Federal Tasks Program "Development of Nuclear Power Complex of Russia on a period of 2007 - 2015 " - accepted in 2006

  - NPP construction

- Federal Tasks Program "Nuclear and Radiation Safety" (2008-2015) - accepted in 2007

  - RAW Heritage

- Federal Tasks Program "New Generation Nuclear Energy Technologies" (2010-2020) – on a final preparation Stage

  - Innovations:

  - *Pyro reprocessing,*
  - *Advanced FR (MFTR, Commercial BN-type, BREST, SVBR)*
  - *RAW advanced management*
  - *Others…*

НИИАР

Federal Tasks Program
"New Generation Nuclear Energy Technologies"
RIAR planned participation

- Multi-functional Fast Test Reactor (MFTR) – 2016 →2020 (loops)
- Large Multi-Purpose Pyrochemical Reprocessing Complex - 2015
  - Molten salt Reprocessing Facility
    - ✓ capacity – up to 2 500 kg of FR SNF per Year (fuel type: oxide, nitride, metallic, IMF)
  - Fluoride volatility Reprocessing Facility,
    - ✓ capacity – up to 1000 kg of SNF per Year (mainly – LWR SNF)
- New Lab for Experimental and Innovative Fuel Production – 2010-1012 (incl. Fuel and Targets with MA)
- Demonstration of Closing Fuel Cycle based on Pyrochemical technologies - 2016-2020-… on a levels:
  - Up to 50 spent FAs of BN-600/800
  - Full scale CFC for MFTR from initial fuel loading
  - Other experimental implementations

New Russian Sodium Fast Test Reactor – Multi-functional Fast Test Reactor (MFTR)

Location – RIAR site

НИИАР

Characteristic	Value
Maximum flux ? max, n/cm2·sec	~ 6.0·10^{15}
Thermal power, MWth	~ 150
Electric power, MWe	~ 50
Number of independent experimental loops (~1 MWth, sodium, heavy metal and gas coolant + salt coolants)	3 (+1 behind reactor vessel)
Driven Fuel	Vi-pack MOX, (PuN+UN)
Core height, mm	400-500
Maximum heat rate, kW/l	1100
Fuel Cycle	Full Scale Closed FC based on Pyro Processes
Test Fuel	Innovative Fuels, MA Fuels and targets
Maximum fluence in one year, n/cm2	~ 1,2·10^{23} (up to 55dpa)
Design lifetime	50 year
RR creation time (no more than, years)	9 (2008 – 2016)

Start of BN Closed fuel Cycle based on RIAR technologies

- **2011 - start of vi-pack MOX-fuel production for BN-800**
- **2012 – start of BN-800 operation**
- **2016..2020 – demonstration of BN-800 closed fuel cycle technologies**

Key final official decisions:

- MOX fuel production by pyroelectrochemistry and vibropacking
- Trend to closing of fuel cycle by compact dry technologies
- Development and testing of new fuel and new technologies

RIAR R&D International cooperation in the field of advanced FC

	Fuel production		Repro-cessing	P&T	Other	Cladding materials	Concept Studies	Funda-mental Studies
	MOX	other						
France	-	MA oxide	-	Am/Cm recovery	Pyro	+	FS	Cm
INPRO	-	-	-	-	-	-	CP RUS-2	-
Japan	MOX vibro	-	MOX	MA/REE separ.	Fluorex/MoO_4^{2-}	ODS	FS	MA
Korea	-	-	Metalliz./ vibro-DUPIC	MA/REE separ.	Pyro	-	-	-
US?	*TRU fuel ?*		*UREX+1 ?*	*TRU fuel?*	-	-	-	*Pu in RTTL's*
EU	-	MA nitride	-	-	MSR fuel	-	-	Cm

Red color – DOVITA-1/2 activities

НИИАР

MOX Fuel Pyrochemical Reprocessing

(BN-800 Closed Fuel Cycle R&D Program)

MOX Fuel Pyrochemical Reprocessing

SNF Decladding
(SNF Vol-oxidation)
SNF Dissolution (Chlorination)

MOX Cathode Deposits Production

Cathode deposits obtaining out of prepared portions is made at their conversion in chloride salt melt. NaCl-2CsCl mixture is the basis of salt systems. All chemical operations are made in one and the same unit – chlorinator-electrolyzer in pyrographite bath (crucible). Salt transference is not made. Crucible is replaced, when its service life is ended. Salt phosphate cleaning is made as required during Am, Cs and impurities accumulation in electrolyte for the purpose to reduce personnel radiation dose and ensure the granulate MOX-fuel quality

Cathode Deposit Crushing

Cathode deposit crushing is made for the purpose to obtain granulate of given granulometric compound

Granulate Washing

Granulate washing is made for the purpose to clean it from captured components of the salt system

Granulate Vacuum Driving-off

Vacuum driving-off of granulate is made for the purpose to clean it after washing till admixtures content required parameters

Granulate Classification

Granulate classification is made with the aim of its grading according to fractions

Granulate Batch Preparation

Granulate portion preparation with given granulometric compound and given weight characteristics is made at the bay of various granulate fractions

Pins Fabrication

The following initial materials and as-built components are used during pins fabrication: granulate portions, metallic U powder (up to 7% from granulate fuel mass), envelope with bottom plug, top plug, element for fuel core fixing, bottom screen pellets

MOX Granulate production lay out

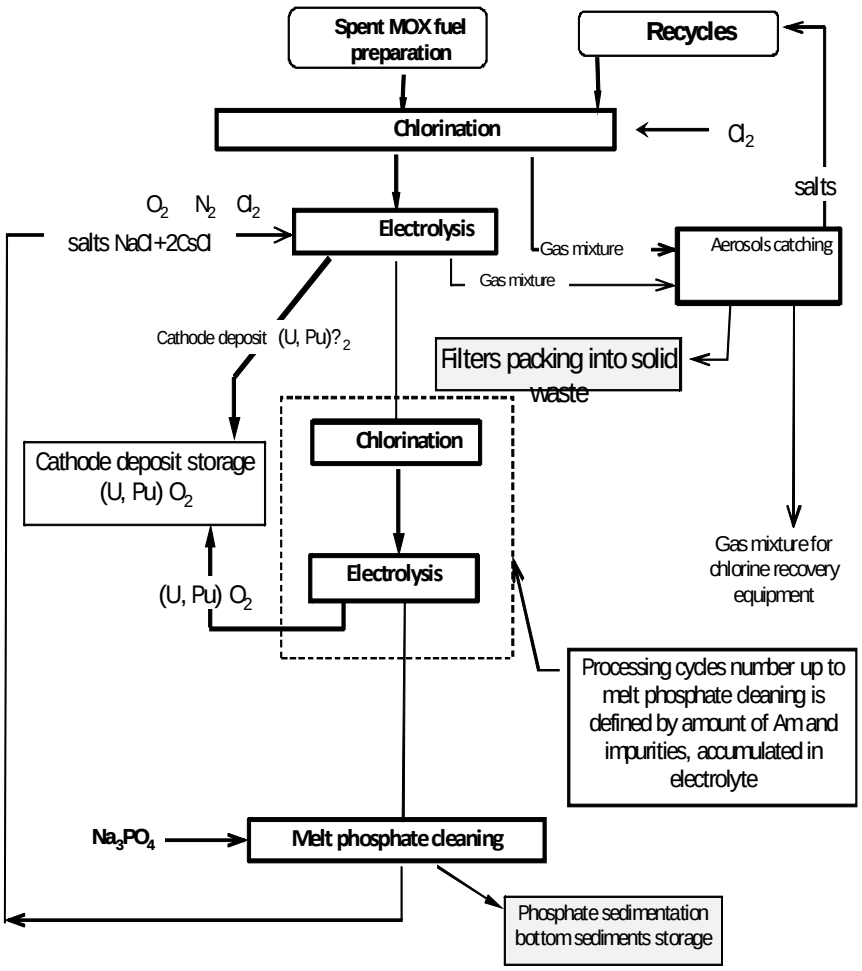

Pins fabrication and monitoring Flow-sheet

НИИАР

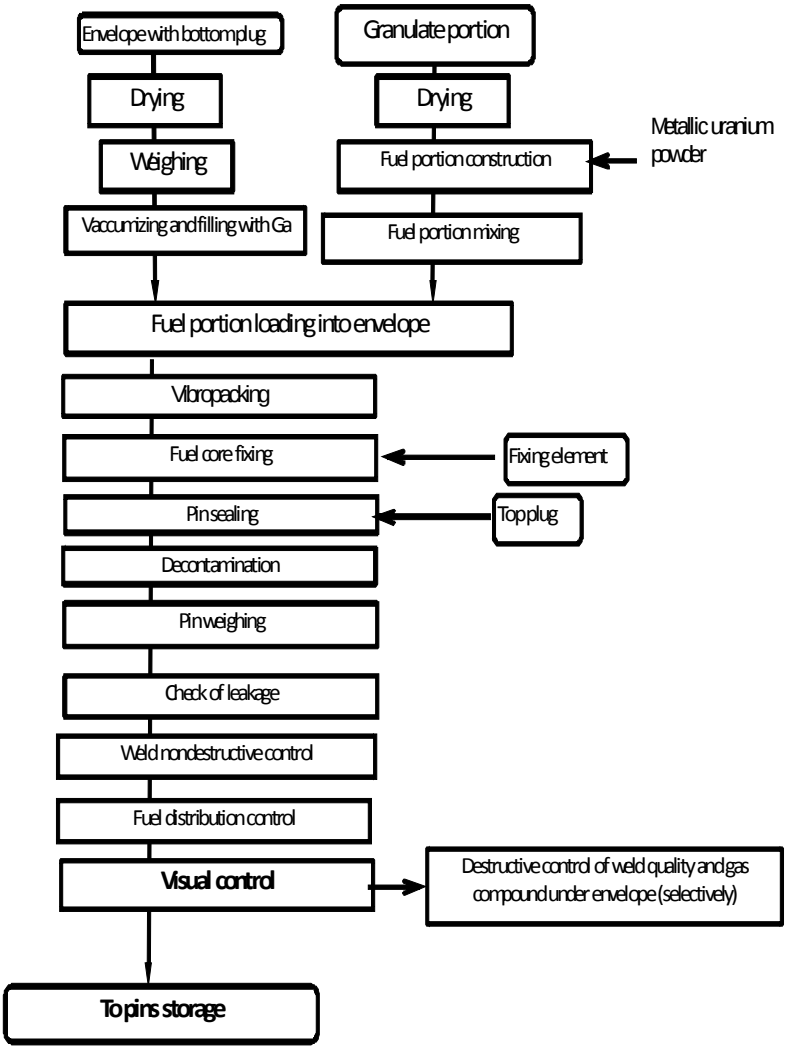

НИИАР

The Nitride Fuel Pyrochemical Reprocessing

(BREST Reactor Closed Fuel Cycle R&D Program)

НИИАР

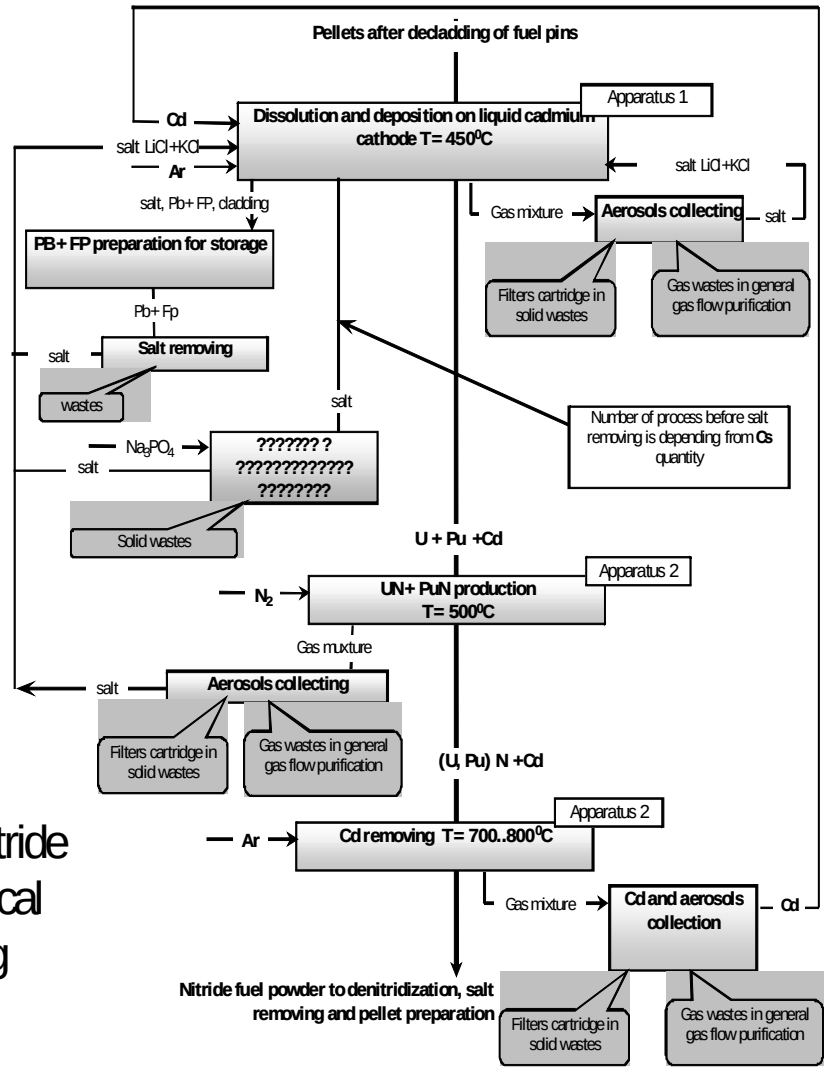

Flow-sheet of nitride fuel pyrochemical reprocessing

НИИАР

Flow-sheet of nitride pellet fuel pins manufacturing

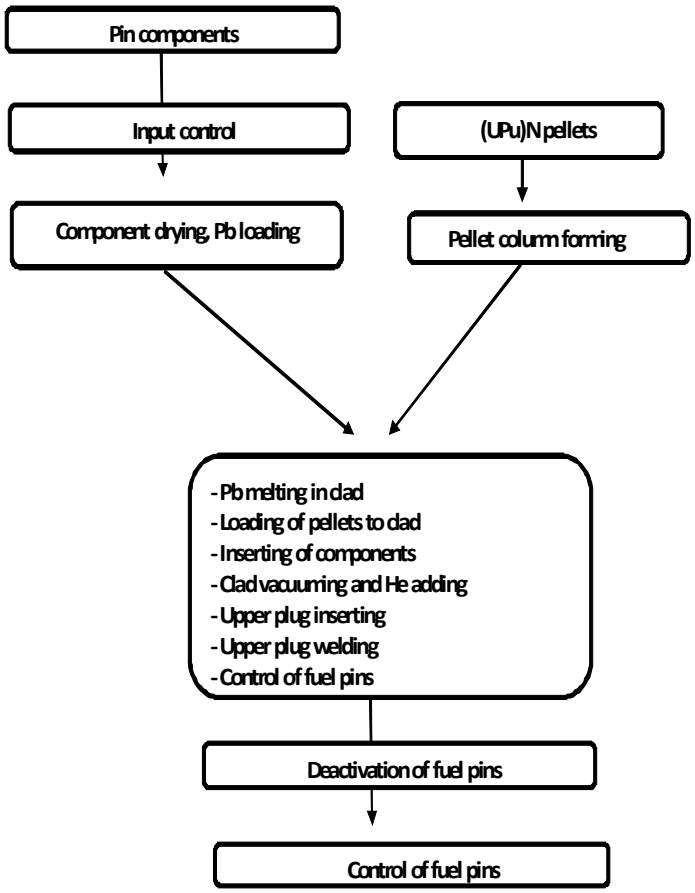

Flow-sheet of material flows

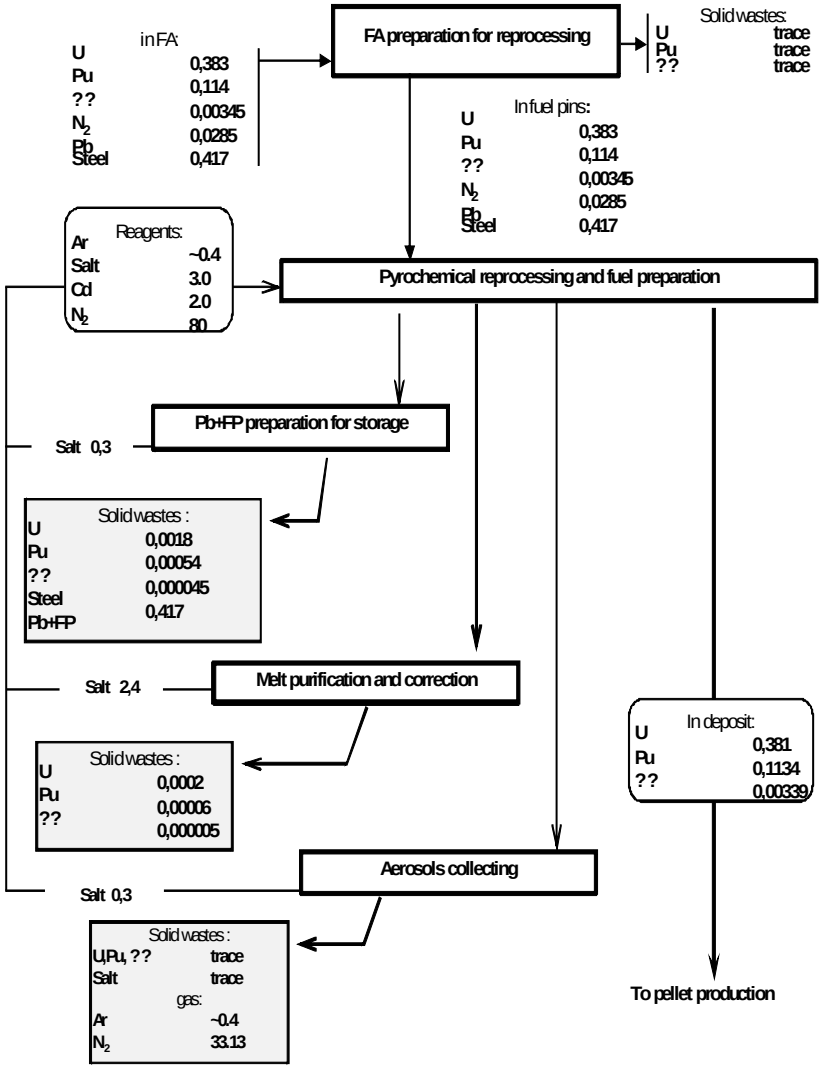

List of contributors

Chair

Pascal Baron (CEA, France)

Scientific Secretary

Yong-Joon Choi (OECD/NEA)

Chapter 1: Hydrometallurgy process

1.1. Standard PUREX

Peter Rance (NNL, UK)

Dave Fox (NNL, UK : retired)

1.2. Extended PUREX

Pascal Baron (CEA, France)

1.3. UREX+3

Emory Collins (ORNL, USA)

1.4. Grind/Leach

Emory Collins (ORNL, USA)

Chapter 2: Pyrometallurgy process

2.1. Pyroprocess (CRIEPI - Japan)

Tadafumi Koyama (CRIEPI, Japan)

2.2. 4-group partitioning process

Kazuo Minato (JAEA, Japan)

2.3. Pyroprocess (KAERI – Korea)

Eung-Ho KIM (KAERI, Korea)

2.4. Direct electrochemical processing of metallic fuel

Mark Williamson (ANL, USA)

2.5. PyroGreen (reduce radiotoxicity to the level of low-and intermediate-level waste) (LILW)

Il-Soon Hwang (SNU, Korea)

Chapter 3: Fluoride volatility process

Victor Ignatiev (KIAE, Russia)

Mikhail Kormilitsyn (RIAR, Russa)

Appendix A: Flowsheet studies of RIAR (Russian Federation)

Mikhail Kormilitsyn (RIAR, Russa)

Members of the expert group

Canada	
HYLAND, Bronwyn	AECL
Czech Republic	
UHLIR, Jan	NRI
France	
BARON, Pascal (Chair)	CEA
WARIN, Dominique	CEA
Italy	
DE ANGELIS, Giorgio	ENEA
LUCE, Alfredo	ENEA
Japan	
INOUE, Tadashi	CRIEPI
MORITA, Yasuji	JAEA
MINATO, Kazuo	JAEA
Korea	
LEE, Han Soo	KAERI
Russian Federation	
IGNATIEV, Victor V.	KIAE
KORMILITSYN, Mikhail V.	RIAR
Spain	
CARAVACA, Concepcion	CIEMAT

United Kingdom

LEWIN, Robert G.	NNL
TAYLOR, Robin J.	NNL

United States of America

COLLINS, Emory D.	ORNL
LAIDLER , James J.	ANL

International Organisations

CHOI, Yong-Joon (Secretary)	NEA
GLATZ, Jean-Paul	EC